NASA Technical Memorandum 107760

Thermal Coatings for Titanium-Aluminum Alloys

George R. Cunnington
Lockheed Missiles & Space Company, Inc.
Palo Alto, California

Ronald K. Clark
NASA Langley Research Center
Hampton, Virginia

John C. Robinson
Lockheed Missiles & Space Company, Inc.
Palo Alto, California

April 1993

National Aeronautics and Space Administration

Langley Research Center
Hampton, Virginia 23681-0001

FOREWORD

This report was prepared jointly by the Research and Development Division of the Lockheed Missiles and Space Company, Inc. (LMSC) and the Materials Division of the Langley Research Center for the National Aeronautics and Space Administration (NASA). The purpose of the research was to develop chemical vapor deposition coatings which would be suitable as environmental protection and thermal control coatings for selected titanium-aluminide and titanium alloys being considered for use in hypersonic vehicle applications.

The NASA project manager was Dr. Ronald K. Clark of the Langley Research Center, and the LMSC project manager was Mr. George R. Cunnington. The authors gratefully acknowledge the following persons for their assistance during the conduct of the program: S. N. Sankaran and K. E. Wiedemann of Analytical Services and Materials, Inc.; T. A. Wallace of Langley Research Center; and A. L. Ambrosio, R. Jamison, A. I. Funai, and B. Wallingford of LMSC.

ABSTRACT

Titanium aluminides and titanium alloys are candidate materials for use in hot-structure and heat-shield components of hypersonic vehicles because of their good strength-to-weight characteristics at elevated temperature. However, in order to utilize their maximum temperature capability, they must be coated to resist oxidation and to have a high total emittance. Also, surface catalysis for recombination of dissociated species in the aerodynamic boundary layer must be minimized. Very thin chemical vapor deposition (CVD) coatings are attractive candidates for this application because of durability and very light weight. To demonstrate this concept, coatings of boron-silicon and aluminum-boron-silicon compositions were applied to the titanium-aluminides alpha2 (Ti-14Al-21Nb), super-alpha2 (Ti-14Al-23-Nb-2V), and gamma (Ti-33Al-6Nb-1Ta) and to the titanium alloy beta-21S (Ti-15Mo-3Al-3Nb-0.2Si). Coated specimens of each alloy were subjected to a set of simulated hypersonic vehicle environmental tests to determine their properties of oxidation resistance, surface catalysis, radiative emittance, and thermal shock resistance. Surface catalysis results should be viewed as relative performance only of the several coating-alloy combinations tested under the specific environmental conditions of the Langley Research Center Hypersonic Materials Environmental Test System (HYMETS) arc-plasma-heated hypersonic wind tunnel. Tests were also conducted to evaluate the hydrogen transport properties of the coatings and any effects of the coating processing itself on fatigue life of the base alloys.

Results are presented for three types of coatings, which are: (1) a single layer boron-silicon coating, (2) a single layer aluminum-boron-silicon coating and (3) a multilayer coating consisting of an aluminum-boron-silicon sublayer with a boron-silicon outer layer. The range of coating thicknesses investigated was 2.4 to 19.6 μm, and coating weights were 0.0056 to 0.0446 kg/m^2. Oxidation protection afforded by all coatings was excellent, and total emittance was 0.80 or greater in all cases. Surface catalysis, expressed as recombination efficiency, was 0.04 or less for the multilayer and the single-layer boron-silicon coatings. Recombination efficiency was 0.06 or less for the single-layer aluminum-boron-silicon coating.

CONTENTS

Section **Page**

Appendix

ILLUSTRATIONS

Figure **Page**

Tables

Section 1
INTRODUCTION

Titanium-aluminide alloys are candidate materials for high-temperature structural elements and heat shields in hypersonic vehicles because of their very favorable strength-to-weight properties at temperatures in the range of 1000 to 1250 K. However, their use in the earth's atmosphere is limited by their susceptibility to oxidation at elevated temperatures with a subsequent reduction in mechanical properties. Protective coatings which prevent oxidation are needed to permit the use of these alloys at higher temperatures for earth reentry vehicles. Furthermore, if the coatings provide a high thermal emittance and low-recombination-efficiency surface, the net heating to vehicle surfaces in a hypersonic flight environment is significantly reduced. The recombination of the dissociated nitrogen and oxygen present in the hypersonic boundary layer is an exothermic reaction. If this reaction occurs at the surface, the energy produced is a heat flux into the vehicle which is in addition to the purely convective heating. Minimization of the surface recombination heating depends on having a surface that does not catalyze the reaction by lowering the activation energy of the rate-determining steps in the reaction process.

The effect of surface recombination efficiency and emittance on the temperature of an insulated hypersonic vehicle surface is illustrated in Figure 1. The flow conditions used for the calculation are typical for those for a test of a coated metal at a surface temperature of nominally 1250 K in the Langley Research Center Hypersonic Materials Environmental Test System (HYMETS). Chemical equilibrium calculations indicate that the oxygen in the flow is totally dissociated and the nitrogen dissociation is on the order of 5%. It should be noted that these calculations are subject to the uncertainties discussed in Section 3.2; they are presented to illustrate the relative importance of emittance and recombination efficiency. The fully catalytic heating rate (convective plus recombination) for this condition is 2.75 times the purely convective heating rate.

Conventional oxidation-protection coatings for metallic materials in high-temperature corrosive environments are commercially available. Coatings for titanium-based alloys are typically formed by applying a slurry mixture to the surface followed by a high-temperature furnace cure. During the cure, the coating reacts with the alloy to form an intermetallic layer. Typical thicknesses for this type of coating are 25 to 50 μm. Concerns with use of this type of coating are that coating consumes substrate material, a very low ductility intermetallic layer at the surface may reduce fracture toughness of the alloy, and thick coatings are a weight penalty.

Physical vapor deposition has limited potential for producing good oxidation-protection coatings because of the difficulty in forming thin defect-free layers. Two approaches for producing defect-free coatings having overall thicknesses in the 2- to 5-μm range are based on chemical vapor deposition (CVD) and on the sol-gel

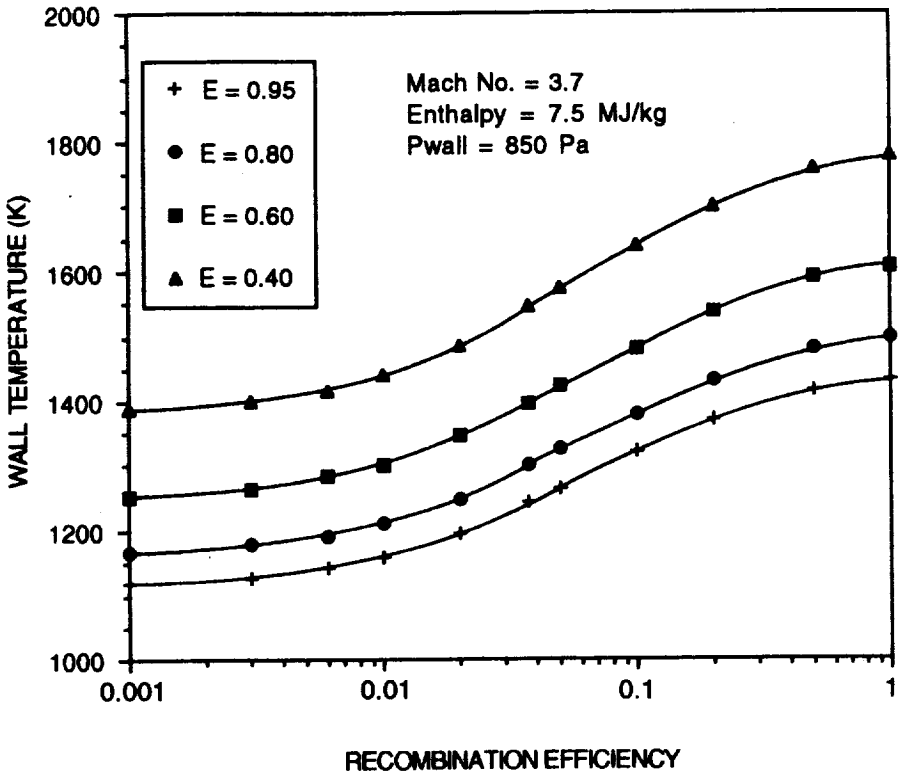

Figure 1. Influence of recombination efficiency and total hemispherical emittance on adiabatic wall temperature for typical HYMETS test conditions.

processes (Ref. 1). Development of the sol-gel coating compositions and processing techniques is being carried out in the laboratories at Langley Research Center. Development of the CVD coatings is the subject of the research reported herein. Coating development and application was carried out by LMSC, and testing was conducted at both LMSC and Langley Research Center. The CVD coatings are of boron-silicon and aluminum-boron-silicon compositions.

The LMSC CVD coating was first applied to metallic heat shield materials in the time period of 1983 to 1985 under contract NAS1-16423 (Ref. 2). The coating was of the aluminum-boron-silicon composition, and it was applied to the inherently oxidation-resistant Inconel 617 and MA 956 superalloys for use in the temperature range 1250 to 1350 K. Tests of coated materials in the HYMETS facility demonstrated a significant reduction in recombination efficiency over that of the natural oxide protective surfaces. The coating also provided a high-total-emittance surface. A subsequent cooperative development effort between LMSC and Langley Research Center established the feasibility of the CVD approach for use with titanium alloys and

titanium-aluminides, and this led to the present contractual effort, the results of which are summarized in this report.

The objective of the coating development activities reported here was to develop a lightweight oxidation protection and thermal control coating for the alpha2, super-alpha2 and gamma titanium-aluminides and the beta-21S titanium alloy for use in hypersonic vehicle applications. Coating weight goals were less than 0.015 kg/m^2, which corresponds to a maximum coating thickness of 7 μm. Thermal control goals were a total hemispherical emittance equal to or greater than 0.80 and recombination efficiency less than 0.020. The goal for useful life of a coating was a minimum of 10 h at maximum temperature in the HYMETS simulated hypersonic flight environment. The maximum temperatures considered to be appropriate for the flight vehicle application are 1094 K for the beta-21s alloy and 1255 K for the titanium-aluminides.

Section 2
DESCRIPTION OF COATINGS

A hydrogenated boron-silicon alloy is the basic coating used for this investigation. The film is produced by thermal decomposition of mixtures of silane (SiH_4) and diborane (B_2H_6) in a hydrogen carrier gas. The film as deposited is amorphous, composed of B-H and Si-H bonds, and contains up to 45 vol % hydrogen. It forms a very tenacious chemical bond over all exposed surfaces, including internal voids and passages, by saturation of free surface bonds. During subsequent heat treatment, hydrogen is evolved, resulting in a residual highly reactive film free to react with a substrate alloying layer and oxygen from the environment.

Three basic compositions of the CVD coating were applied to four titanium-aluminum alloys. These coatings, all of the boron-silicon and the aluminum-boron-silicon compositions, are covered under five LMSC Patents (Refs. 3–7). Both single- and two-layer coatings were investigated in an attempt to optimize oxidation resistance, thermal emittance, and recombination efficiency in a single coating. The coatings were applied to the following aluminides and alloy substrate materials (numbers are weight percents of the elements, with the balance titanium):

- Ti-14Al-21Nb (alpha2 titanium-aluminide)
- Ti-14Al-23Nb-2V (super-alpha2 titanium-aluminide)
- Ti-33Al-6Nb-1Ta (gamma titanium-aluminide)
- Ti-15Mo-3Al-3Nb-0.2Si (beta-21S titanium alloy)

The substrate materials were furnished by the Government in the form of sheet material, except for the initial test specimens of the gamma material, which were machined from bar stock. The alpha2 specimens were from two different sheets of material, 0.00045 and 0.00055 m thick. The super-alpha2 sheet stock was 0.00095 m thick. The specimens of gamma from sheet stock were 0.00075 m thick and the machined specimens were 0.00047 m thick. The beta-21S sheet was 0.00065 m thick. All test specimens were coated in the finished shape required for a specific test. Environmental test specimens were circular disks, and the fatigue and thermogravimetric (TGA) specimens were rectangular.

2.1 COATING DESIGNS

The two basic designs for the coatings are (1) a single layer of either aluminum-boron-silicon or boron-silicon and (2) a multilayer configuration having a boron-silicon exterior layer over either an aluminum-boron-silicon or a silicon hexaboride-like layer. The configurations are illustrated schematically in Figure 2. The multilayer configuration, designated Type 1, consists of a nominally 2-μm-thick sublayer with a nominally 3-μm-thick outer layer. A variation of this type of construction has a silicon

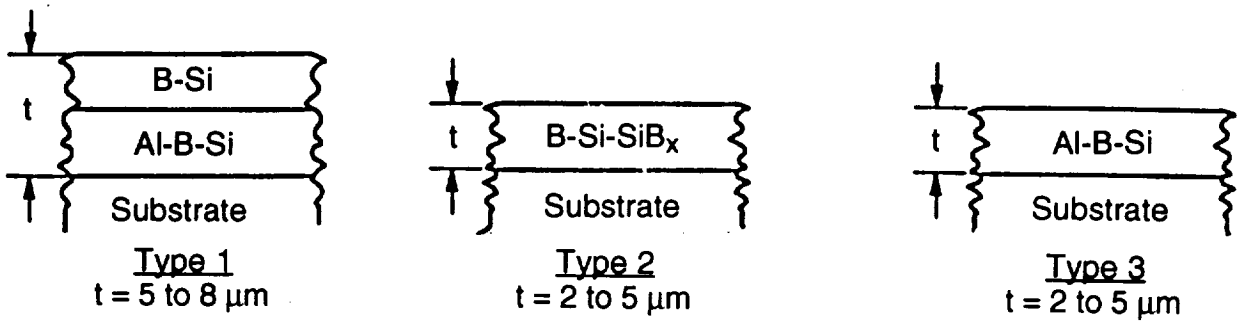

Coating Weight = 7 to 35 g/cm^2

Figure 2. Schematic representation of the coating constructions.

hexaboride sublayer applied directly to the substrate as a finely divided dispersion of submicrometer size particles. The boron-silicon outer layer is then applied by CVD. The single-layer constructions are designated Types 2 and 3. For Type 2, the layer composition may be made boron rich so that a nominal hexaboride-like composition is formed in-situ during a post-coating heat treatment.

The outer layer of boron-silicon composition was chosen to provide the low-recombination-efficiency surface. Upon oxidation, the boron-silicon layer becomes similar in composition and structure to a borosilicate glass which has been reported to have the lowest level of efficiency for the recombination of atomic oxygen on its surface (Ref. 8). Aluminum was added to the boron-silicon sublayer of the Type 1 coating and to the Type 3 coating to improve oxidation resistance and susceptibility to thermally induced stress cracking. Aluminum in the coating is believed to occupy vacancy sites which would otherwise be available for oxygen transport, as well as forming aluminum oxide in the lattice, which impedes ion migration. Aluminum increases thermal expansion of the coating to be more compatible with the substrate. It also forms a lower melting temperature eutectic with both boron and silicon which permits some flow at operating temperature to reduce probability of cracking. The addition of aluminum was also found to increase the thermal emittance of the surface.

The definition of recombination efficiency as used in the context of this research is the measure of the heterogeneous catalytic activity on the rate at which the recombination reaction proceeds from the lowering of the activation energy of the rate-determining step of the overall reaction. The generally accepted reaction mechanism for the recombination of atomic oxygen at a surface follows two steps, which are:

$$\text{Step 1: } O\ (\text{gas}) + e^-\ (\text{solid}) = O^-\ (\text{adsorbed})$$

$$\text{Step 2: } O^-\ (\text{adsorbed}) + O\ (\text{gas}) = O_2\ (\text{gas}) + e^-\ (\text{solid})$$

where the second formula gives the rate-determining step.

The order of recombination efficiency data for surfaces, from a purely electronic material standpoint, is that insulators are the lowest followed by n-type semiconductors and then p-type semiconductors. Experimental data obtained in the temperature range of 300 to 800 K for pure compounds (Refs. 2 and 9) show that recombination efficiency increases from the 10^{-4} range to the 10^{-2} range as we go from:

Pyrex<SiO_2<Al_2O_3<Cr_2O_3<FeO<TiO_2<V_2O_5<Fe_2O_3<Co_3O_4<NiO<CuO<MoO,

which takes us from insulator to p-type electronic behavior.

The insulator provides the lowest value of the recombination efficiency because the gas-phase atom is only physically adsorbed at the surface and there is no electron transfer. This is the lowest bond energy reaction, as it is dependent on the van der Waals dipole/dipole effect. The activation energy is very low, on the order of 0.2 eV. Thus, thermally induced desorption of the atom readily occurs at the surface temperatures experienced in the hypersonic application, and the probability of collision of an incident neutral atom with an adsorbed atom is very small. Considering the rate-controlling Step 2, above, the number density of O^- (adsorbed) is small. The physisorbed atom vibrates from thermal excitation in the shallow potential well, and it is easily displaced from the surface. Lifetimes of physisorbed species are typically 10^{-8} s at a temperature of 300 K and 10^{-11} s at 1000 K. Surface coverage is low, and the O^-(adsorbed) term of Step 1 becomes the rate-controlling mechanism.

Adsorption on semiconducting surfaces is by ionosorption, as the surface provides for electron transfer. The p-type semiconductor is dependent upon hole exchange between the valance band, which increases the electronic conductivity of the solid. The Fermi levels of p-type materials are relatively low, which accounts for a low energy level to the released electron. This decreases the activation energy for the donor reaction of Step 2. Because of the exchange with the valance band, the activation energy for the rate-controlling reaction is low, and there is a high coverage of the surface with atomic species such as oxygen or nitrogen. For n-type surfaces, where there is a wide band gap and electron transfer is with the conduction band, there is a lower coverage of the surface with adsorbed atomic species. Also, the activation energy is higher because of the higher Fermi level. Chemisorption is the result of the formation of chemical bonds, usually covalent, and this results in the strongest bond energies, on the order of 2 to 3 eV. Desorption as the molecular species does not readily occur, as neither the thermal energy nor the kinetic energy of the incident atom is sufficient to promote the molecular-formation reaction.

The understanding of the catalytic activity of real surfaces is very poor because of the influence of imperfections and defects which alter the adsorption and desorption processes. The contamination of the surface with either higher or lower altervalent ions generally leads to an increase in catalytic activity for oxygen atom recombination. These other ions may come from the substrate and migrate to the surface, or they may be the result of ions present in the boundary layer or of contamination during handling.

2.2 COATING PROCESS

The basic coating process used is low-temperature, low-pressure chemical vapor deposition (CVD) of a hydrogenated boron-silicon alloy film, followed by heat treatment to remove hydrogen and to react the boron-silicon film with the substrate to form a surface bond. The aluminum-boron-silicon coating is formed by physical vapor deposition of a thin aluminum layer over the boron-silicon layer, followed by 1/2 h of heat treatment in vacuum or inert atmosphere. Heat treatment is carried out in the temperature range 1000 to 1300 K. The final processing step, after all coating layers have been applied, is static oxidation of the coating in air at atmospheric pressure at a temperature of 1094 or 1255 K for a period of 1/2 h.

The CVD processing of the boron-silicon film is carried out in either a hot-wall or a cold-wall reactor, shown schematically in Figure 3. In the cold-wall reactor only the substrate is heated, and in the hot-wall reactor the entire deposition region of the apparatus is heated. In both cases the reactants flow in the laminar regime over the substrate, whose surface is parallel to the direction of flow. The hot-wall reactor offers the advantage of simultaneously coating all surfaces of a specimen suspended in its nearly isothermal environment. The cold-wall reactor requires two coating runs because one surface of a specimen is in contact with the heating platen. The cold-wall reactor is more adaptable to large parts because it is not necessary to heat the entire chamber. The flow and controls system for the reactors is shown in Figure 4. Typical operating conditions are a chamber total pressure of 300 Pa and a substrate temperature of 600 K. The composition of the reactants is 2 vol % SiH_4 and 1 vol % B_2H_6 with the balance hydrogen.

2.3 SAMPLE PREPARATION

Test specimen substrates were either die-stamped or machined to the shape and dimension required for each test. Specimens for reentry simulation (HYMETS), thermal shock, water immersion, hydrogen exposure, and cyclic-oxidation tests were 0.0254-m-diameter disks. Fatigue specimens were rectangular bars 0.0127 m wide by 0.102 m long. TGA specimens were 0.015 m long by 0.010 m wide.

The substrate materials were prepared using the following steps:

- Vapor degrease
- Rinse with deionized water
- Etch with hot HF/HNO_3 (50% HNO_3, 3% HF)
- Rinse with deionized water and ethyl alcohol and hot-air dry

The cleaned specimens were stored in a dessicator prior to coating.

Type 1 and Type 2 coatings were applied to specimens of all four substrate materials. The Type 3 coating was used only on the alpha2 material. A summary of the coating/substrate combinations, the types of tests, and the number of specimens prepared for each test is given in Table 1.

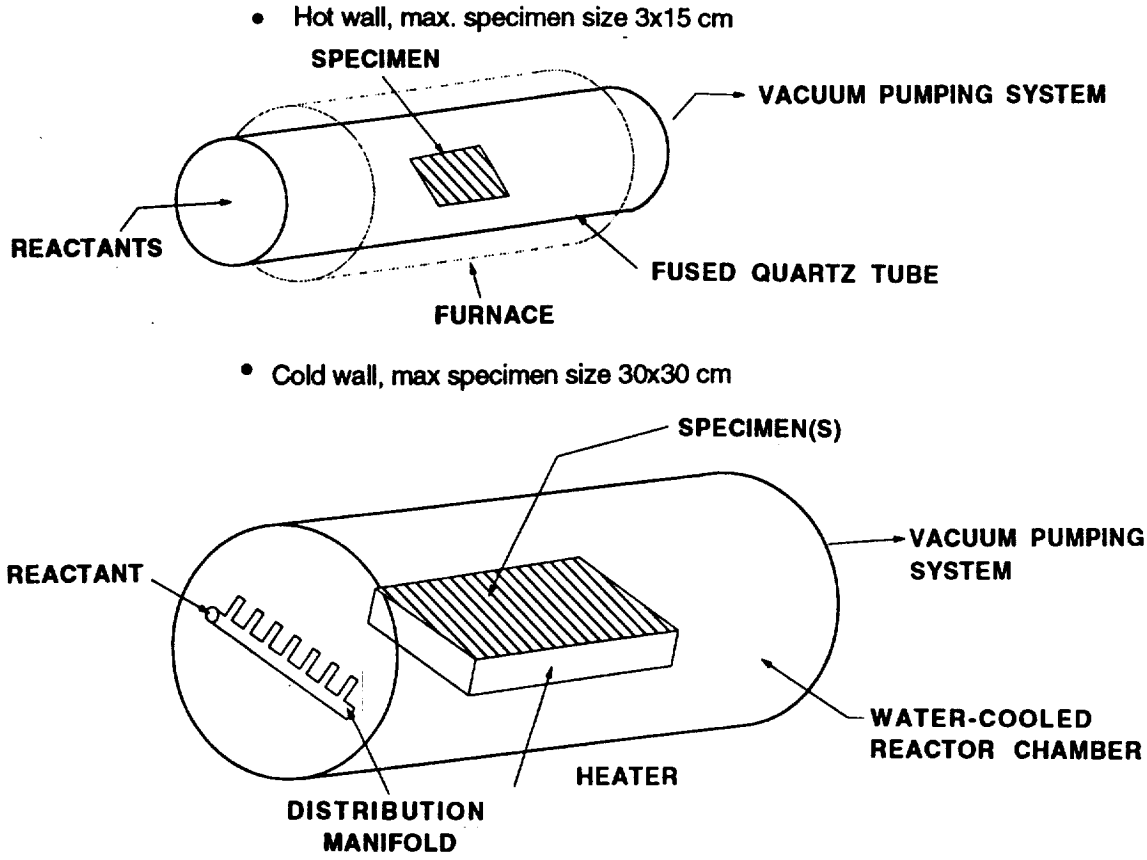

Figure 3. Schematics of LMSC CVD hot-wall and cold-wall reactors.

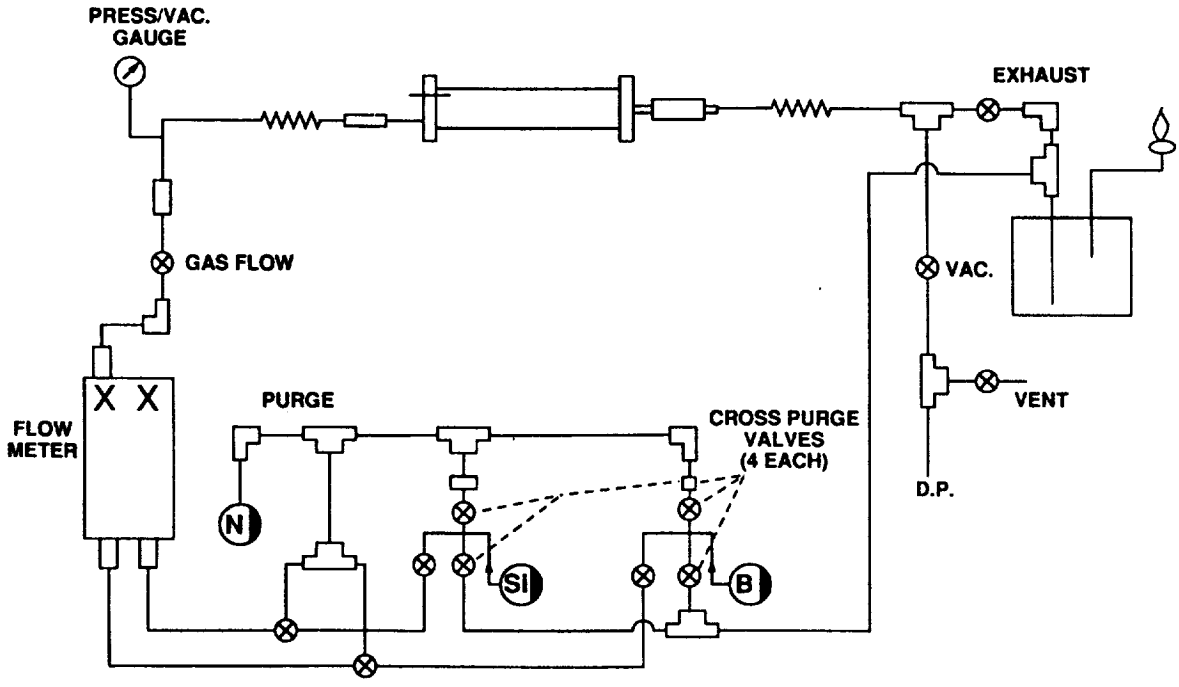

Figure 4. Flow loop and controls schematic for the LMSC CVD reactors.

Table 1. Test Specimen Summary.

	Coating Type					
Ti Alloy	T_1	T_2	T_{2a}	T_3	T_{3a}	T_{3b}
alpha2 Ti-14Al-21Nb	10 HY, 1 Ts, 1 Bw, 9 F 20 TGA	—	4 HY	4 HY 1 SO	2 HY	2 HY
super alpha2 Ti-14Al-23Nb-2V	7 HY, 1 CO, 2 Bw, 2Ts, 5 F	1 HY	—	—	—	—
gamma Ti-33Al-4Nb-1 Ta	3 HY 5 TGA	1 HY	4 F	—	5 F	—
beta21S Ti-15 Mo-3Al-3 Nb-0.2 Si	1 HY	1 Bw, 4 HY 1 Ts, 11 F	—	—	—	—

Notes: Numbers represent number of samples in each type of test.

Test Type: TGA = Thermogravimetric analysis, HY = HYMETS, Ts = Thermal shock, Bw = Boiling water, SO = Static oxidation, CO = Cyclic oxidation, F = Fatigue

2.4 PROCESS SCALE-UP

The feasibility of using the LMSC CVD process for coating large panels, up to 2 m by 4 m, was the subject of a brief study. The coating of panels up to a 2 m maximum dimension is well within the current state of technology for this type of process. Since 1988, CVD processing has been used for coating mirrors up to 2-m diameter. Estimated cost for a reactor for the LMSC process with a 2-m size capability is $500,000 (1992 dollars). In order to achieve coating uniformity over large planar areas, a plasma-assisted CVD process is desirable. This approach greatly reduces the problems that are encountered in conventional reactors with substrate temperature uniformity and reactant flow nonuniformities in mass flux and composition at the substrate surface.

It is believed that additional reactor technology development will be required to permit coating of parts as large as 4 to 5 m. Very large reactors are used in the processing of carbon-carbon structures; however, contamination problems and

process control are not as critical in that application. The LMSC coating does not require the stringent compositional control needed in the semiconductor industry, but it does approach their needs for control of temperature, pressure, and reactant concentrations. The principal technology advancement requirement is in the area of flow modeling and the application of the results to hardware. A final concern with the large-scale application of the LMSC coating lies with the quantities of diborane, a hazardous material, which are associated with the large-scale processing. Costs of suitable handling facilities for this chemical may be very high.

Section 3
EXPERIMENTAL APPARATUS AND PROCEDURES

The primary experimental facility used to evaluate the oxidation resistance and thermal control properties of the coatings was the Langley Research Center Hypersonic Materials Environmental Test System (HYMETS). The HYMETS is a 100-kW hypersonic arc-plasma-heated wind tunnel. This apparatus provided a simulation of the earth ascent and reentry environments under conditions of exposure to high-temperature dissociated air with supersonic flow conditions. The simulation of the broad range of Mach numbers and altitudes encountered by hypersonic vehicles is not achievable in ground-test facilities. However, as the use-temperature limitations of the titanium-aluminides and titanium alloys are dictated by their mechanical properties, the simulation tests were conducted under a set of environmental conditions that would produce these maximum materials temperatures to evaluate oxidation resistance, recombination efficiency, and thermal emittance. Additional test facilities were used to provide preliminary screening data for oxidation resistance in static air, hydrogen transport through the coatings, effects of coating on fatigue life of the metallic substrates, and limited environmental conditions of thermal shock and water exposure. Table 2 lists the properties measured, the type of test exposure and the test apparatus used for each.

Table 2. Summary of Properties Measured, Type of Exposure, and Test Apparatus.

Property Measured (Method)	Test Exposure	Test Apparatus
Oxidation Resistance (Weight Change)	Static Air: 100-h isothermal, 100 cycles 300 K to max temp. dynamic, supersonic flow	• TGA at atmos. and low-pres. • Furnace at atmos. pres. • HYMETS
Recombination Efficiency (Energy Balance)	1 to 10 h in 1/2-h cycles	HYMETS
Spectral Normal Emittance (Integration of Room Temp. Spectral Reflectance Data)	Static oxidation, HYMETS, and thermal shock/water immersion	Integrating sphere and heated cavity spectral reflectometers
Fatigue Life (Bending, + to − Stress)	Room temp. after coating and static oxidation	Cantilever-beam cyclic bending apparatus
Hydrogen Resistance (Volume Change to Maintain Constant Pres.)	Hydrogen at 1094 K temp. and a constant pres. of 6 kPa	Constant pres., isothermal exposure chamber
Thermal Shock (Recombination Efficiency Meas.)	Drop from furnace at 1255 K into liquid nitrogen	HYMETS
Water Immersion (Recombination Efficiency Meas.)	Boiling distilled, deionized water for 24 h	HYMETS

The ascent/reentry simulation tests were conducted in HYMETS. Spectral room-temperature near-normal reflectance was measured on specimens during HYMETS

testing. Oxidation-resistance studies using a thermogravimetric apparatus (TGA) were also carried out by NASA. The other testing and compositional and morphological analyses of the coatings were conducted at the Palo Alto Research Laboratory of LMSC.

3.1 OXIDATION RESISTANCE

Two types of test apparatus were used to evaluate oxidation performance. One was an isothermal exposure in a TGA using dry air at both atmospheric and reduced pressure. Weight change was measured continuously during the tests, which were of 24 to 100 h duration. The second type of test was cyclic, with the specimen alternately heated and cooled between ambient and the maximum temperature. Two types of cycles were used. The first was a rapid cycle, during which the specimen was heated in 1 min and cooled in 3 min with a 26-min dwell at the maximum test temperature. The second was a profiled cycle using programmed rates to heat the specimen in 15 min, hold at temperature for 15 min, and then cool to ambient temperature in 15 min. Both cyclic tests were conducted in air at atmospheric pressure. The specimens were suspended in a fused quartz tube furnace, and room air, heated to the test temperature, flowed past the specimen in the furnace at a velocity of 3 m/min. The specimen was removed from the furnace periodically for weighing. A second control specimen, instrumented with a platinum/platinum-rhodium thermocouple, was located in the furnace adjacent to the test specimen for temperature determination.

Test specimen dimensions were 0.01 m by 0.015 m for the TGA and 0.0254 m in diameter for the cyclic tests. The specimens were kept in a desiccator prior to the initial weight measurement. For the cyclic tests, they were placed in a desiccator after removal from the furnace, then weighed and returned to the desiccator until they were reinstalled in the furnace. Specimens were weighed with a balance having an accuracy of 3 μg. Weight change data are reported in terms of weight per unit area of the specimen with a measurement accuracy of 0.40%.

3.2 REENTRY SIMULATION (HYMETS)

Specimens are exposed to simulated hypersonic flight conditions in the HYMETS facility, which uses air plus nitrogen and oxygen in ratios equivalent to air. The test system consists of a segmented constrictor arc heater, test chamber with three insertion stings and a continuous-duty vacuum pumping system. High-purity nitrogen is introduced at the downstream end of the cathode and is heated in the arc section. High-purity oxygen and air are introduced into the plenum and mixing chambers between the arc section and the downstream hypersonic nozzle. The nozzle discharges into a test chamber that contains a diffuser which is linked to a mechanical pumping system.

The test specimen is mounted in a stagnation model adapter attached to an insertion sting. The specimen is instrumented with a single platinum/platinum-rhodium thermocouple (10-mil diameter) spot welded to its rear face at the center. An

insulator of high-temperature fibrous ceramic material, LI2200, is placed at the rear surface of the specimen to reduce heat loss to the holder. A water-cooled heating rate and pressure probe that measures the catalytic cold-wall heating rate and surface pressure is mounted on a different insertion sting. Figure 5a shows schematically the test system and specimen position in the test chamber. Details of the mounting of the specimen in the model holder are shown in Figure 5b.

As discussed earlier, the range of test conditions available in HYMETS does not fully simulate hypersonic flight. However, the heating rate in the presence of high-velocity dissociated air species is the parameter most critical for evaluating the response of the coated metals in hypersonic flight. The boundary layer is almost fully dissociated oxygen (>95%) with a fraction of dissociated nitrogen (Ref. 10). The range of test conditions used for this study is given in Table 3.

Table 3. Range of HYMETS Test Conditions.

Mach Number	3.9 to 4.1
Wall Pressure	525 to 850 Pa
Enthalpy at Boundary-Layer Edge	3.5 to 10.0 MJ/kg
Boundary-Layer Edge Temperature	1500 to 3100 K
Cold-Wall Heating Rate	60 to 425 kW/m^2
Degree of Equilibrium Dissociation	
Oxygen	0 to 95%
Nitrogen	0%

Specimens are subjected to half-hour tests at conditions to produce the desired surface temperature. For each test, the operating conditions of HYMETS and the fully catalytic heating rate are recorded. The fully catalytic heating rate is measured with a silver slug calorimeter which has a catalytic efficiency of 0.25 (Ref. 8). Specimens are cooled to room temperature between the half-hour tests. Periodically, specimens are removed from the HYMETS for spectral reflectance and weight measurements.

Recombination efficiency is calculated from an energy balance at the surface. The aerothermal heating to a specimen in hypersonic flow (q_{aero}) is the sum of the convective heating (q_c) and the catalytic heating (q_d), and these heat rates are determined from Goulard's solution for the stagnation-point laminar heat transfer equation for a surface with a finite recombination efficiency (Ref. 11). The aerothermal heating is balanced by the heat absorbed by the specimen (q_{absorb}) and heat rejected from the specimen by radiation (q_{rad}) and conduction (q_{cond}):

$$q_{aero} = q_{absorb} + q_{rad} + q_{cond} \quad (1)$$

where:

$$q_{absorb} = \rho_s c_{p_s} L_s dT/dt \quad (2)$$

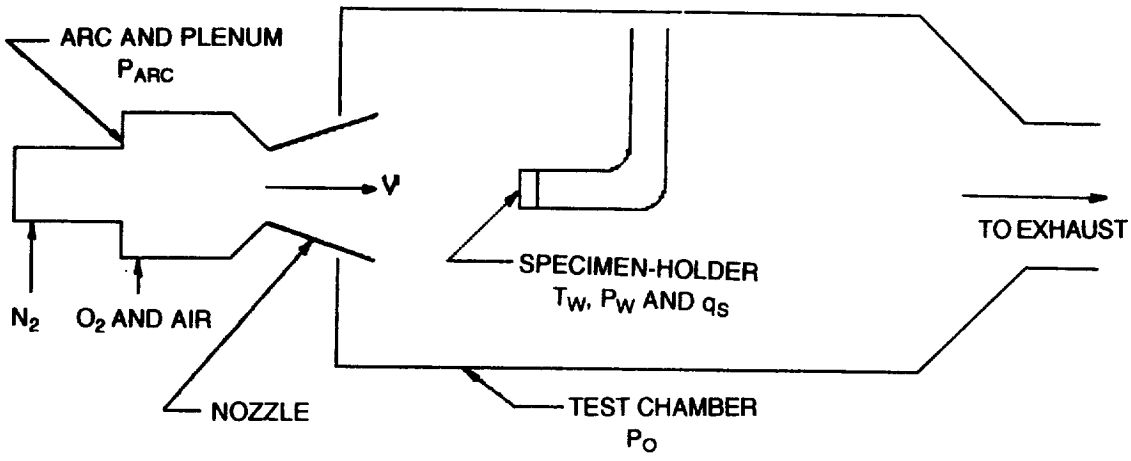

MEASURED TEST PARAMETERS:
- PRESSURES AT ARC CHAMBER, SPECIMEN AND TEST CHAMBER
- TEMPERATURE AT SPECIMEN SURFACE
- CATALYTIC COLD WALL HEATING RATE, q_s
- ELECTRICAL POWER INPUT TO ARC
- MASS FLOW RATES OF GASES INTO ARC AND PLENUM

a. Schematic of HYMETS test facility.

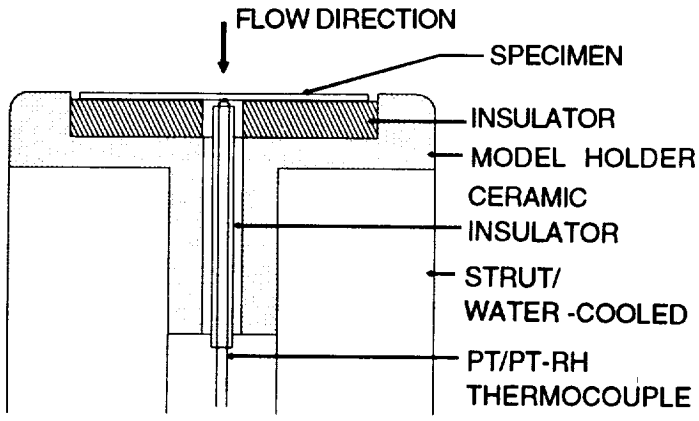

b. Schematic of specimen-holder assembly.

Figure 5. Physical layout of HYMETS test facility and specimen-holder.

$$q_{rad} = \varepsilon_{TH}\sigma T_s^4(1+F_e+F_H) \tag{3}$$

$$q_{cond} = 1.128[\rho_{ins}C_{Pins}k_{ins}(T_s - T_o)dT/dt]^{1/2} \tag{4}$$

for the transient case, and

$$q_{cond} = k_{ins}(T_s - T_b)/L_{ins} + Q_{tc} + Q_{edge\,cond} \tag{5}$$

for the steady-temperature case.

The q_{rad} term of Eq. (3) is made up of three radiation-loss components: the radiative transfer from the exposed surface of the specimen, radiation from the specimen edge, and radiation from the rear of the specimen through the hole in the insulator through which the thermocouple passes (refer to Figure 5b). As the specimen is isothermal and has equal emittance for all surfaces, the latter two terms in this equation are nondimensionalized and appear within the brackets as F_e and F_h for the specimen edge and insulator hole, respectively. The conduction term, Eq. (5), is modified to account for heat losses through the thermocouple leads and its ceramic insulator, Q_{tc}, and gas conduction across the small gap between the edge of the specimen and its holder, $Q_{edge\,cond}$ (see Figure 5b). All of the loss terms must be included for calculation of hot-wall recombination efficiency. The cold-wall recombination efficiency calculation uses only Eqs. (2) and (4) with Eq. (1). As the transient measurement in this case is based on the specimen temperature rise between nominally 300 and 350 K, which takes place in the order of 1 s for the specimens tested in this program, radiation losses from all surfaces of the specimen are insignificant compared to the q_{absorb} term. Also, thermocouple assembly and edge heat-loss terms are negligible.

The influence of specimen-edge and insulator-hole radiation loss and the thermocouple assembly and specimen-edge conduction loss terms, or so-called second-order terms, on the calculation of hot-wall recombination efficiency is significant for low-recombination-efficiency surfaces. As an example, recombination efficiency calculated from actual test data for a Type-2-coated 0.0009-m-thick specimen is 0.013 when the second-order terms are neglected. When the second-order terms are included, the recombination efficiency value increases to 0.019. The test conditions for this case are: Mach number = 4, enthalpy = 8.1 MJ/kg, P_w = 786 Pa, and specimen temperature = 1250 K.

The calculated heating rate from the right side of Eq. (1) and the measured fully catalytic heating rate, q_{aero}, for the same test conditions are used with Goulard's solution to determine the recombination efficiency of the specimen using the relationship:

$$q_{aero} = q_c + \phi q_d \tag{6}$$

where q_c is the heating rate due to convection and ϕq_d is the heating rate resulting from the surface recombination of dissociated boundary layer species. The parameter ϕ is directly related to the recombination efficiency γ from:

$$\gamma = k_w[(2\pi M_{air}) / (R_u T_w)]^{1/2} \tag{7}$$

and,

$$k_w = S / [(1/\phi) - 1] \tag{8}$$

where S is the boundary-layer diffusion rate.

The assumptions for the solution method are: the total flow process is isentropic; the gas is in chemical equilibrium in the arc chamber, free stream, and boundary-layer edge; and the solution to the stagnation laminar boundary-layer equation is valid. The heating to the sample is calculated from the measured specimen temperature, emittance data, and the calculated heat loss parameters, where applicable, using Eqs. (4) or (5), for either a transient or steady-state test. The boundary-layer edge enthalpy is calculated using the heating rate determined by a silver slug calorimeter in Zoby's relationship: (Ref. 12)

$$h_{se} = q_s[(d_{eff} / 2P_w k_{air})]^{1/2} \tag{9}$$

where q_s is the heating rate from the slug calorimeter, d_{eff} is the effective diameter of the blunt body calorimeter, P_w is wall pressure and K_{air} is the dimensionless stagnation-point velocity gradient. This new value of enthalpy is used in the boundary layer equations to compute a new q_{aero} based on a γ of 0.25 for the calorimeter (Ref. 8).

An iterative procedure is employed to converge the calculated and measured values of q_{aero}. A difference factor F_{diff} is computed from

$$F_{diff} = 1 - (q_c + \phi q_d) / q_s \tag{10}$$

This is used to derive a new value of enthalpy at the boundary layer edge from

$$h_{se}(new) = h_{se}(old) + F_{diff}\left\{q_s[d_{eff} / (2P_w k_{air})]^{1/2}\right\} \tag{11}$$

The iteration process is continued until F_{diff} is 0.00001 or less. The parameters of S, q_c, and q_d are then calculated for the converged value of h_{se} together with the experimental values for T_w and P_w. Finally, the recombination efficiency of the test specimen is calculated using Eqs. (6), (7), and (8), where q_{aero} is the specimen heating rate from the right side of the equality sign of Eq. (1).

An analysis was performed to show the effect of errors in experimental measurements and in the calculations of heat-loss parameters and boundary-layer

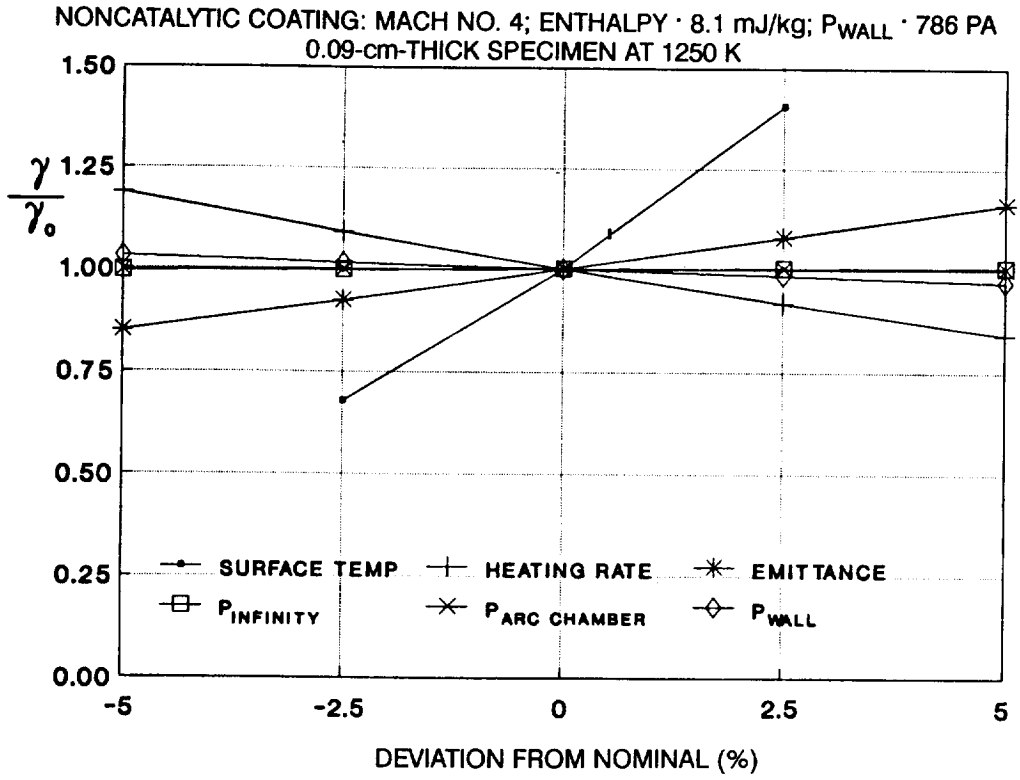

Figure 6. Influence of experimental uncertainties on recombination efficiency.

conditions on the recombination efficiency. The influence of measurement errors on recombination efficiency is shown in Figure 6 for a coating having a nominal recombination efficiency of 0.020. The most sensitive parameter is surface temperature, followed by heating rate, surface emittance, and pressures, in order of decreasing importance. Estimates of maximum uncertainties in measurements of temperature, heating rate, and emittance are 0.50%, 5.0%, and 2.5%, respectively. Pressure measurement accuracies are estimated to be within 5.0%. The maximum uncertainty in recombination efficiency based upon the individual maximum uncertainties is 36.5%, or a recombination efficiency having bounds of 0.013 to 0.027. The contributions of uncertainties in the insulator and second-order heat-loss terms are small. Assuming a 25% maximum uncertainty for each, the maximum uncertainty in recombination efficiency is 0.002 to 0.003 for nominal recombination efficiencies in the range of 0.015 to 0.035.

3.3 EMITTANCE

Room-temperature spectral near-normal reflectance measurements were performed to evaluate the spectral emittance characteristics of the specimens. Spectral normal absorptance of opaque materials is equal to unity minus the spectral normal reflectance, and by Kirchhoff's law, spectral emittance is equal to spectral

absorptance at equal temperatures. The validity of the extension of room-temperature spectral emittance to high-temperature spectral emittance for these types of coatings was established by earlier work (Ref. 2). Total normal emittance is calculated by integrating the spectral data with respect to the Planck blackbody energy distribution function for a given temperature of interest. Again, for these types of coatings, experimental data (Ref. 2) show that the calculated total normal emittance values were within 0.02 emittance units of the actual values measured over the temperature range 1089 to 1367 K. The emittance property required for the data analysis for recombination efficiency is total hemispherical emittance. The ratio of total hemispherical to total normal emittance used was 0.975. This ratio was derived from earlier experimental work (Refs. 13 and 14) done with a number of coated and oxidized metals having a moderate surface roughness.

Spectral reflectance measurements were made using a Gier-Dunkle Model HC-300 heated-cavity reflectometers (Ref. 15) over the wavelength interval 1.5 to 25 μm. A limited number of reflectance measurements were made over the wavelength interval of 0.28 to 2.2 μm using a Varian Cary Model 17 spectrophotometer with an integrating sphere attachment. These data were used to calculate solar absorptance of the coatings.

3.4 FATIGUE

A room-temperature fatigue test was conducted on a series of coated and uncoated specimens of the several substrate alloys to determine if the coating process would seriously degrade the fatigue properties of the base materials. The test approach was to compare the number of cycles to failure for coated and uncoated specimens under the same alternating stress level. The test apparatus used a cantilever specimen 0.1016 m long by 0.0127 m wide, which was clamped at one end over a 0.048-m length. A single strain gauge was bonded to the specimen. The load was applied through a line contact 0.0508 m from the clamping area. An alternating load was applied at a rate of 1 Hz to give a plus and minus deflection of equal amplitude to the beam. One cycle consisted of a stress from zero to a positive value then through zero to an equal negative value and return to zero. The 1-Hz cycle rate did not produce any measurable temperature rise in the specimens. Five specimens were tested simultaneously.

The beam deflection was set to produce a stress level nominally 50% of the yield stress of a material, based upon literature values. The actual stress was determined by strain-gauge measurements. Specimens were cut from sheet stock, the edges were milled and finished with fine sand paper, and thickness was measured with a micrometer.

3.5 THERMAL SHOCK/WATER IMMERSION

A thermal shock test was conducted on coated specimens prior to testing in HYMETS. The test consisted of dropping the specimen from a furnace at either 1094 K (beta-21S) or 1260 K into a dewar of liquid nitrogen. The specimen was first weighed, then

placed in the furnace for 15 min, after which it was dropped into the liquid nitrogen. Upon removal from the dewar, the specimen was allowed to warm to room temperature. It was then weighed and examined for evidence of spallation or crazing of the coating. Finally, the specimen was exposed in HYMETS for 1 h (two 1/2-h cycles) to measure recombination efficiency.

The water immersion test consisted of suspending a specimen in incipient boiling distilled and deionized water for a period of 24 h. The specimen was weighed before and after the test and examined visually for any evidence of coating failure. The specimen was then subjected to a 1-h HYMETS test.

3.6 MORPHOLOGY AND COMPOSITION ANALYSES

Morphological characteristics of surfaces of the coatings were studied using scanning electron microscopy (SEM). Cross sections of the coating-substrate region were examined using both SEM and optical microscopy. Compositional analysis of coating surfaces and coating-substrate cross sections were performed using energy dispersive analysis of x-rays (EDAX) and, to a limited extent, Auger electron spectroscopy (AES). Compositional analyses were qualitative in nature.

3.7 HYDROGEN EXPOSURE

A 24-h exposure test to low-pressure gaseous hydrogen at a temperature of 1094 K was used to obtain a qualitative measure of the degree of protection against substrate hydrogen pickup provided by a coating. The test apparatus consisted of an exposure chamber 0.076 m in diameter by 0.102 m long which was placed in a furnace maintained at a temperature of 1094 K. The exposure chamber was connected to a hydrogen reservoir having a volume of 1×10^{-3} m by a 0.006-m-diameter tube. The hydrogen reservoir was external to the furnace, and it was maintained at a constant temperature of 310 K. A mass flow meter calibrated for hydrogen was located between the reservoir and the hydrogen gas supply. The system was connected to a vacuum pumping station for the evacuation of the entire system. Pressures were measured for the exposure chamber, reservoir, and supply gas using capacitance gauges. Temperature was measured with a thermocouple spot welded to the exterior of the exposure chamber. The specimen was suspended from a fused quartz rod in the chamber.

A specimen was placed in the chamber, and the system was evacuated to 1 Pa. The exposure chamber was brought up to the test temperature with the vacuum pump operating. Vacuum was maintained for 2 h at temperature. The system was then filled with hydrogen at a pressure of 3 kPa, and this pressure was maintained for the 24-h test period by admitting gas into the reservoir. The mass of hydrogen required to hold constant reservoir pressure was assumed to be that picked up by the specimen.

Section 4
EXPERIMENTAL RESULTS

The applicability of the coatings for use in hypersonic vehicle heat shields and hot structures was evaluated on the basis of the results of a series of experiments to measure the oxidation protection provided to the candidate heat shield and structural materials and the thermal control properties, total emittance, and recombination efficiency of the coatings over the useful temperature range of these materials. The stability of these properties for long life and multiple flight cycles was a major aspect of the experimental program. Experiments were also conducted to determine if the coating process conditions will degrade the mechanical properties of the structural materials. Hypersonic flight simulation tests using the HYMETS provided data for recombination efficiency and primary data for emittance properties. Limited oxidation protection data were also derived.

4.1 OXIDATION PROTECTION

The oxidation protection provided by the coatings was assessed by measuring the weight change of coated specimens of each of the titanium-aluminides and the beta-21S alloy. This method is semiquantitative for the CVD coatings, because they are only partially oxidized during the coating process, and the weight gain seen during testing is the result of further oxidation of the coating. Compositional analyses of cross sectioned specimens were made to look for oxygen in the substrate adjacent to the coating layer. However, these measurements are semiquantitative and cannot detect very low levels of oxygen.

Two types of exposure conditions were used for the investigation of oxidation protection. One is a static exposure in which a specimen is exposed to a flow of low-velocity (0.5 m/s) air. Tests were conducted under both isothermal and cyclic temperature conditions. The second type of test used the HYMETS, where the specimen was exposed to thermally dissociated oxygen in a hypersonic-flow environment.

Weight gains from static-air oxidation tests of Type-1 coated and uncoated alpha2 titanium-aluminide at 1255 K and atmospheric pressure are shown in Figure 7 for both isothermal and cyclic (coated specimens only) tests. Coating thickness is nominally 5 μm in all cases. The weight gain due to complete oxidation of the coating itself is calculated to be approximately 1.5 mg/cm^2. The initial oxidation of the coating for 1/2 h during the final coating processing step typically results in a weight gain of approximately 0.15 mg/cm^2. Thus, the expected weight gain for a fully oxidized coating at the conclusion of the 100-h oxidation test would be 1.35 mg/cm^2. The test data suggest that the coating is only 50% oxidized at the end of the 100-h

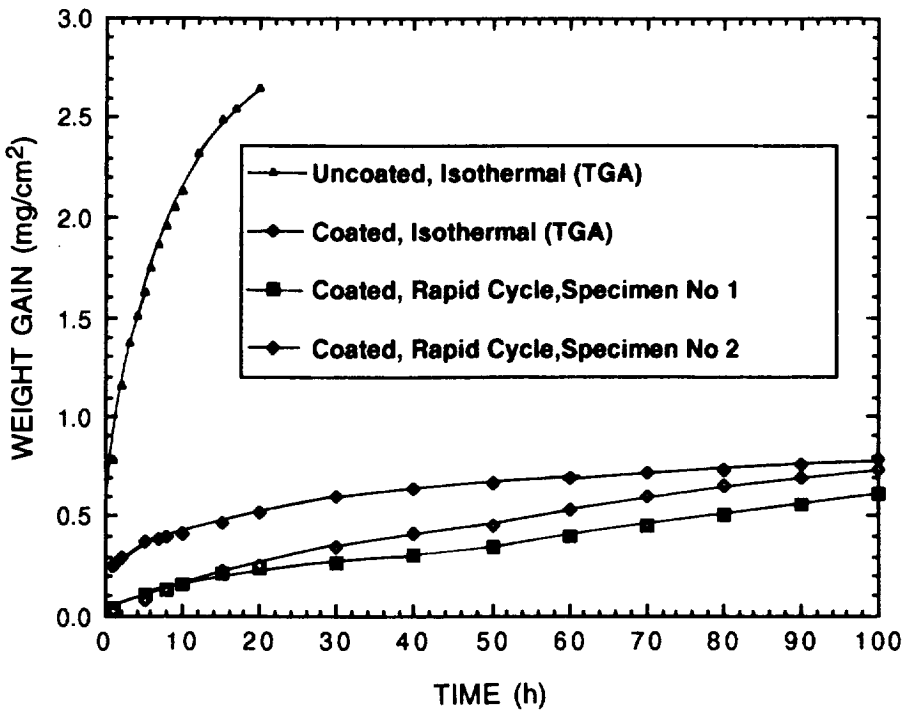

Figure 7. Weight gain data for isothermal and cyclic oxidation tests at 1255 K for uncoated and Type 1 coated alpha2 substrates.

test. Comparing the data at the end of the 20-h isothermal exposure, the weight gain of the coated specimens is only 20% of that of the uncoated material. The isothermal exposure data for a coated specimen show a greater initial weight gain than is observed for the cyclic test. The reason for this difference is not apparent. For the isothermal test, the specimen is maintained at constant temperatures for the entire exposure period. In the cyclic tests, the specimen is cooled to ambient temperature between each cycle. This transient temperature may result is some microspallation of the coating although none was visually detected during a cyclic test. However, at the end of the 100-h exposure, weight gains for isothermal and cyclic tests are essentially the same.

Comparative weight-gain data between rapid-cycle and profiled-cycle tests are shown in Figure 8. Exposure time for the profiled data is calculated as the product of the number of cycles and the time at maximum temperature (15 min) for each cycle. Little difference in weight gain is seen between the two exposure conditions. The slightly greater weight gain for the profiled-cycle tests is probably the result of a longer time near the maximum temperature because of the particular time-temperature profiles used for the heating and cooling portions of the cycle. The weight gain differences seen between Rapid Cycles No. 1 and No. 2 may be the result of some microspallation of the No. 1 specimen coating (which was not observed visually) under the very rapid thermal transient conditions of this test.

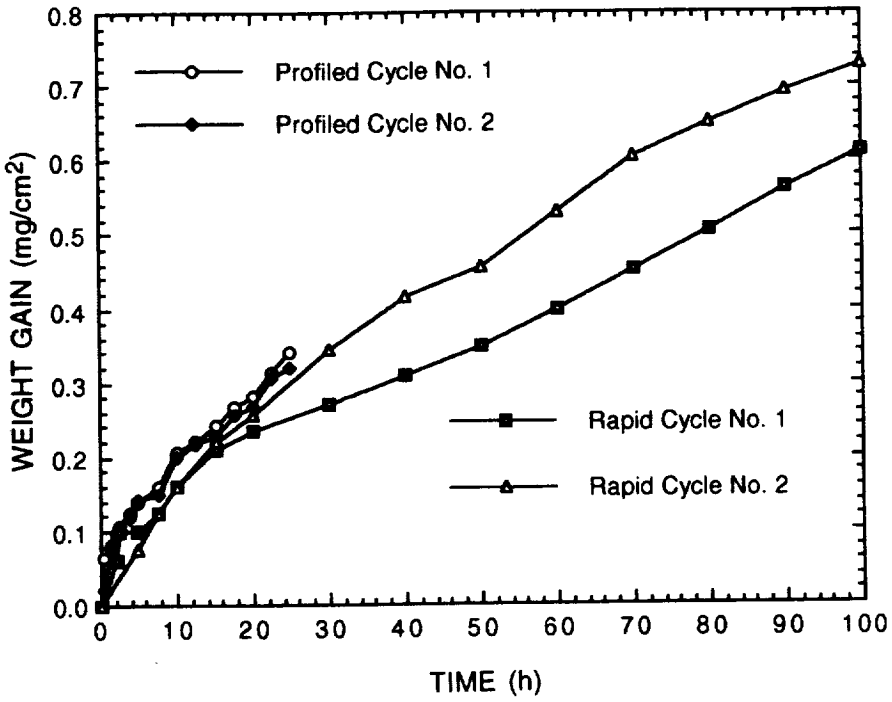

Figure 8. Comparison of weight gain data for rapid- and profiled-cycle oxidation tests at 1255 K for Type 1 coated alpha2 substrates.

Profiled-cycle oxidation data at a temperature of 1255 K for alpha2 and super-alpha2 substrates with the Type 1 coating are shown in Figure 9. The measured weight gains are essentially the same for both substrate materials. The small differences between the two alpha2 specimens and the super-alpha2 specimen may be due to some slight variations in the CVD processing, such as a difference in the silicon-to-boron ratio, or in the amount of aluminum deposited on the sublayer. The super-alpha2 and alpha2 specimens were prepared at different times. Final weight gains correspond to approximately 20% of that of a fully oxidized coating after the equivalent of 25 h at 1255 K. Assuming that the coating oxidation follows a parabolic rate behavior, it would take on the order of 400 to 500 h to fully oxidize the typical Type 1 coating, 5 to 6 μm thick.

Isothermal (TGA) weight gain data at four temperatures for uncoated and Type 1 coated super-alpha2 specimens are shown in Figures 10 and 11, respectively. Weight gain of the uncoated specimens increases exponentially with increasing temperature between 978 K and 1255 K. Little difference in weight gain is seen between temperatures of 922 K and 978 K. Weight gain for the coated specimens (c.f., Figure 11) is essentially equal for temperatures of 922 K and 978 K. However, at a temperature of 1089 K, the weight gain data are significantly less than those observed at the lower temperatures. This behavior may be due to some difference in the mechanisms of oxygen transport within the boron-silicon layer, or it may be related to a surface-controlled oxygen-dissociation reaction. Molecular oxygen incident

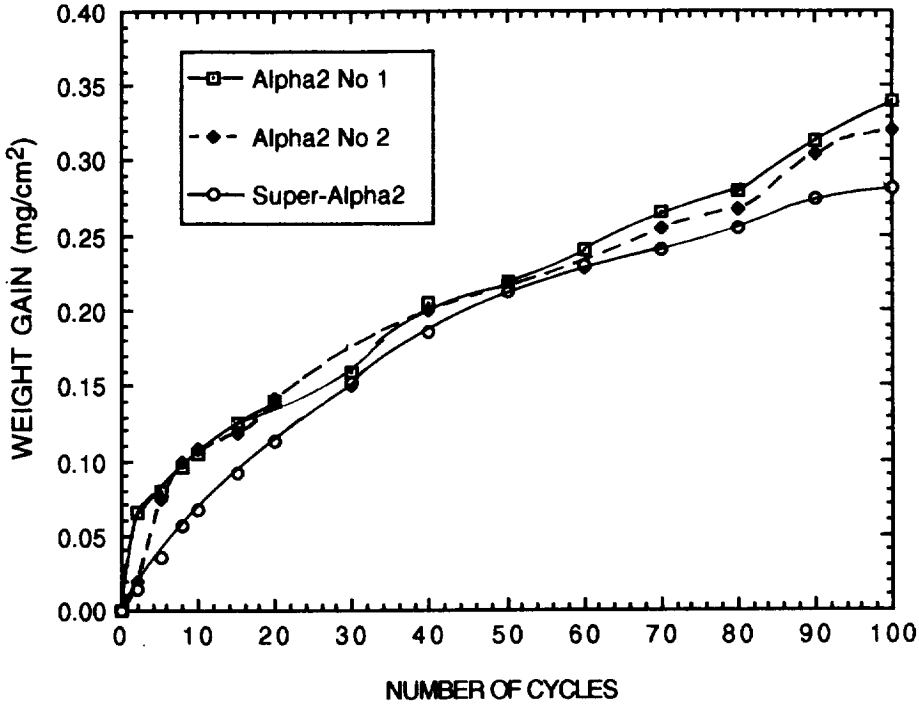

Figure 9. Profiled-cycle oxidation weight gain data for Type 1 coated alpha2 and super-alpha2 substrates at 1255 K.

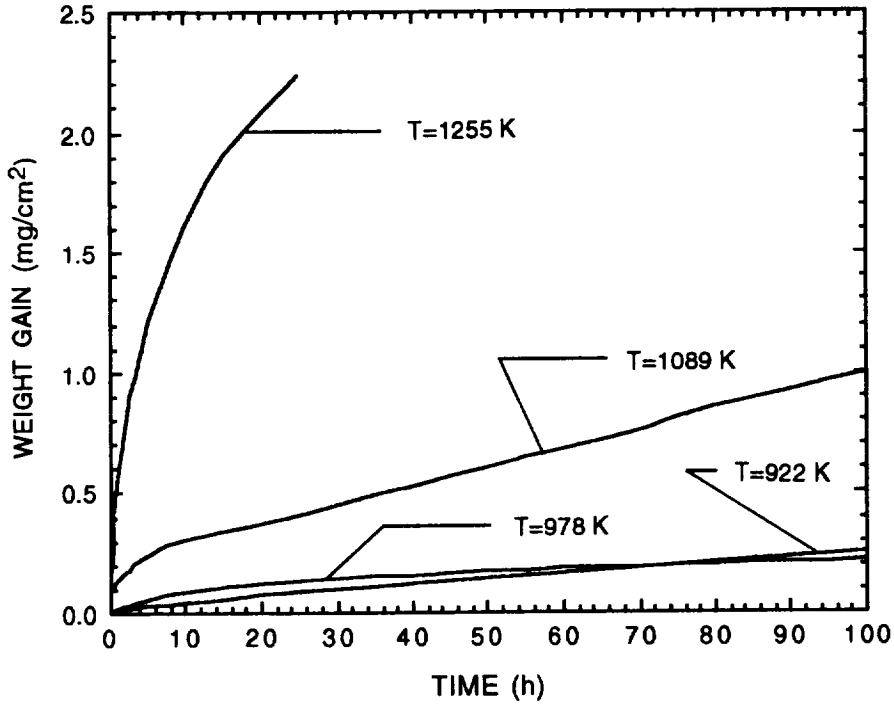

Figure 10. Isothermal (TGA) weight gain data for uncoated super-alpha2 at four temperatures in air at a pressure of 100 kPa.

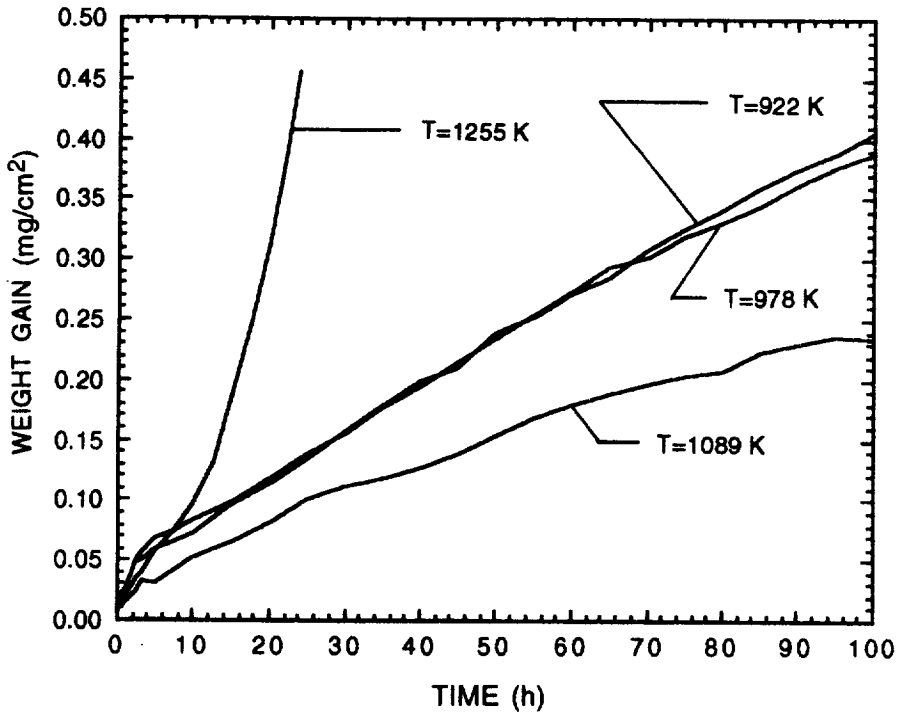

Figure 11. Isothermal (TGA) weight gain data for Type 1 coating on super-alpha2 at four temperatures in air at a pressure of 100 kPa.

on the coating surface must dissociate before it is transported in the coating lattice. The surface may be less "catalytic" in this regard at that particular temperature. This result may also simply be an anomaly for the particular specimen, as only a single set of data was obtained under these conditions. Weight gain at a temperature of 1255 K appears to depend exponentially on exposure time, which is opposite to that seen for the same coating on alpha2 (c.f., Figure 7).

The effect of air pressure at an oxidation temperature of 1255 K is seen from the TGA data shown in Figure 12. Weight gain at low pressure is greater than that at atmospheric pressure for both uncoated and Type 1 coated super-alpha2 specimens. The mechanism for this behavior is not understood at this time. This result suggests that additional oxidation testing should be carried out as a function of pressure as well as temperature.

Weight-gain data for three specimens of the Type 2 coating are compared with similar data for the Type 1 coating in Figure 13. The substrate material is super-alpha2 in all cases, and the test conditions are profiled cyclic oxidation at 1255 K. The greater weight gains for the Type 2 coated specimens may be the result of a more open lattice structure, in the single layer of boron-silicon composition. In the Type 1 coating, the aluminum-boron-silicon sublayer has a tighter lattice structure, which is more resistant to oxygen ion transport. Also, this layer has a thermal expansion coefficient intermediate to those of the substrate and the outer layer,

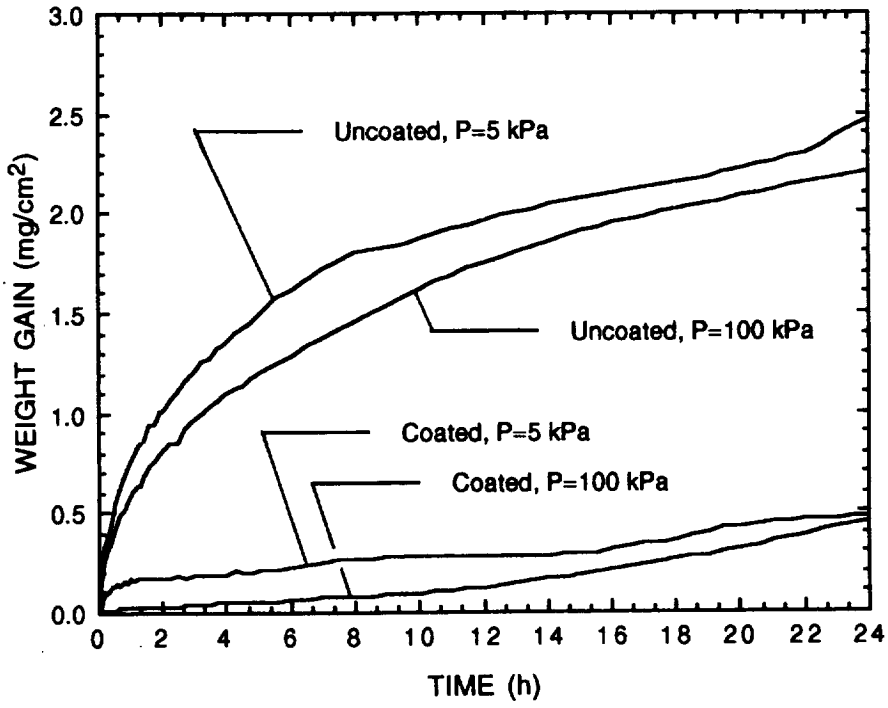

Figure 12. Isothermal (TGA) weight gain data at 1255 K in air for uncoated and Type 1 coated super-alpha2 substrates at pressures of 5 and 100 kPa.

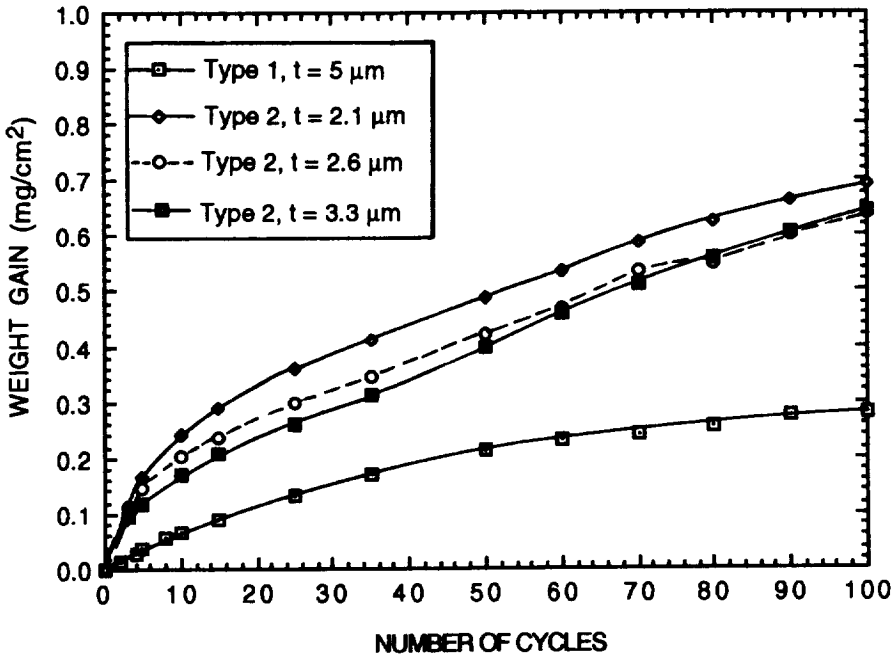

Figure 13. Comparison of 1255 K profiled-cycle oxidation weight gain data for three thicknesses of Type 1 and Type 2 coated super-alpha2 substrates.

which is basically the Type 2 composition. This may serve as a strain moderator which reduces the tensile stress on heating in the low-thermal-expansion outer layer, thereby reducing oxygen transport. The increasing weight gain with decreasing Type 2 coating thickness may be due to a reduction in strain near the surface of this coating with increasing thickness. Fully oxidized Type 2 coating weight gains are estimated to be 0.57 and 0.90 mg/cm^2 for thicknesses of 2.1 and 3.3 μm, respectively. Comparing these values with the test data, there may be some substrate oxygen pickup for the specimen with the thinnest coating.

Weight-gain data for uncoated and Type 1 and Type 2 coated gamma titanium-aluminide from profiled-cycle oxidation tests at a temperature of 1255 K are shown in Figure 14. Weight gain for the Type 2 coating again is slightly greater than that for the Type 1 coating. The weight gain at 100 cycles for the Type 1 coating on gamma is greater than that measured for this coating on both alpha2 or super-alpha2 substrates, 0.60 mg/cm^2 for gamma versus 0.30 to 0.35 mg/cm^2 for the others. No explanation for this difference was found. Weight gain results for the Type 2 coating are similar for all three of the titanium-aluminides.

Weight gain data from profiled-cycle oxidation tests at 1089 K on uncoated and Type 1 coated beta-21S titanium alloy specimens are shown in Figure 15. At the end of the 25-h oxidation period (100 cycles), the oxygen pickup of the coated specimen is 12% that of the uncoated specimen, and it has reached a nearly constant value.

No evidence of coating failures such as crazing, spalling, or delamination was seen visually for any of the oxidation tests. The weight gain in these tests is less than the weight increase calculated for complete oxidation of the coating layers themselves, with the exception of the thinnest Type 2 coating layer tested, 2.1 μm thick, as is discussed above. Oxygen analyses of cross sections of several specimens did not detect the presence of oxygen in the substrates. Elemental profiles of two Type 1 coated alpha2 specimens are shown by Figure 16. The as-coated specimen is shown in Figure 16a and the post oxidation specimen in Figure 16b. After the oxidation test, a depletion of aluminum and niobium is seen in the substrate region adjacent to the coating interface, with titanium migration into the coating. It is postulated that both aluminum and niobium ions migrate to the coating with the titanium. Also, silicon has penetrated into the substrate to a depth of 1 to 2 μm. No evidence of oxygen is seen in the substrate for either case. Cross-sectional elemental analyses were not conducted on specimens of the other alloys as it is believed that migration of aluminum, niobium, and titanium would be similar for the same coating.

Weight-change data were obtained from 22 specimens tested in the HYMETS. Weight measurements were made at time intervals when a specimen was removed from a test for spectral near-normal reflectance measurements. The specimen was reinstalled in the model holder and the test continued. A number of the data sets show a weight loss, which may be the result of coating spallation due to stresses from the severe heating and cooling transients inherent in this type of test. A second possible cause for the weight loss is some coating damage, particularly at the edge of a specimen, during handling for these periodic measurements. Also, the majority of the specimens

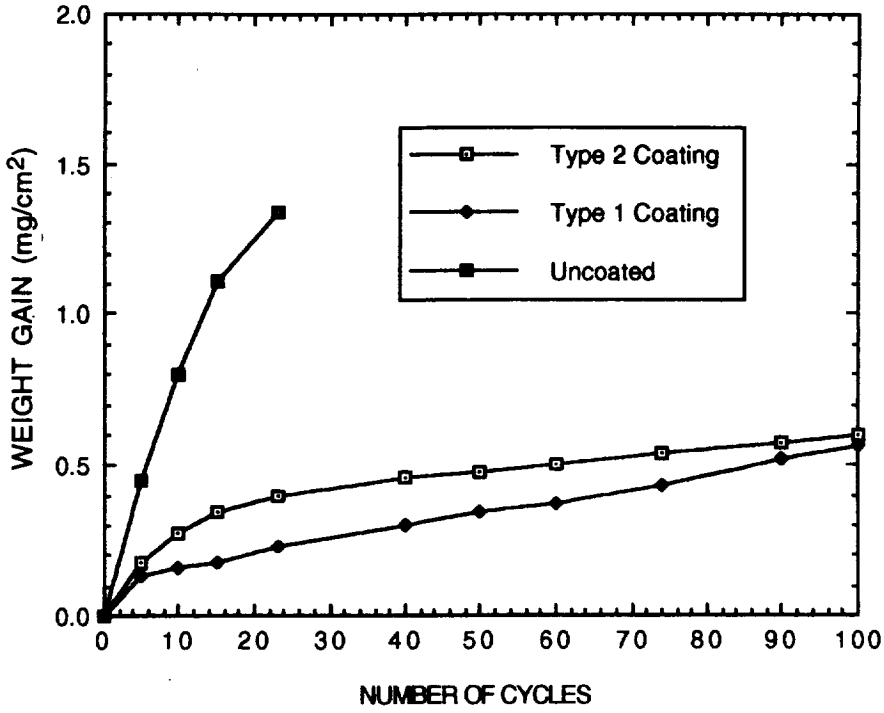

Figure 14. Weight gain data for uncoated and Types 1 and 2 coated gamma in profiled cycle oxidation tests in air at 1255 K and atmospheric pressure.

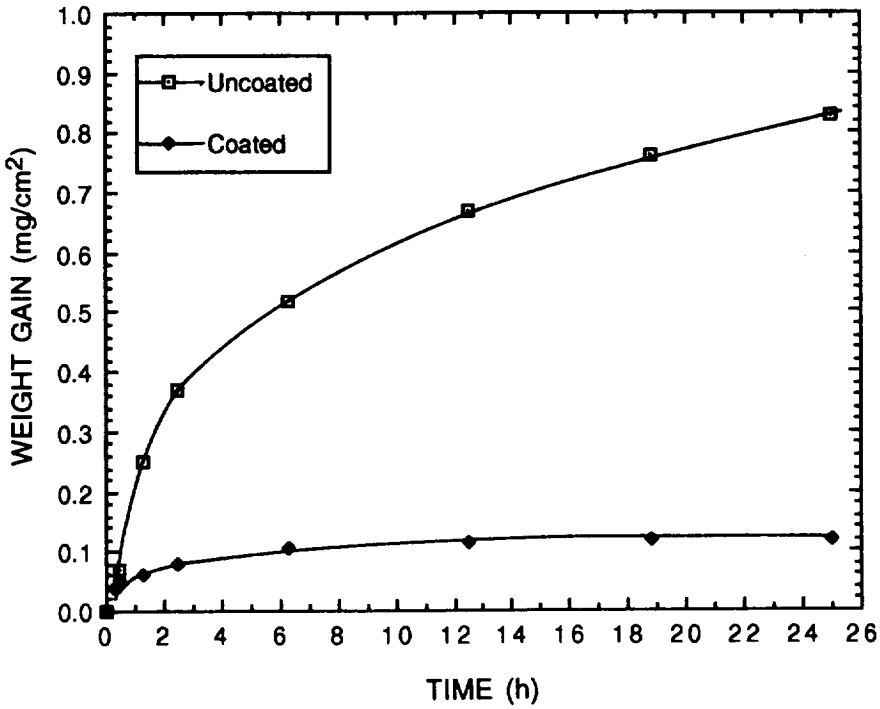

Figure 15. Weight gain data for profiled-cycle oxidation tests at 1089 K for uncoated and Type 1 coated beta-21S substrates.

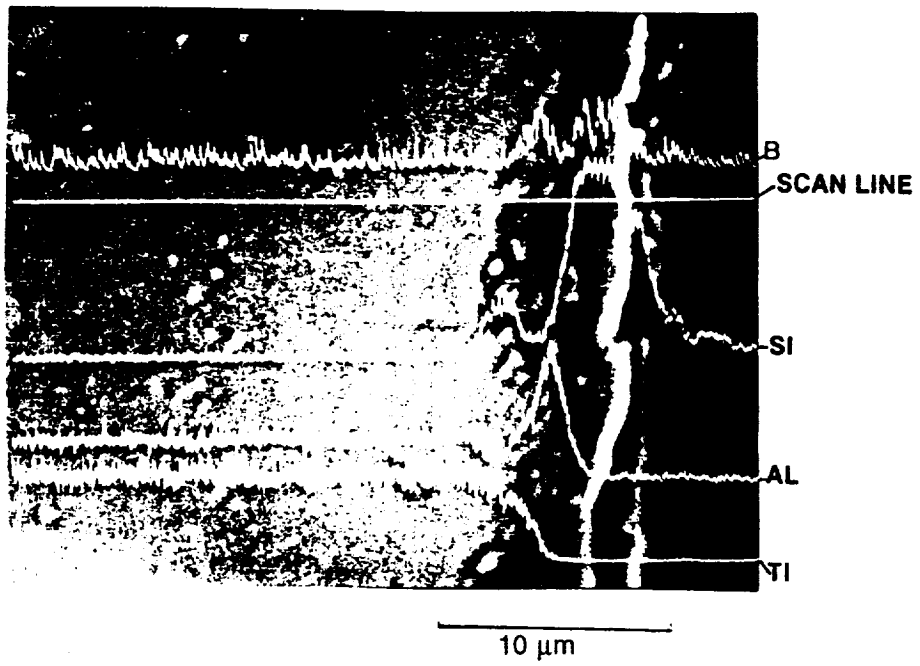

a. As coated.

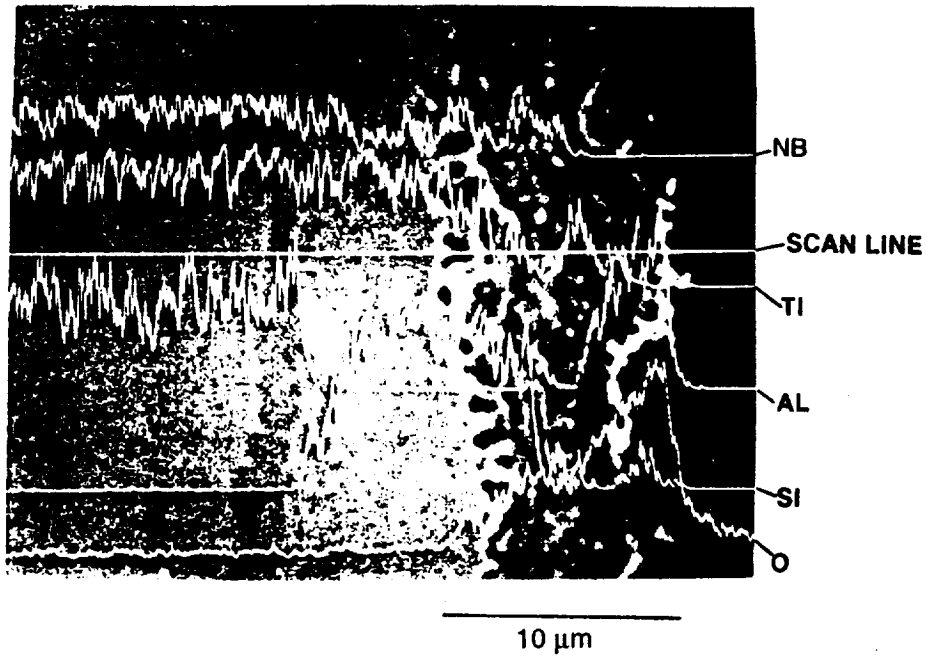

b. After 100 profiled oxidation cycles at 1255 K.

Figure 16. SEM photographs of cross sections of Type 1 coated alpha2 titanium-aluminide as coated and after 100-cycle profiled oxidation test at 1255 K.

were instrumented with a thermocouple for the primary measurement of recombination efficiency. The thermocouple was removed for the weight and reflectance measurements, and then it was reattached to continue the test. Table 4 summarizes Types 1 and 2 coating weight change data for the HYMETS tests. No data were obtained for the Type 3 coating. Nine specimens show moderate to large weight loss, the most severe occurring with specimen NG6, for which the initial coating weight was 0.56 mg/cm^2, but the weight loss is 2.36 mg/cm^2.

Table 4. Summary of Specimen Weight Change Data from HYMETS Tests.

Specimen	Coating	Substrate	Test	Weight Change (mg/cm*2) at Exposure Time (hr)						
Number	Type	Material	Temperature	1	2	4	5	6	8	10
N2	1	Alpha2	1260K	0.214	0.228	-	-	-	-	-
N3	1	Alpha2	1260K	0.067	-	-	-	-	-	-
N5	1	Alpha2	1260K	0.751	-	-	-	-	-	-
N6	1	Alpha2	1260K	-0.114	-	-	-	-	-	-
N9	1	Super-Alpha2	1205K	0.137	0.257	0.385	-	0.367	-	0.312
N11	1	Super-Alpha2	1205K	0.192	0.257	0.302	-	0.174	-	-0.156
N12	1	Super-Alpha2	1260K	-0.110	-	-	-	-	-	-
N14	1	Super-Alpha2	1260K	0.231	0.248	0.183	-	-	-	-
N15	1	Super-Alpha2	1260K	-0.009	-	-	-	-	-	-
N16	1	Super-Alpha2	1260K	-0.267	-	-	-	-	-	-
N1A	1	Alpha2	1205K	0.167	-	-	0.573	-	-	0.714
N2A	1	Alpha2	1205K	-0.567	-	-	-1.516	-	-	-1.346
N3A	1	Alpha2	1205K	-0.161	-	-	-	-	-	-
N4A	1	Alpha2	1205K	0.142	-	-	-	-	-	-
NG2	2	Gamma	1260K	0.056	-	-	-	-	-	-
NG6	2	Gamma	1260K	-	-1.350	-	-1.703	-	-2.225	-2.364
NG3	2	Gamma	1260K	0.307	-	-	-	-	-	-
NG12	1	Gamma	1260K	-	-0.214	-	-0.130	-	-0.559	-0.605
N7(A)	2	Beta-21S	1094K	0.0009	-	0.0094	0.160	-	-	-
N8(A)	2	Beta-21S	1094K	-	0.0000	-	-	-	-	-
NSJR6	2	Super-Alpha2	1260K	-	0.147	-	-0.866	-	-	-
Beta 21S	None	Beta-21S	1094K	0.592	1.034	-	1.673	-	-	-

Weight gain data from HYMETS and profiled oxidation tests of uncoated beta-21S titanium alloy specimens are shown in Figure 17. The solid curve in the figure is the cyclic-oxidation test and the individual data points are HYMETS results. At the conclusion of the 5-h HYMETS test, weight gain is 3 times greater than that measured in the static oxidation test in air at atmospheric pressure. A comparison between HYMETS and static oxidation weight gain data for Type 1 coated alpha2 material is seen in Figure 18. Again, HYMETS test conditions resulted in a significantly greater weight gain than was measured during either isothermal (TGA) or profiled-cycle static oxidation tests. From these limited data, HYMETS appears to be a more energetic oxidation environment. One possible reason is that oxygen which is fully dissociated in the high-temperature boundary layer is incident on the surface. Oxygen atom diffusion in the coating layer is then the rate-limiting reaction. However, in the static oxidation test, molecular oxygen from the environment must first dissociate at the coating surface before oxygen can diffuse within the coating itself. This dissociation reaction may be the rate-limiting reaction to the overall oxygen transport process. Another

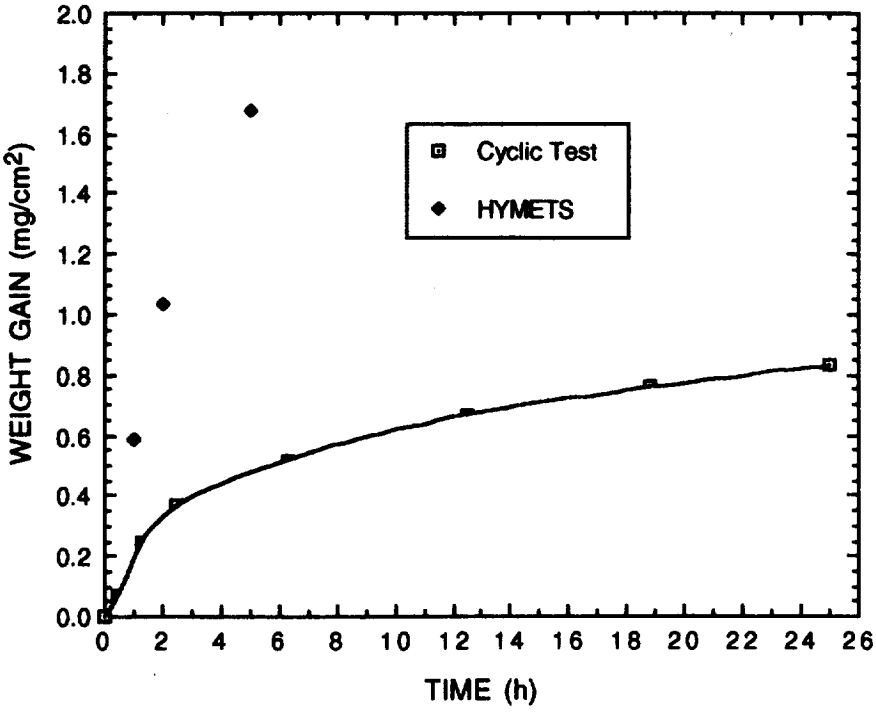

Figure 17. Comparison of weight gain data measured during profiled cyclic oxidation and HYMETS tests at 1089 K for uncoated beta-21S.

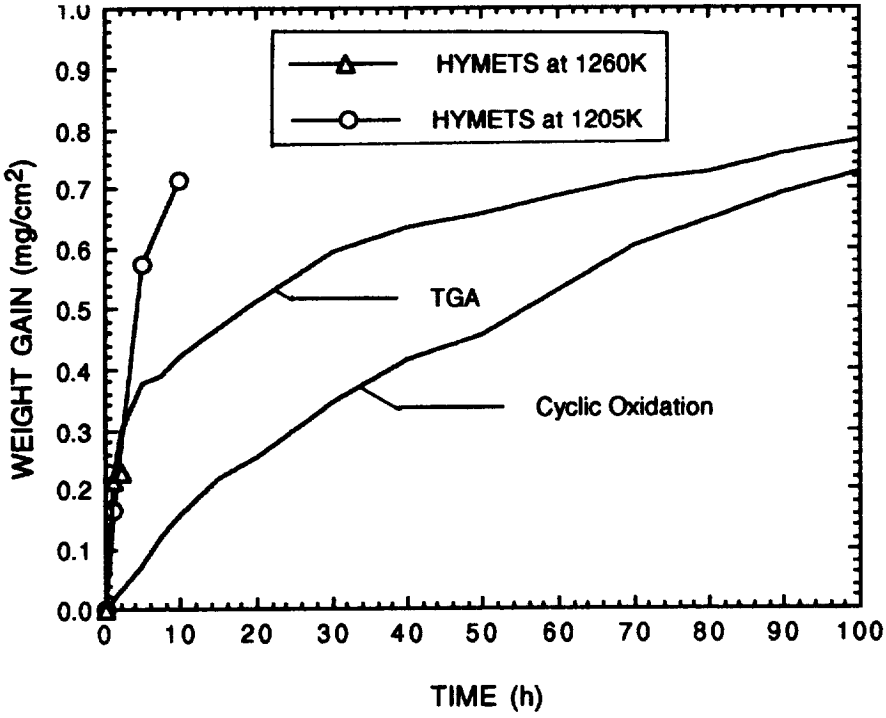

Figure 18. Comparison of weight gain data measured during static oxidation (1255 K) and HYMETS tests for Type 1 coated alpha2.

potential cause for the observed difference in weight gain may be the severe thermal transients experienced by a specimen during a HYMETS cycle.

A comparison of weight gain data for Type 1 coated super-alpha2 measured in both HYMETS and static oxidation tests is shown in Figure 19. Again, weight gains for HYMETS tests up to 4 h of exposure are significantly greater than those observed in the static oxidation test environments. At longer HYMETS exposure times, a decrease in weight is seen. This may be due to some microspallation of the coating with handling or thermally induced stresses. It is interesting to note that the TGA data at a pressure of 5 kPa are closer to the HYMETS data than either the TGA or cyclic-oxidation data at a pressure of 100 kPa. Sufficient data in terms of pressure, temperature, and specimen population are not available to draw any conclusions in regard to the possible reasons for these results.

Final evaluation of these types of coatings for use as exterior surfaces of hypersonic vehicles should be carried out in a test environment which simulates the boundary layer temperature, pressure, and species and their concentrations for hypersonic flight. For interior use of the coatings, the low-pressure static oxidation test is probably an adequate approach for oxidation protection studies.

4.2 RECOMBINATION EFFICIENCY

A total of 38 coated specimens were tested in the HYMETS to measure recombination efficiencies of the three coating types with four substrate materials. Of this lot of specimens, 13 were exposed for 5 h and 7 were exposed for 10 h. The tests were

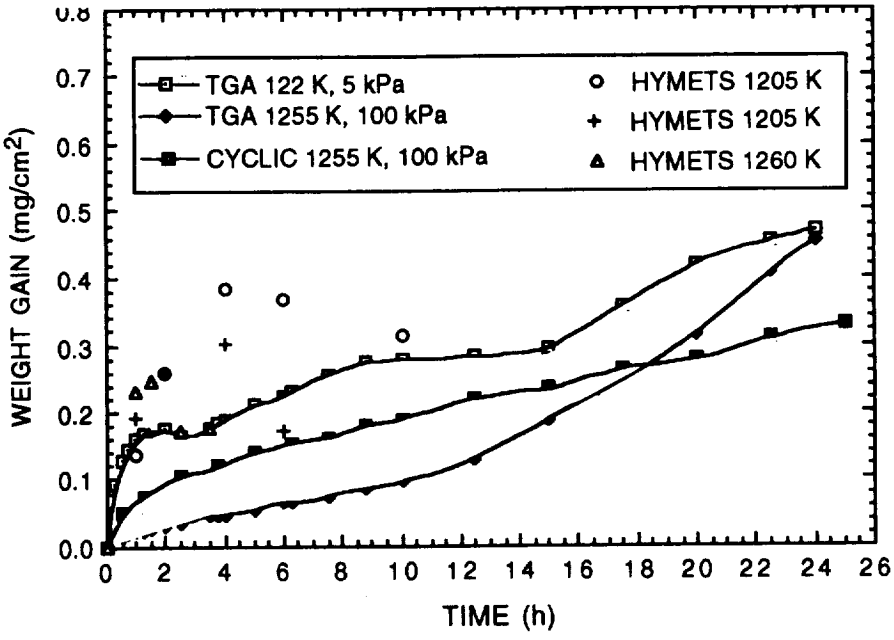

Figure 19. Comparison of weight gain data from HYMETS and static-air oxidation tests at two pressures for Type 1 coated super-alpha2.

conducted in cycles of 1/2 h in the hypersonic flow stream followed by 1/2 h out of the flow. Coated alpha2 and super-alpha2 specimens were tested at temperatures of 1205 K and 1260 K, gamma specimens at 1260 K, and beta-21S specimens at 1089 K.

Recombination efficiency data are summarized in Table 5. The data shown for the hot-wall recombination efficiencies are derived from smoothed values of the individual data points plotted as a function of exposure time. For many of the tests, there appear to be anomalous points which are not consistent with the overall trend in change in recombination efficiency with time. As discussed in Section 3.2, the uncertainty of the recombination efficiency value is estimated to be 0.007. Also, it is to be emphasized that these data in the absolute sense are valid only for the HYMETS hypersonic-flow conditions, and they should not be used for actual vehicle design. However, the data are valid for comparing performance of the various coatings and for ranking their effectiveness, as the precision of the measurement of recombination efficiency is estimated to be 0.004. Data for each test are given in detail in Appendix A to this report.

Results of post-test surface analysis of a number of the specimens are summarized in the last column of Table 5. It should be noted that for all of the tests of the beta-21S specimens, copper was detected on the surfaces. This apparently is from arc electrode contamination of the stream at the operating conditions required to maintain the lower maximum use temperature, 1089 K, for this material. Tungsten was also present on three of these specimens. Iron was detected on two specimens, one which was tested at 1260 K. The source of this element is not known. Finally, calcium was present on several specimens. This is believed to be from water contamination which probably occurred during the spectral reflectance measurements. Titanium and niobium were detected near the surface for most of the specimens analyzed. Detection depth of EDAX used for the analysis is on the order of 1 μm, so the results are not indicative of the actual surface by itself. However, one assumes there is a continuous elemental profile gradient in the region near the free surface, and when an element is detected by EDAX, that element is assumed to be present on the surface. The presence of niobium and titanium compounds is believed to increase catalytic efficiency.

A comparison of hot-wall catalytic efficiency as a function of HYMETS exposure time at a temperature of 1260 K for the three basic types of coatings on alpha2 substrates is shown in Figure 20. These values are the average for multiple specimens. The Type 3 coating, which includes aluminum in its composition, was dropped from further evaluation because of its poor performance relative to the Type 1 and Type 2 coatings, which do not contain aluminum in the surface layer. The superior performance of these two coatings which have a boron-silicon composition for the surface, is consistent with the lower recombination efficiency of borosilicate glasses with respect to Al_2O_3, as discussed in Section 2.1. The initial values of hot-wall recombination efficiency for the Types 1 and 2 coating are equal. However, after 3 h of exposure, the single-layer coating, Type 2, has a lower efficiency, 0.018 compared

Table 5. Summary of HYMETS Test Specimens, Recombination Efficiency Data, and Surface Elemental Analysis Results.

Coating Type: Design [a]	Specimen Number	Substrate Alloy	Coating		Test		Hot-Wall Recombination Efficiency at Time (h)							Contaminant Elements on Surface of Specimen at End of HYMETS Test[b]
			Weight (10^{-2} kg/m^2)	Thickness (μm)	Temperature (K)	Time (h)	0.5	1.0	2.0	3.0	5.0	7.5	10.0	
Type 3: Al + 3SiB + SO	L-29	Alpha2	0.90	3.8	1260	5	0.035	0.045	0.067	0.065	0.063	–	–	Ti-m, Nb-w
	L-31	Alpha2	0.89	3.7	1260	5	0.025	0.028	0.041	0.045	0.039	–	–	Ti-vs, Nb-vw
	L-33	Alpha2	0.99	4.1	1260	5	0.025	0.030	0.072	0.073	0.090	–	–	Ti-vs, Nb-w
Type 3a: Al + SiB + SO + Al + SiB + SO	L-15	Alpha2	1.28	5.3	1260	5.5	0.036	0.036	0.035	0.035	0.034	–	–	Ti-m, Nb-w
Type 3b: SiB + VHT + Al + 3SiB + SO	L-35	Alpha2	0.76	3.2	1260	3	0.020	0.021	0.039	0.051	–	–	–	Ti-m, Nb-w
Type 3c: SiB + Al + VHT + Al + 3SiB + SO	L-36	Alpha2	1.52	6.3	1260	3	0.043	0.037	0.074	0.067	–	–	–	Ti-m
Type 1: SiB + Al + VHT + 3SiB + SO	L-37	Alpha2	1.05	4.4	1260	5	0.013	0.014	0.032	0.015	0.029	–	–	Ti-m to vs, Nb-w to m
	L-58	Alpha2	0.85	3.5	1260	5	0.019	0.025	0.021	0.027	0.029	–	–	
	N-2	Alpha2	1.36	5.7	1260	2	0.001	0.007	0.015	–	–	–	–	Start of coating spallation
	N-3	Alpha2	1.41	5.9	1260	1.5	0.009	0.015	–	–	–	–	–	
	N-8	Alpha2	1.52	6.3	1260	1.5	0.007	0.009	–	–	–	–	–	Ti-tr
	N1A	Alpha2	1.51	6.3	1205	10	0.005	0.007	0.014	0.010	0.018	0.025	0.023	Ti-s, Nb-m; see Fig. 45
	N2A	Alpha2	1.54	6.4	1205	1	0.015	0.016	–	–	–	–	–	
	N3A	Alpha2	1.39	5.8	1205	1	0.008	0.009	–	–	–	–	–	
	N4A	Alpha2	1.51	6.3	1205	10	0.015	0.018	0.022	0.050	0.046	0.023	0.023	
	N9	Super-alpha2	1.65	6.9	1205	10	0.015	0.021	0.023	0.020	0.029	0.069	0.073	Ti-w, Nb-vw, Ca-tr
	N12	Super-alpha2	1.37	5.7	1260	1	0.012	0.015	–	–	–	–	–	
	N13	Super-alpha2	1.58	6.6	1260	3.5	0.020	0.021	0.055	0.046	–	–	–	Ti-m, Cu-tr, Fe-tr
	N14	Super-alpha2	1.85	7.7	1260	3.5	–	–	–	–	–	–	–	None of above as seen for N13
	N15	Super-alpha2	1.89	7.9	1260	1	0.023	0.029	–	–	–	–	–	
	N16	Super-alpha2	1.67	7.8	1260	1	0.031	0.023	–	–	–	–	–	
	PG1	Gamma	1.27	5.3	1255	1	0.015	0.012	–	–	–	–	–	
	PG2	Gamma	1.03	4.3	1255	5	0.014	0.015	0.020	0.018	0.014	–	–	
	NGAMMA12	Gamma	1.56	6.5	1255	10	0.012	0.030	0.037	0.035	0.039	0.063	0.048	Ti-vw
	NA4	Beta-21S	1.53	6.4	1094	10	0.005	0.006	0.010	0.009	0.025	0.048	0.122	Ti-s, Cu-m, W-m, Fe-w
Type 2a: SiBx-Air Brush + SiB + SO	L-42	Alpha2	1.86	8.0	1260	5	0.026	0.024	0.037	0.031	0.023	–	–	None
	L-47	Alpha2	3.98	17.2	1260	5	0.001	0.001	0.002	0.002	0.001	–	–	
	L-48	Alpha2	0.93	4.0	1260	5	0.004	0.014	0.012	0.016	0.023	–	–	
Type 2b: SiB-Boron Rich + SiB + SO	L-59	Alpha2	4.46	19.2	1260	5	0.028	0.025	0.027	0.034	0.045	–	–	
Type 2: 3SiB + SO	NSJR2	Super-alpha2	1.09	4.7	1167-1322	4.5	0.017	0.017	0.021	0.013	–	–	–	
	NSJR6	Super-alpha2	0.84	3.6	1260	10	0.016	0.016	0.018	0.018	0.021	0.030	0.033	Ti-s, Nb-m; see Fig. 52
	NG2	Gamma	0.74	3.1	1260	1	0.027	0.032	–	–	–	–	–	
	NG3	Gamma	0.80	3.4	1260	1	0.026	0.048	–	–	–	–	–	
	NGAMMA6	Gamma	0.56	2.4	1260	10	0.020	0.023	0.026	0.034	0.035	0.023	0.020	
	N6 (A)	Beta-21S	0.99	4.3	1094	1	0.078	0.074	–	–	–	–	–	Ti-vs, Nb-w, Cu-tr
	N7 (A)	Beta-21S	1.04	4.5	1094	5	–	0.014	0.013	0.007	0.317	–	–	Ti-vw, Cu-w, W-tr, Ca-w
	N8 (A)	Beta-21S	0.94	4.0	1094	2	0.023	0.04	0.162	–	–	–	–	Ti-vs, Nb-w, W-tr, Cu-w
	N9 (A)	Beta-21S	0.98	4.2	1094	1	–	–	–	–	–	–	–	

3032_MMEM

(a) Letters a, b, or c following the numerical in the coating type designation denote variations of the basic coating type. Nomenclature for coating construction: Al is 1 μm of aluminum, SiB is 1 μm of boron-silicon, 3SiB is 3 μm of boron-silicon, VHT is 1/2-h vacuum heat treatment, and SO is 1/2-h static oxidation in air.

(b) vs = very strong, s = strong, m = medium, w = weak, vw = very weak, and tr = trace

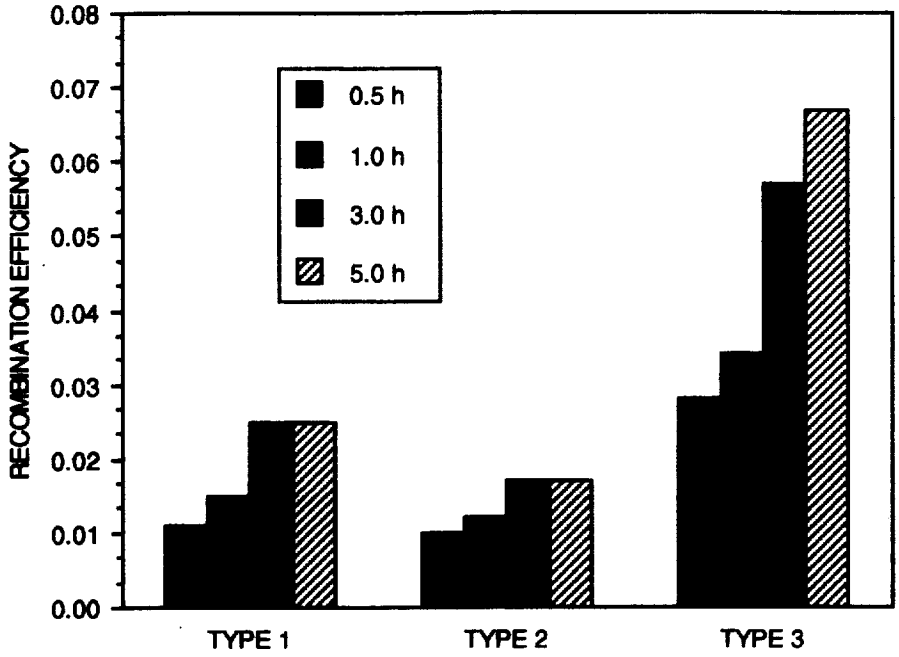

Figure 20. Hot-wall recombination efficiency of coating Types 1, 2, and 3 on alpha2 substrates as a function of exposure time in HYMETS at 1260 K.

to 0.025. As a point of reference, the hot-wall recombination efficiency of uncoated alpha2 was 0.055 after 1-h HYMETS exposure.

Hot-wall recombination efficiency data for the Type 1 coating on the four substrate materials for exposure times to 10 h are shown in Figure 21. Specimen temperatures are 1205 K for alpha2 and super-alpha2, 1260 K for gamma, and 1089 K for beta-21S. Hot-wall recombination efficiency values through 5 h of testing are the average value for multiple specimens. Data for 7.5 and 10.0 h are for a single specimen, with the exception of the alpha2 material which represents two specimens. The large increase in recombination efficiency for super-alpha2 at 10 h may be due to contamination. Calcium was found on the surface of this specimen at the conclusion of the test. The large increase in recombination efficiency for the beta-21S coating after 5 h is probably also the result of contamination. Copper and tungsten, probably from the arc heater electrodes, was present on the coating. Both of these elements form oxides that have moderately high recombination efficiencies for oxygen.

Figure 22 shows hot-wall recombination efficiency data for the Type 2 coating on the four substrate materials. Test temperatures were 1260 K for alpha2 and gamma, 1205 K for super-alpha2, and 1089 K for beta-21S. The dramatic increase in recombination efficiency at 5 h for beta-21S is probably the result of copper contamination. Differences in efficiencies between alpha2 and super-alpha2 are small, and they are probably due to sample-to-sample processing variations.

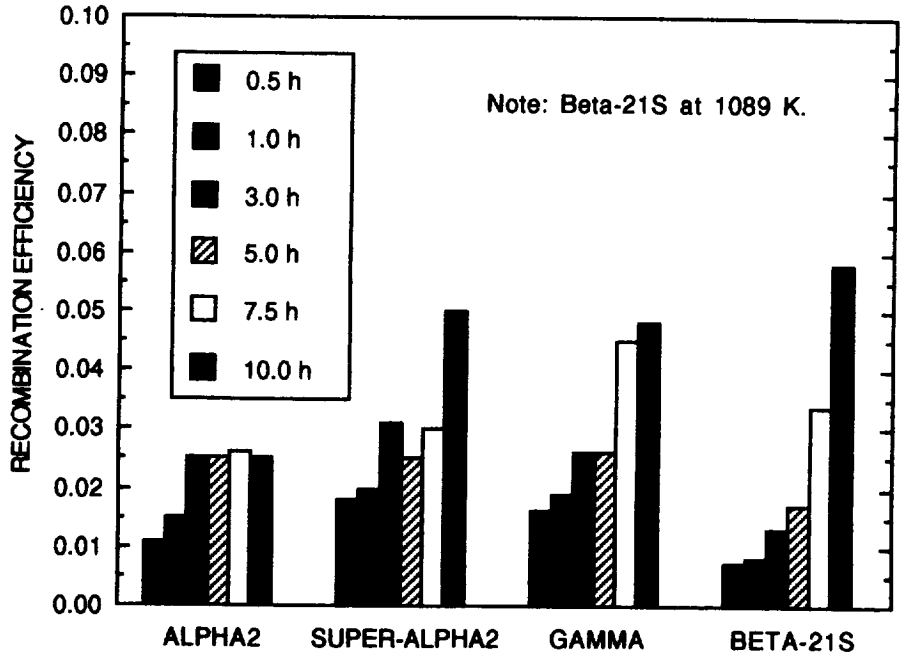

Figure 21. Hot-wall recombination efficiency of the Type 1 coating on four types of substrates as a function of exposure time in HYMETS.

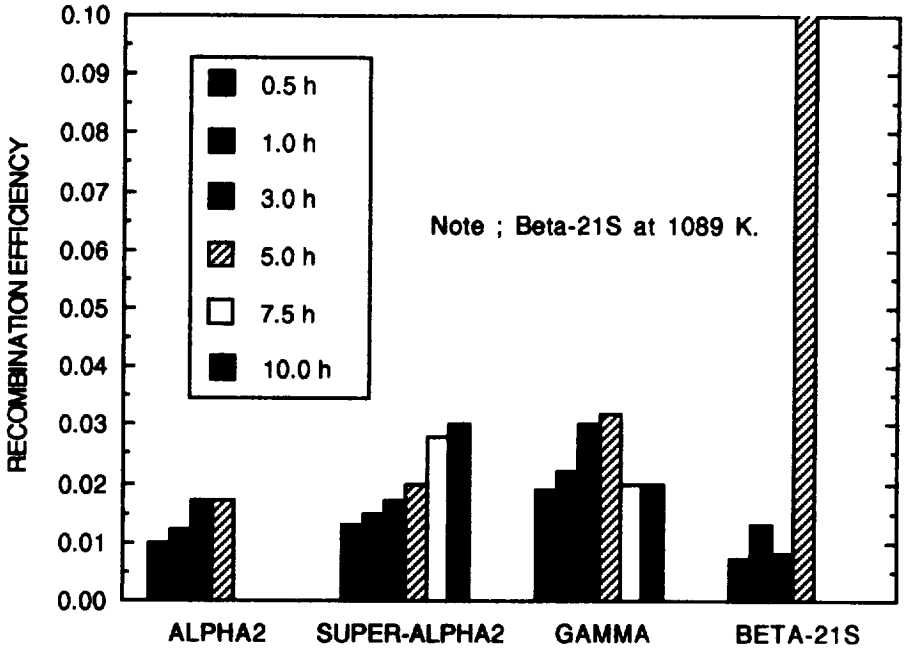

Figure 22. Hot-wall recombination efficiency of the Type 2 coating on four types of substrates as a function of exposure time in HYMETS.

Hot-wall recombination efficiencies of Type 1 and Type 2 coatings on super-alpha2 are shown in Figure 23. Similar data are shown in Figure 24 for the gamma material. Hot-wall recombination efficiency of uncoated gamma after 1 h in HYMETS at a temperature of 1260 K is 0.068. The Type 2 coating has the lower hot-wall recombination efficiency on both of these titanium-aluminides. This coating shows better stability of recombination efficiency with increasing time of exposure. In the case of the Type 1 coated specimens, aluminum and silicon are present at the surface, but aluminum is not detected for the Type 2 coating. Aluminum from the sublayer of the Type 1 coating appears to migrate to the surface with increasing exposure time. The presence of aluminum-bearing compounds at the surface increases recombination efficiency, as discussed in Section 2.1 of this report.

Representative cold-wall and hot-wall recombination efficiency is shown a function of HYMETS exposure time in Figures 25 and 26. The times at which a specimen was removed from HYMETS for reflectance measurements are indicated by the vertical bars along the upper axis of the figures. The small step-like decrease in hot-wall recombination efficiency seen after 2 h in Figure 25 could be the result of this procedure. However, similar changes are not seen after the 1-, 4- and 6-h removal times. A review of all of the test data revealed no consistent correlation between specimen removal and abrupt change in efficiency. The increase in hot-wall recombination efficiency after 4.5 h for this specimen (N9) may be due to the presence of niobium and/or titanium near the surface (c.f., Table 5) which leads to a semiconductor contamination of the basic insulator electronic structure of the coating. Abrupt decreases in efficiency at 5.5 and 9 h may be the result of the removal of some surface contaminant(s) during thermal transients. This specimen also showed a trace of calcium contamination, probably from contact with cooling water during a reflectance measurement. The cold-wall recombination efficiency follows a similar trend in time-dependent changes. The cold-wall values are much lower in all cases. The effect of temperature is to change the energy gap and broaden the energy levels. As temperature increases, the lattice expands and the oscillations of the atoms about their equilibrium lattice points increase. Recombination efficiency should increase with temperature because of increasing charge mobility and energy. At some point, the efficiency should then start to decrease as temperature is further increased as the energy of oxygen atoms resident on a surface increased and they are more readily desorbed reducing their surface number density.

Cold-wall and hot-wall recombination efficiencies are shown as a function of HYMETS exposure time for a typical Type 2 coated specimen at a test temperature of 1260 K in Figure 26. The slowly increasing hot-wall efficiency may be due to (1) migration of substrate ions to the surface as discussed above, or (2) surface morphological changes such as roughening which increases recombination efficiency at a surface. The step-like change in hot-wall efficiency at 5.25 h correlates with specimen removal after the 5.0 h. If the 0.006 step increase in efficiency between 5.00 and 5.25 h is subtracted from the data for longer exposure times, the recombination efficiency is 0.025 at 10 h. Cold-wall recombination efficiency was nearly constant at 0.003 to 0.004 throughout the test. The surface region of this

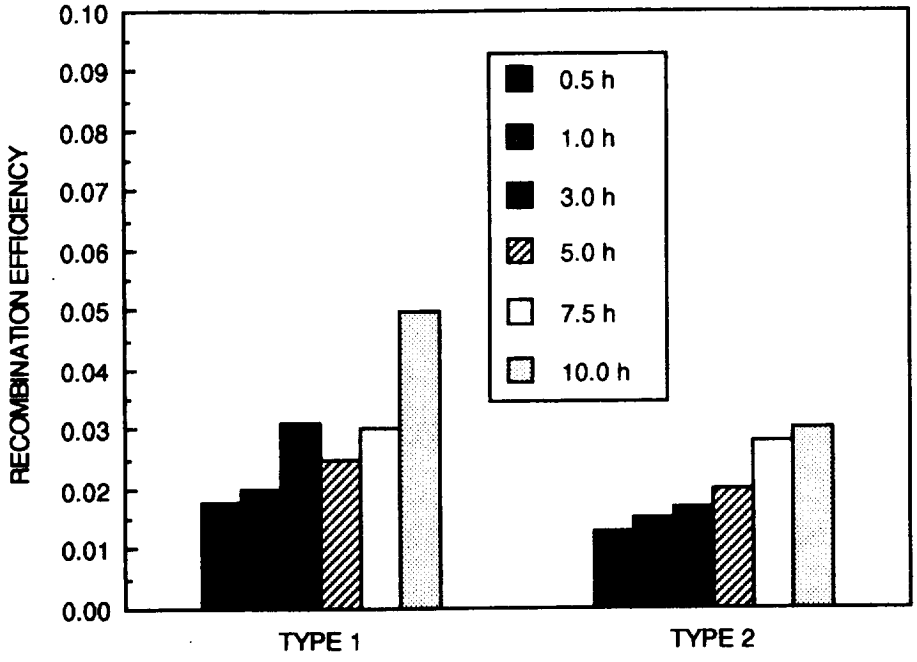

Figure 23. Hot-wall recombination efficiencies of Type 1 and 2 coatings on super-alpha2 substrates as a function of exposure time in HYMETS at 1205 to 1260 K.

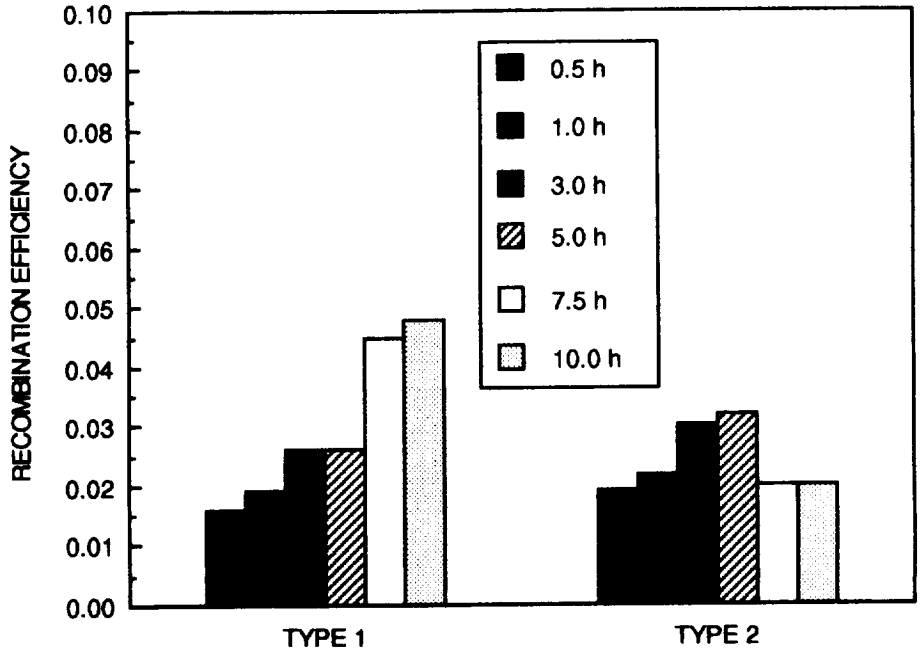

Figure 24. Hot-wall recombination efficiencies of Types 1 and 2 coatings on gamma substrates as a function of exposure time in HYMETS at 1260 K.

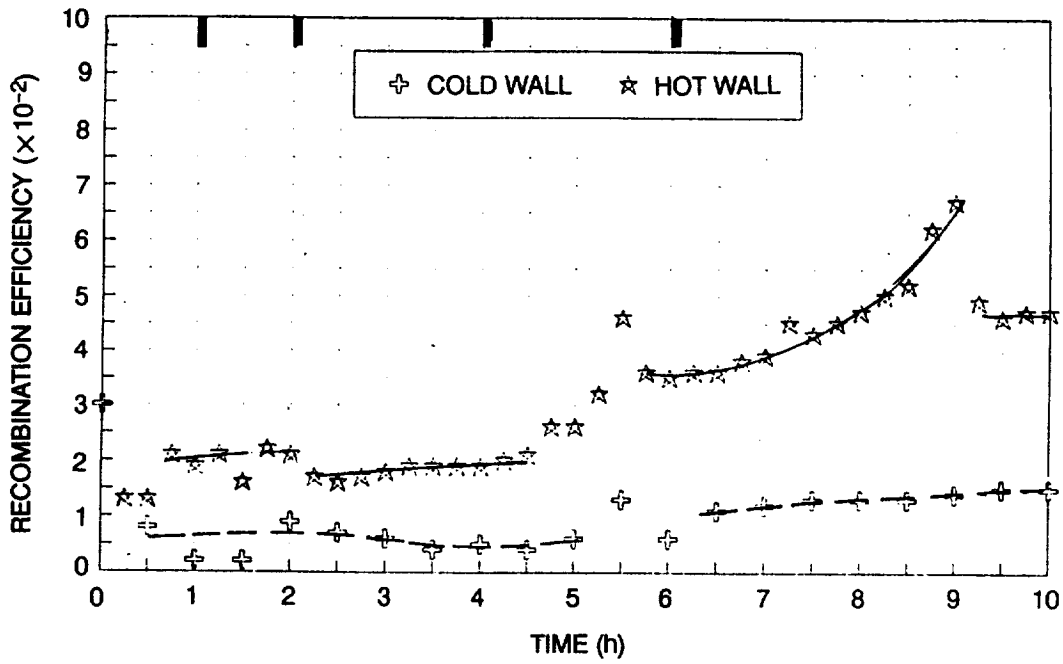

Figure 25. Hot- and cold-wall recombination efficiencies as a function of exposure time at 1205 K for Type 1 coated super-alpha2, Specimen No. N9.

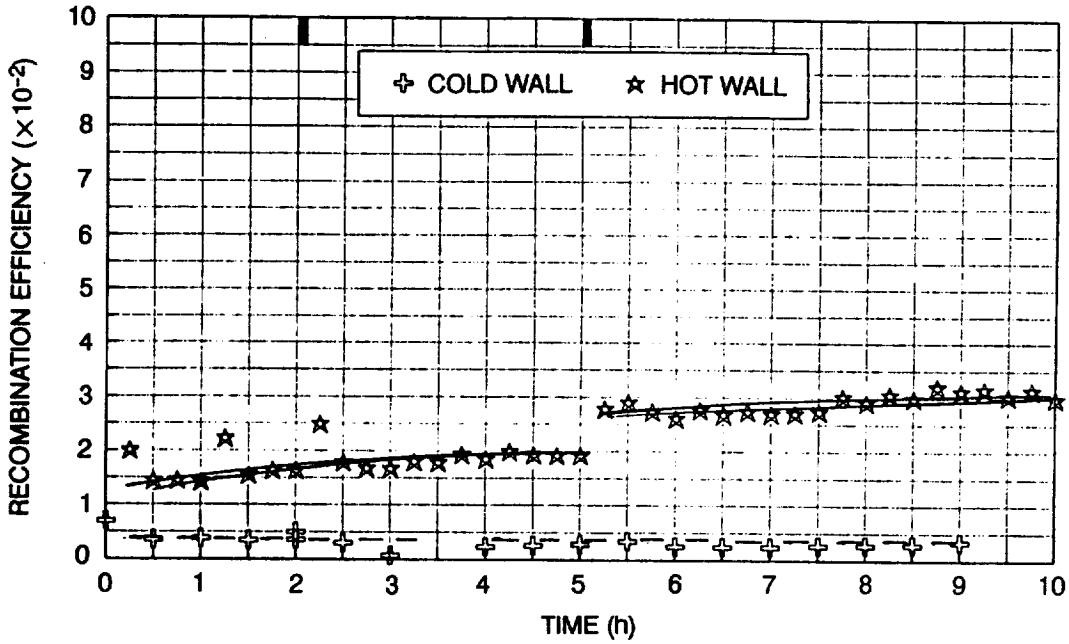

Figure 26. Hot- and cold-wall recombination efficiencies as a function of HYMETS exposure time at 1260 K for Type 2 coated super-alpha2, Specimen No. NSJR6.

specimen at the conclusion of the test showed the presence of niobium and titanium, but the absence of aluminum.

Hot-wall recombination efficiencies for four specimens of Type 1 coated alpha2 specimens are shown in Figure 27. The coating thickness for Specimen L58 was 3.5 μm, and coating thickness for the remaining specimens was 6.3 to 6.4 μm. The recombination efficiency behavior of specimen N4A between 3 h and 8 h is very erratic when compared to the other specimens. Specimens N1A and N2A were processed in the same batch as N4A, and presumably they are identical coatings. Reflectance measurements were made after 1 and 5 h of exposure, and the correspondence of these times with changes in efficiency is inconclusive. Similar trends are seen for specimen N1A, but the magnitude of change is much smaller. Potential causes of these changes may be cyclic changes in composition or an anomaly in arc heater performance leading to surface contamination which is removed during subsequent test cycles. There is insufficent information to support any reason for the observed behavior. Similar trends are observed with Specimen N1A, but the magnitudes of the changes are much smaller.

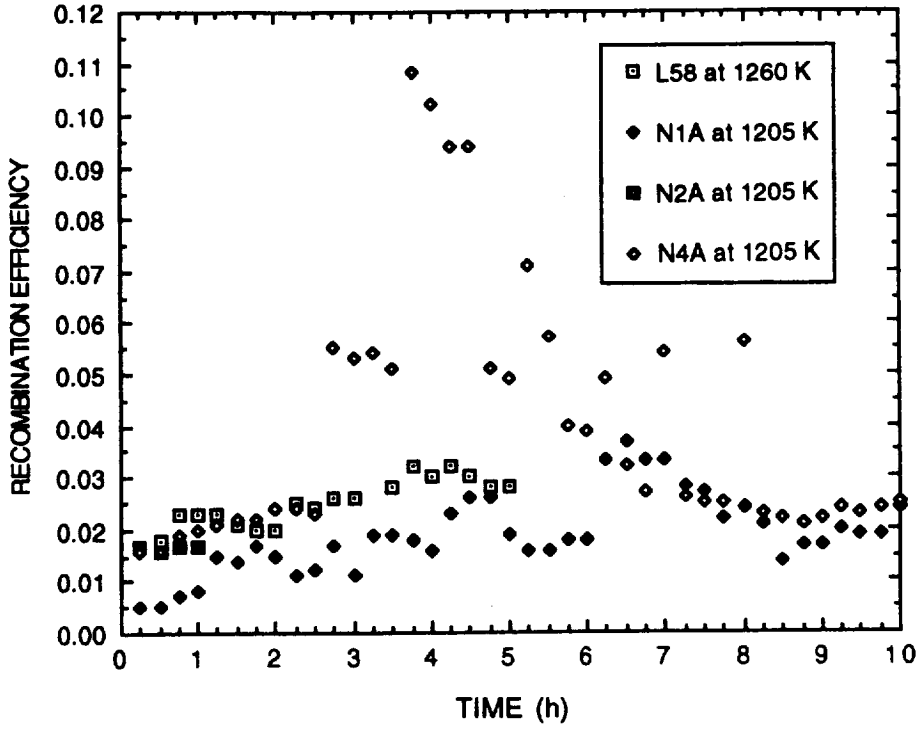

Figure 27. Hot-wall recombination efficiencies of four specimens of Type 1 coated alpha2 as a function of HYMETS exposure time.

Hot-wall recombination efficiency data during a 10-h HYMETS test at 1089 K for a Type 1 coated beta-21S specimen, No. NA4, are shown in Figure 28. The surface of this specimen was found to be contaminated with copper, iron, and tungsten at the conclusion of the test. Continued deposition of these contaminants from the arc probably led to the monotonic increase in efficiency seen after 6 h of exposure. Copper contamination was observed for all tests at 1089 K. At the higher test temperatures, the copper and tungsten compounds were not found on the surface of any of the specimens. These contaminants may still be present in the flow stream, but they may be volatile at the higher surface temperatures.

Figure 29 shows the variation in hot-wall recombination efficiency with HYMETS exposure time for a Type 2 coated gamma titanium-aluminide specimen, No. NG6, tested at 1260 K for 10 h. This specimen was removed from HYMETS after 2, 5, and 8 h of the test. A Type 1 coated gamma substrate specimen, No. PG2, tested earlier for 5 h in HYMETS at the same temperature, is also shown in the figure for comparison. These latter data do not show the step-like changes in efficiency seen between 2.5 and 5 h for Specimen NG6.

4.3 EMITTANCE

Total normal emittance data for the as-prepared coatings are summarized in Table 6. The ranges in emittance values shown for each temperature are based on data for multiple specimens for each coating type. The lower emittance of the coated beta-21S with both Type 1 and Type 2 coatings is the result of the lower static oxidation temperature (1089 K) used during processing to be consistent with the maximum use temperature of this alloy. Increasing the oxidation time to 2 h raises the emittance to 0.80–0.83 at 1089 K. After 25 h of static oxidation, total normal emittance increases to 0.85–0.88 at 1089 K.

The Type 2 coating has slightly higher total normal emittance than the Type 1 coating on alpha2 and gamma substrates. However, on super-alpha2, the Type 1 coating has the higher emittance at both 1089 K and 1255 K. The differences in emittance for a given temperature is probably due to processing variability, particularly the boron-to-silicon ratio. Heat treatment of the boron-silicon layer is believed to form a Si_xB_y compound which has strong optical absorption characteristics and is the governing factor in emittance. Variations in the fraction of boron deposited will influence the amount of this compound which is formed in the coating during heat treatment. It is believed that when heat treated (statically oxidized) at 1260 K, the boron-silicon layer is optically thick when the physical thickness of the layer is greater than 2 μm.

Stability of total emittance at elevated temperatures is a primary consideration in the evaluation of candidate coatings. Changes in total emittance with time during HYMETS tests are determined using the spectral near-normal reflectance data measured before, during, and at the conclusion of the test. These data are integrated over the Planck function to calculate temperature-dependent total normal emittance. All of the spectral data obtained from the HYMETS test series, presented as room-temperature

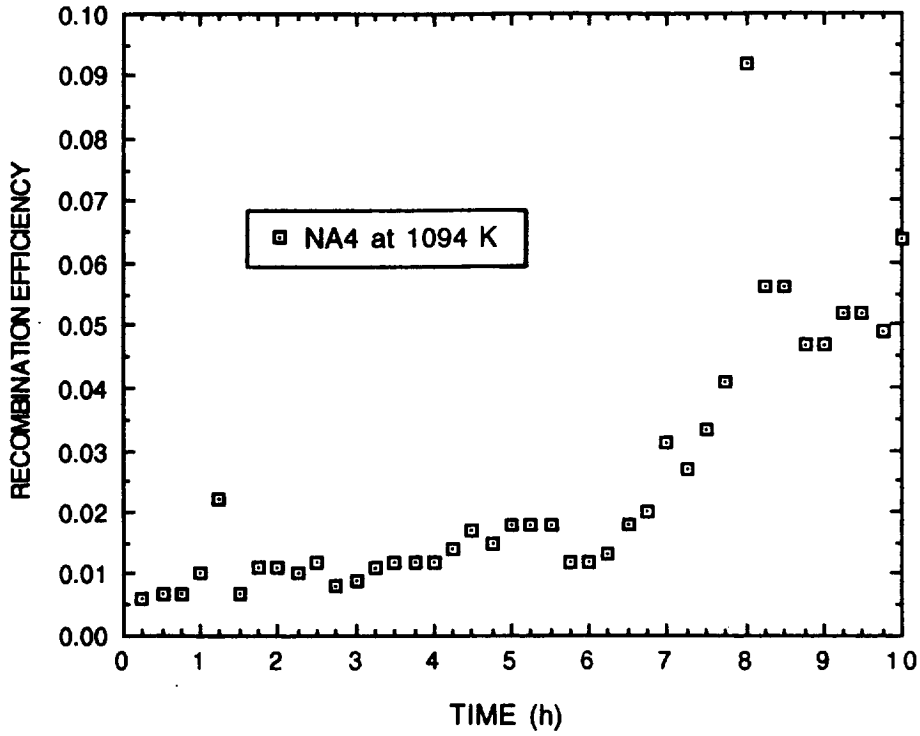

Figure 28. Hot-wall recombination efficiency as a function of HYMETS exposure time at 1089 K for Type 1 coated beta-21S, Specimen No. NA4.

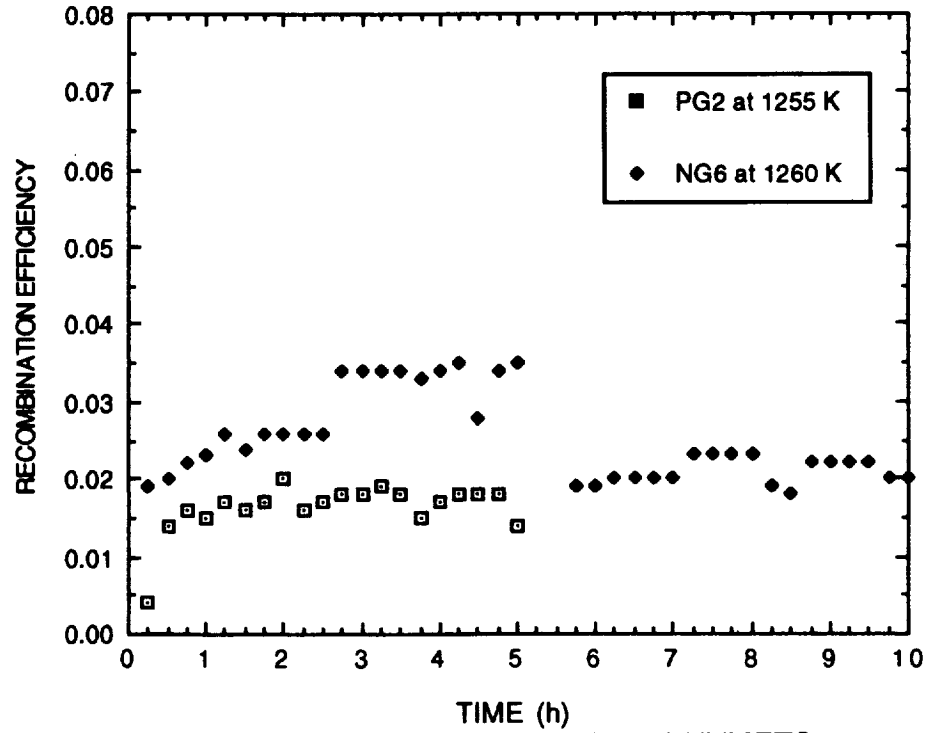

Figure 29. Hot-wall recombination efficiency as a function of HYMETS exposure time at 1260 K for Type 2 coated gamma (NG6) and Type 1 coated gamma (PG2).

Table 6. Summary of Total Normal Emittance Data for As-Prepared Coatings at Two Temperatures.

Coating Type	Substrate	Total Normal Emittance	
		at 1089 K	at 1255 K
Type 1	alpha2	0.81–0.85	0.81–0.87
	super-alpha2	0.82–0.88	0.88–0.91
	gamma	0.79–0.82	0.82–0.84
	beta-21S	0.77–0.78	0.76–0.79
Type 2	alpha2	0.85–0.91	0.87–0.92
	super-alpha2	0.80–0.82	0.82–0.85
	gamma	0.83–0.85	0.83–0.86
	beta-21S	0.78–0.79	0.79–0.80
Type 3	alpha2	0.87–0.89	0.88–0.90

near-normal spectral emittance, are contained in Appendix B of this report. Comparisons of the spectral data at increasing exposure times are useful in evaluating compositional changes in a coating.

The temperature dependence of total normal emittance over the range 300 to 1255 K is shown as a function of exposure times up to 10 h in HYMETS in Figures 30 and 31 for two specimens each of Type 1 coated alpha2 and super-alpha2, respectively. In all cases, total normal emittance increases with increasing HYMETS exposure time. For the alpha2 specimens of Figure 30, total normal emittance at 1255 K, which initially is 0.81 for both specimens, increases to 0.84 after 1 h of HYMETS exposure. After 10 h, total normal emittance is 0.85 and 0.87 for specimens N1A and N4A, respectively. The initial value of total normal emittance at 1255 K for the super-alpha2 specimens is 0.87, and it increases to 0.89 to 0.91 after 10 h (Figure 31).

Total normal emittance of the Type 1 coating on alpha2 decreases slightly with increasing temperature because the spectral emittance of the coating is greater in the wavelength interval of 12 to 20 μm than it is in the wavelength interval of 1 to 6 μm, as is seen from Figure B-11 of Appendix B. This is because of strong absorption by an optically thick SiO_2 phase of the coating at the longer wavelengths. The emittance spectra centered around the wavelengths of 9.5 and 22 μm, as is seen in Figure B-11, are typical of an amorphous silica phase.

The temperature dependence of total normal emittance of the Type 1 coating on super-alpha2 (c.f., Fig 31) is increasing emittance with increasing temperature. Referring to the spectral data of Figures B-14 and B-15, spectral emittance is lower in the 10- to 20-μm-wavelength region and higher in the 1- to 6-μm region than is seen for alpha2. Also, the magnitude of the 8- to 10-μm reflection peak is less, indicating less of the silica form, particularly in the initial condition. The higher spectral emittance from 1 to 6 μm in wavelength for the alpha2 may be the result of more Si_xB_y formation or the presence of compounds formed from substrate ions.

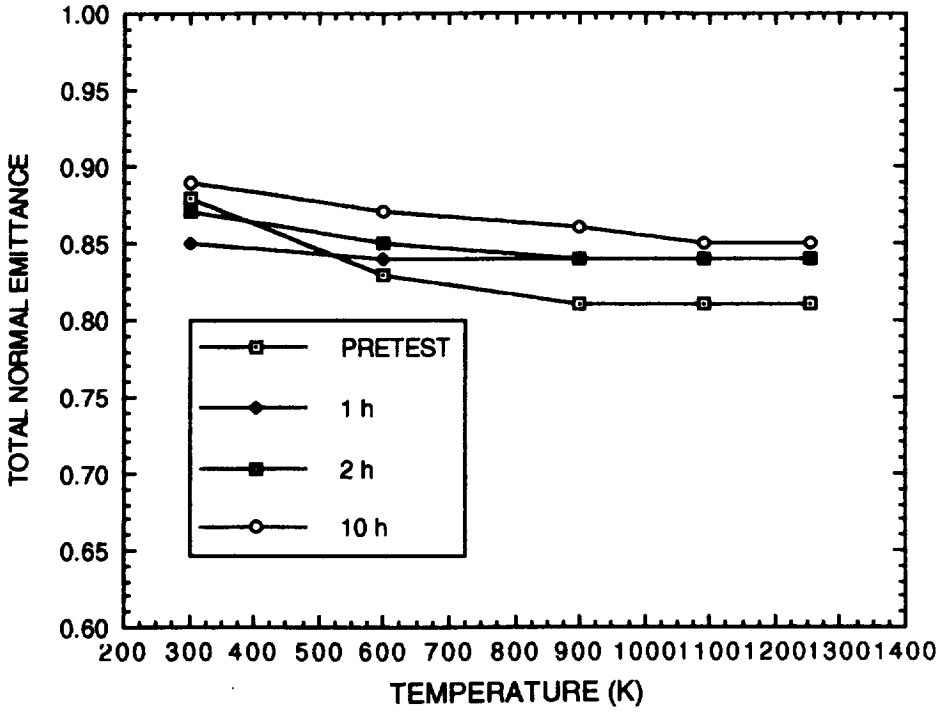

a. Specimen N1A.

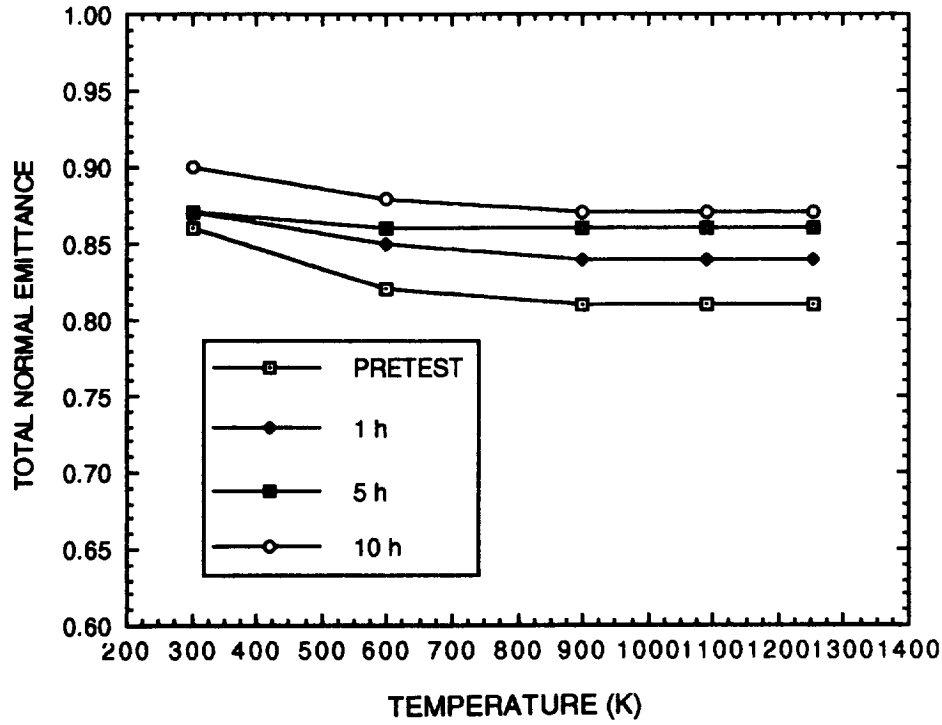

b. Specimen N4A.

Figure 30. Temperature dependence of total normal emittance of two Type 1 coated alpha2 specimens as a function of HYMETS exposure time at 1255 K.

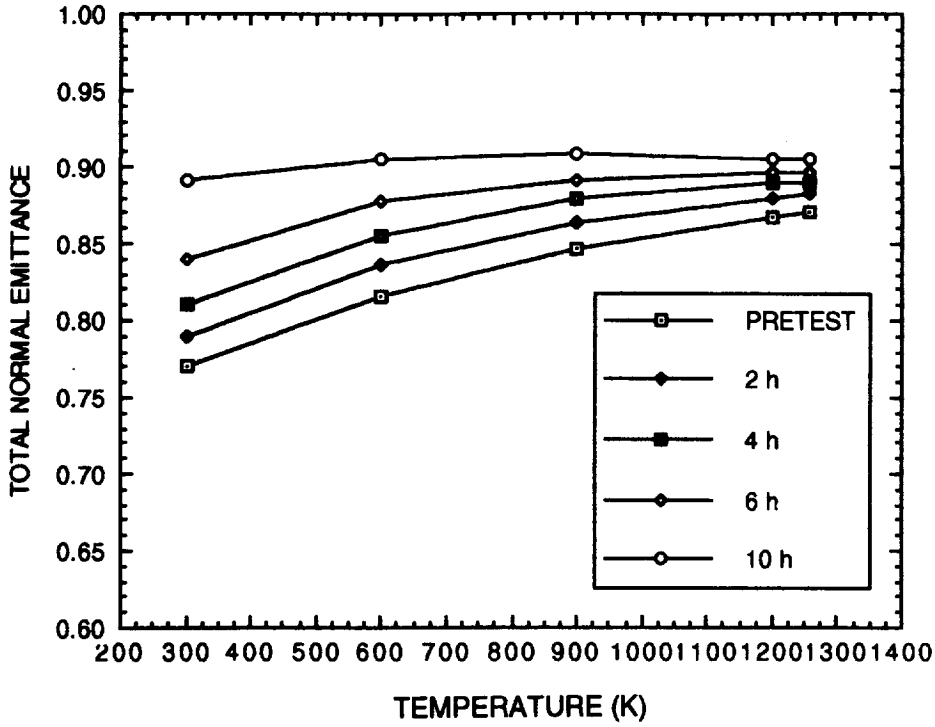

a. Specimen N9.

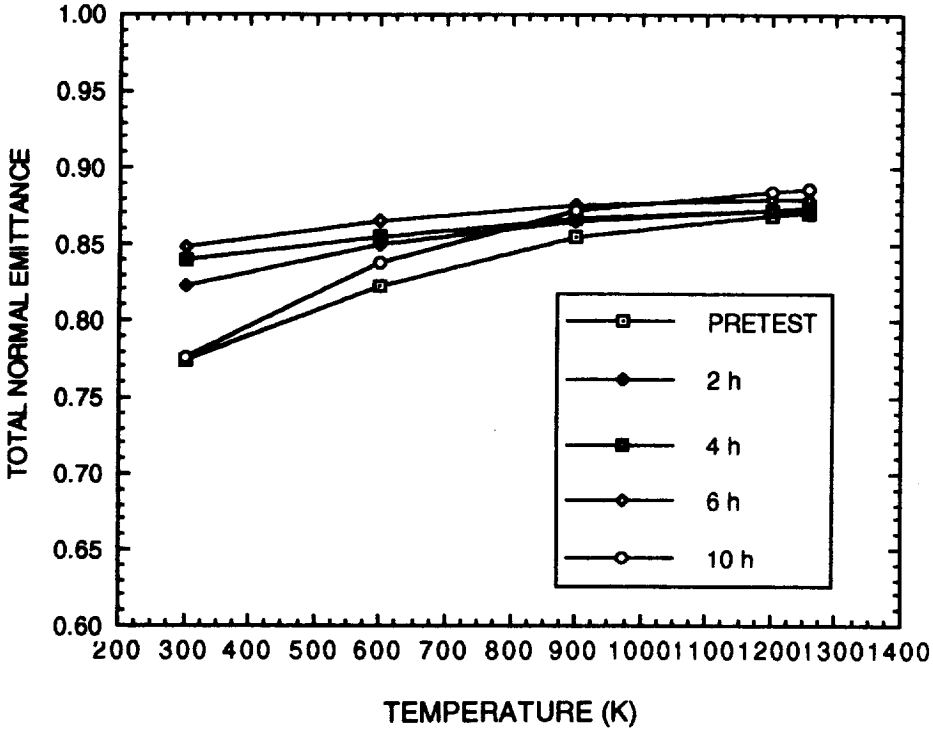

b. Specimen N11.

Figure 31. Temperature dependence of total normal emittance of two specimens of Type 1 coated super-alpha2 as a function of HYMETS exposure time at 1205 K.

The total normal emittance of Type 1 coated gamma titanium-aluminide shows little temperature dependence from 300 K to 1255 K, as is seen in Figure 32. HYMETS exposure, however, results in a strong increase in emittance over that of the as-prepared coating. The total normal emittance at 1255 K is initially 0.79, and it increases to 0.84 after 1 h and 0.87 after 10 h. Spectral emittance data for this specimen (c.f., Fig B-22) do not show the typical silica reflection spectra, as was seen for this Type 1 coating on both alpha2 and super-alpha2. Spectral emittance is relatively flat with wavelength, resulting in the small change in total emittance with temperature. Emittance spectra for the as-prepared coating are somewhat similar to that of a silicide (Ref. 13).

Total normal emittance data for Type 1 coated beta-21S alloy are shown as a function of temperature in Figure 33. Total normal emittance remains essentially constant with exposure time and shows a moderate decrease with increasing temperature to 900 K. Referring to the spectral data shown in Figure B-23, a strong silica-like spectra is present, which results in the higher total emittance at the lower temperatures. Spectral emittance is low in the wavelength interval of 1 to 7 μm. This is probably due to decreased Si_xB_y formation at the lower temperature (1089 K). Continued exposure at this temperature in HYMETS does not appear to promote additional formation of this species, as the spectral data remain relatively constant with exposure time. Heat treatment at a temperature greater than 1089 K is needed to increase emittance of the boron-silicon coating.

Total normal emittance as a function of temperature and HYMETS exposure time for the Type 2 coating on super-alpha2, gamma, and beta-21S substrates is shown in Figures 34, 35, and 36, respectively. The data for temperatures of 900 K and greater are similar to those for the Type 1 coating on the same substrates. Temperature dependence is small, and total normal emittance is between 0.81 and 0.87 for super-alpha2 and gamma and 0.73 to 0.78 for the beta-21S alloy.

The spectral emittance of the Type 2 coating on super-alpha2 (see Figure B-28) shows a very strong silica reflectance band in the 8- to 10-μm-wavelength interval. The overall spectrum is also very similar to that of the Type 1 coating on the same substrate material, with the exception of the pretest Type 2 coating in the wavelength region of 12 to 20 μm. The lower spectral emittance in this region is attributed to a lesser degree of oxidation during processing. Optical absorption is smaller at the longer wavelengths because of oxygen deficiency in-depth in the coating. As the coating is more fully oxidized during the HYMETS test, the absorption coefficient becomes larger and emittance increases.

The spectral emittance of the Type 2 coating on the gamma substrate (see Figure B-29) shows a small change with exposure time which is quite different from that seen with the Type 1 coating (c.f., Figure B-22). In the latter case, spectral emittance continuously increased with increasing exposure time. Also, the strong silica reflectance peak is present in all of the Type 2 spectra.

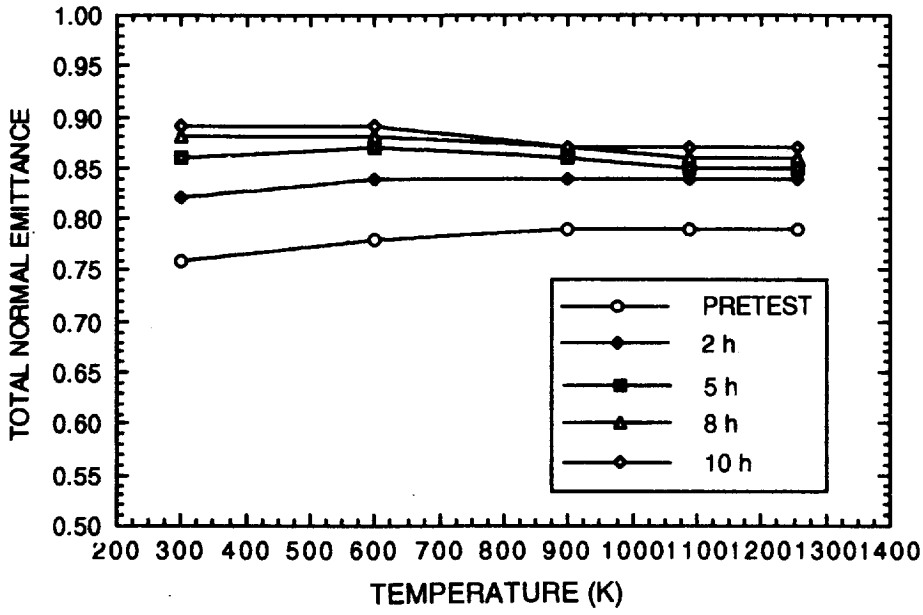

Figure 32. Temperature dependence of total normal emittance of Type 1 coated gamma, Specimen No. NG12, as a function of HYMETS exposure time at 1255 K.

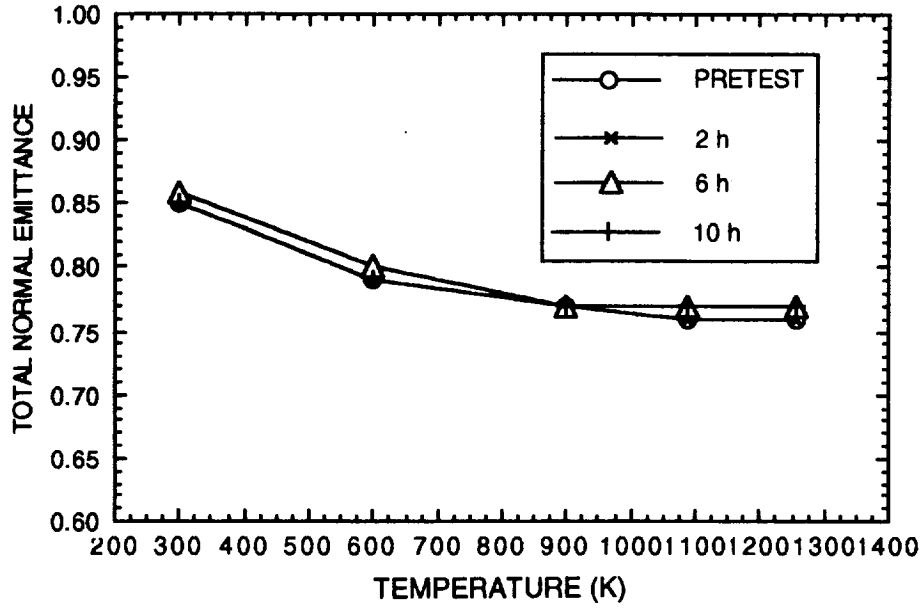

Figure 33. Temperature dependence of total normal emittance of Type 1 coated beta-21S, Specimen No. NA4, as a function of HYMETS exposure time at 1089 K.

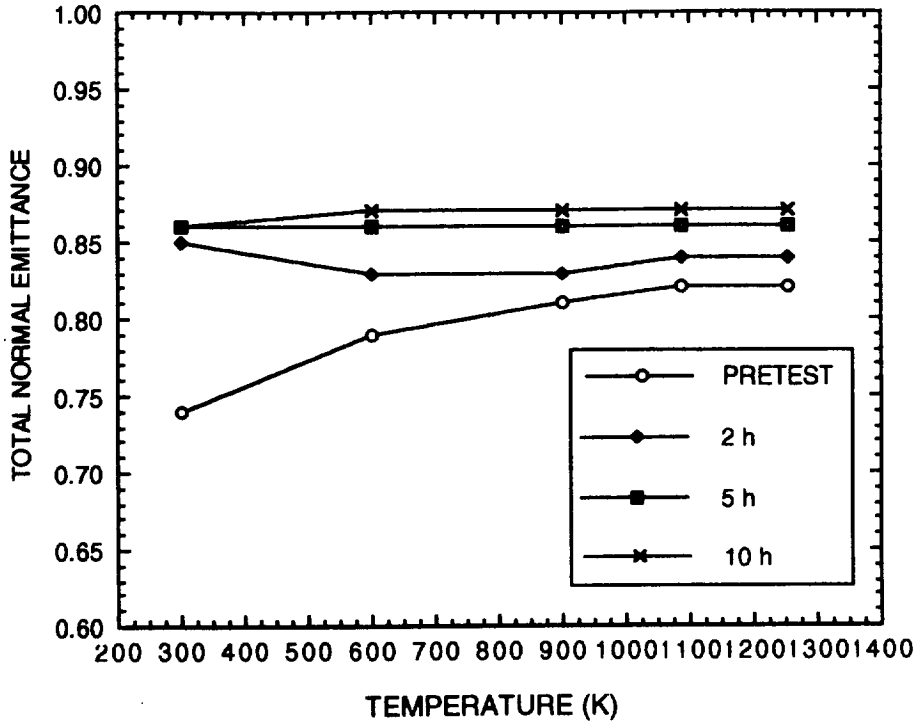

Figure 34. Temperature dependence of total normal emittance of Type 2 coated super-alpha2, Specimen No. NSJR6, as a function of HYMETS exposure time at 1255 K.

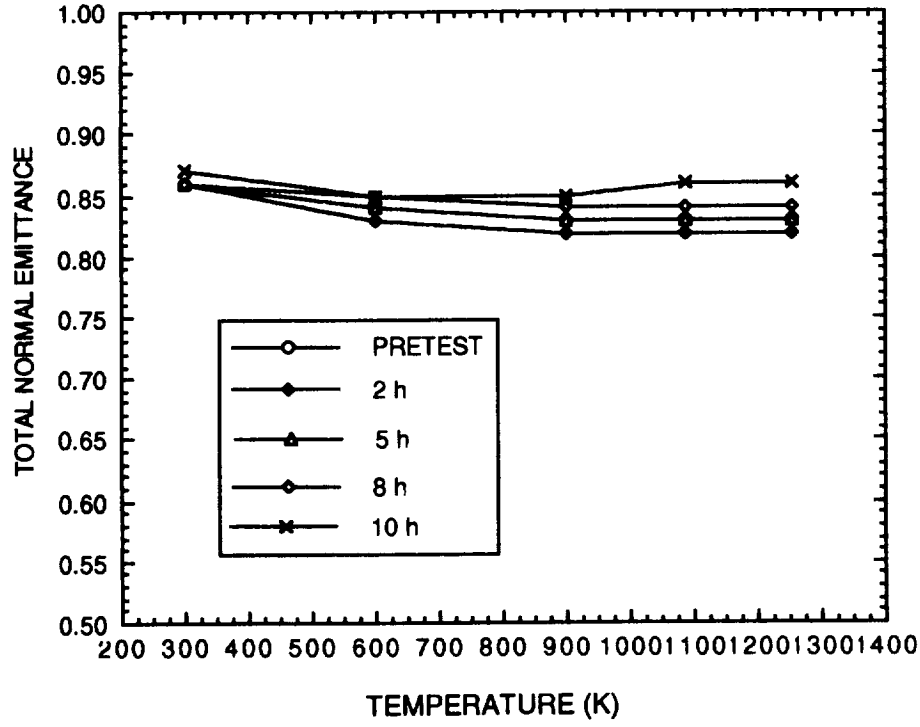

Figure 35. Temperature dependence of total normal emittance of Type 2 coated gamma, Specimen No. NG6, as a function of HYMETS exposure time at 1255 K.

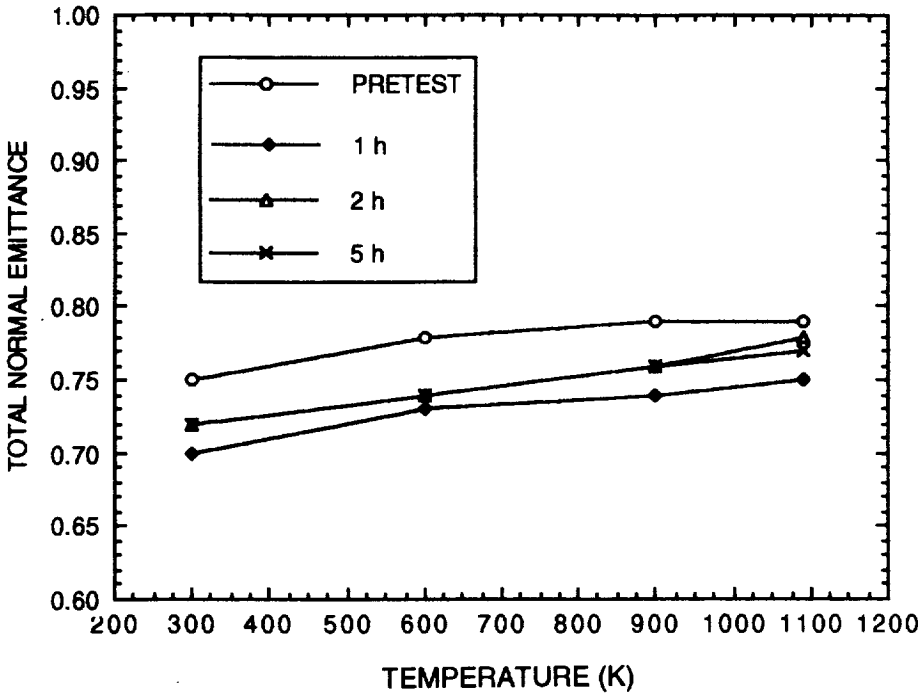

Figure 36. Temperature dependence of total normal emittance of Type 2 coated beta-21S, Specimen No. N7(A), as a function of HYMETS exposure time at 1089 K.

The total normal emittance of the Type 2 coating on beta-21S shows a small increase with increasing temperature, as is seen in Figure 36. The emittance of the Type 1 coating decreased with increasing temperature. The reflectance spectra for the two coatings for this low-temperature application are quite different (c.f., Figure B-32 and Figure B-23). Without the formation of the Si_xB_y constituent in the coating, the lower layer of the Type 1 coating has the major effect on emittance, particularly in the 14- to 25-μm-wavelength interval. Spectral emittance of the as-prepared Type 2 coating on super-alpha2 (Figure B-28) is similar to that of this coating on beta-21S. However, HYMETS testing of gamma at the higher temperature promotes a significant increase in longer wavelength emittance from enhanced oxidation of the coating at 1260 K.

The total normal emittance characteristics of coated specimens that were subjected to static oxidation tests were similar to those of HYMETS test specimens for temperatures of 900 K to 1255 K. A typical comparison of temperature-dependent total normal emittance data for two HYMETS tests and 100-cycle profiled static-oxidation test is shown in Figure 37.

Figures 38 and 39 show composites of the total normal emittance characteristics of Types 1 and 2 coatings on the four substrate materials at their maximum-use temperatures as a function of HYMETS exposure time. Total normal emittance is comparable for both coating types, and it is independent of substrate composition

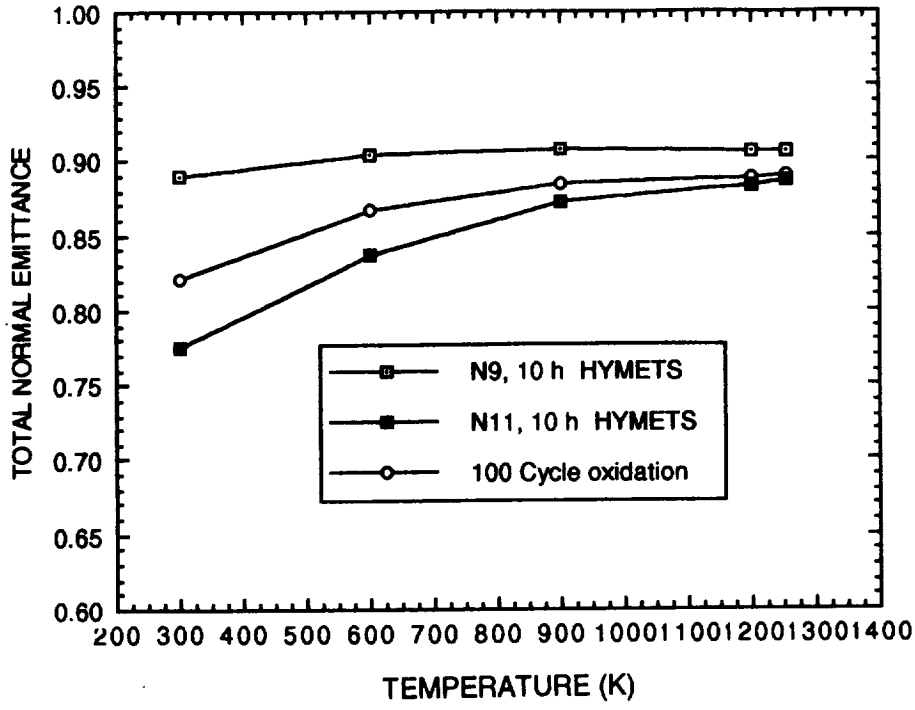

Figure 37. Comparison of total normal emittance for HYMETS and cyclic oxidation tests for Type 1 coated super-alpha2.

for the titanium-aluminides and the titanium alloy investigated in this program. The Type 2 coating is the one recommended because of its simpler process requirements.

The effect of thickness of the as-prepared Type 2 coating on spectral near normal emittance on super-alpha2 is shown in Figure 40. These data show that the coating is optically thick at a coating thickness of 2.3 μm, and that it is strongly absorbing over the wavelength interval applicable to the high-temperature use. The decrease in spectral emittance over the wavelength interval of 8 to 10 μm is the result of the strong change in optical constants of silica in the region of the bremsstrahlung frequency. For the temperature range of 900 K to 1255 K, spectral normal emittance, and therefore total normal emittance, is essentially independent of thickness for 2.3- to 4.0-μm-thick coatings initially statically oxidized at 1260 K. This may not be true at the lower temperature of 1089 K used for the beta-21S alloy, The small differences in spectral emittance between the three thicknesses in Figure 40 are probably due to processing variability.

4.4 FATIGUE

Room-temperature fatigue tests were conducted on specimens of Type 1 coated alpha2 and super-alpha2 titanium aluminides and the beta-21S titanium alloy to determine if the coating composition and/or processing had an adverse effect on the mechanical properties of these materials. The Type 1 coating was chosen for this

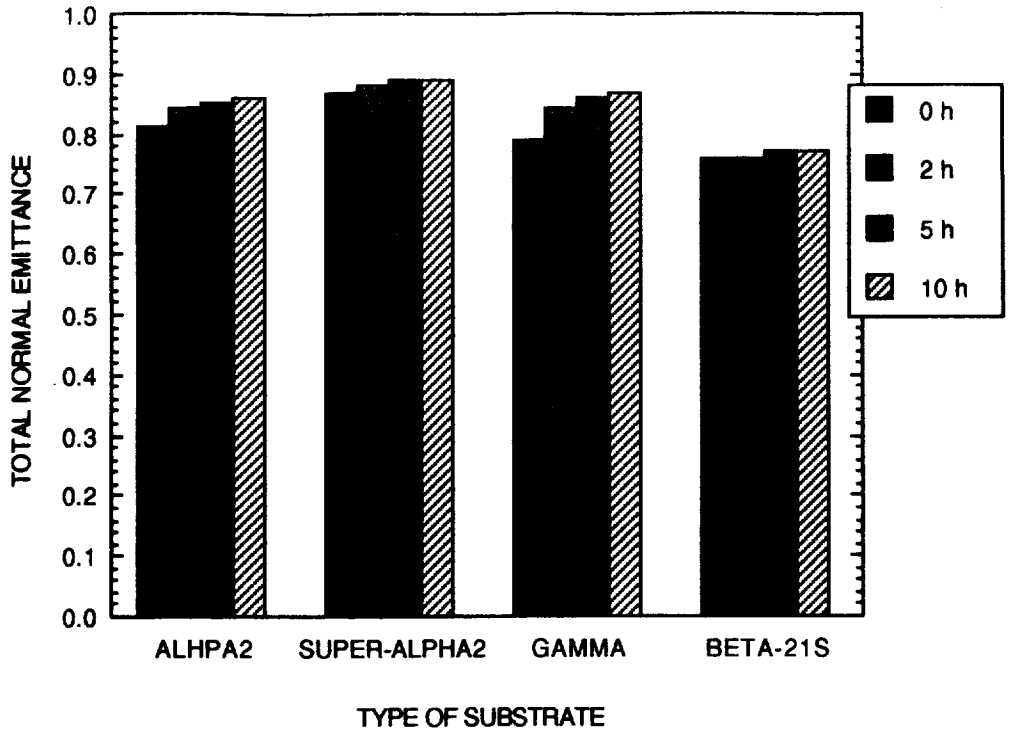

Figure 38. Total normal emittance of Type 1 coating on four types of substrate at 0, 2, 5, and 10 h of HYMETS exposure; beta-21S at 1089 K, all others at 1255 K.

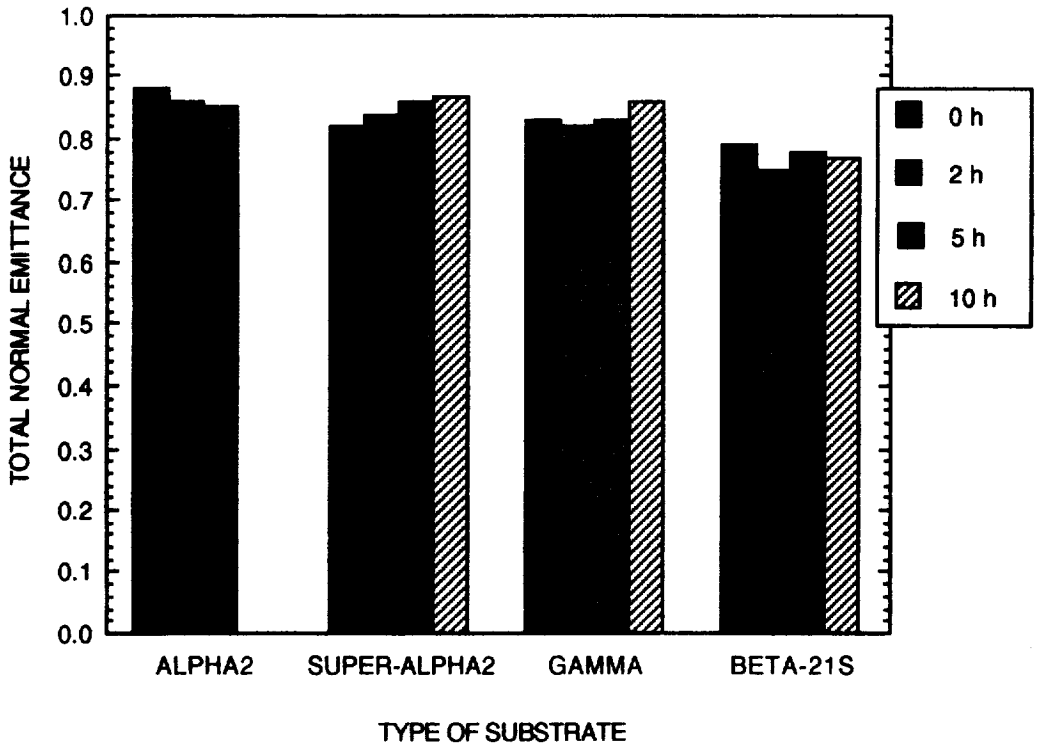

Figure 39. Total normal emittance of Type 2 coating on four types of substrate at 0, 2, 5, and 10 h of HYMETS exposure; beta-21S at 1089 K, all others at 1255 K.

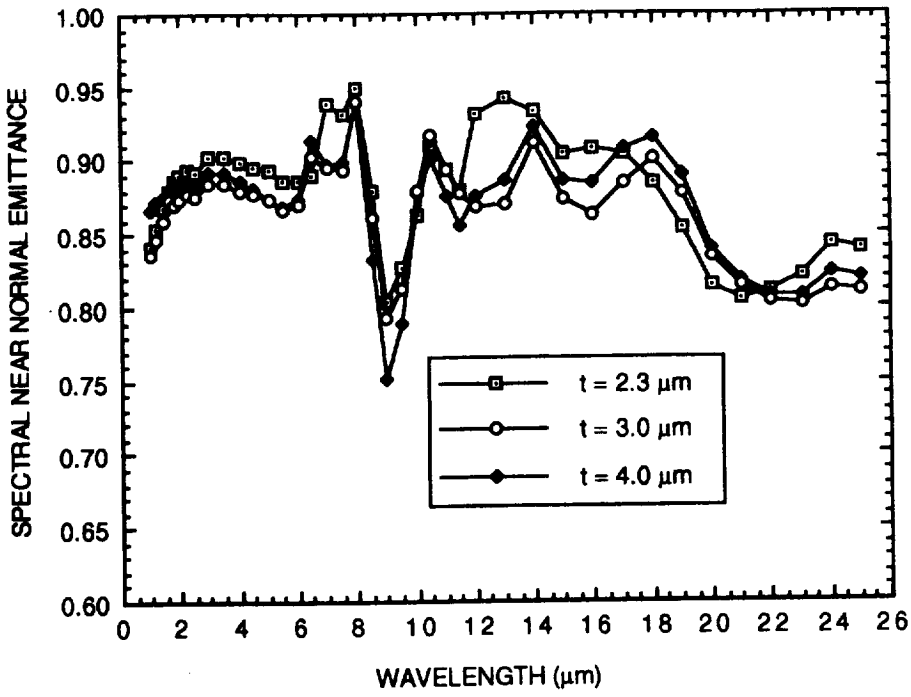

Figure 40. Effect of Type 2 coating thickness on spectral near-normal emittance of coated super-alpha2 substrates.

investigation because it contains all of the elements used for the coating concepts, and it requires an intermediate heat treatment step which may promote silicide formation at the coating-substrate interface prior to coating oxidation. The fatigue data are expressed as the number of cycles to failure in the cyclic bending test described in Section 3.4. Uncoated specimen sets were also tested to establish a baseline for the comparison. These results should be viewed only to compare the uncoated and coated specimens. They are not intended to represent actual fatigue life information because of the small sample population.

The specimen sets included five specimens for each of the uncoated and coated substrates for the three materials. Two additional sets of super-alpha2 specimens were statically oxidized for 100 h, one set at 1255 K and the other at 1205 K, and then tested to examine long-term oxidation effects on fatigue performance. The coated specimens were all statically oxidized in air for 1/2 h (1089 K for beta-21S and 1255 K for other alloys) prior to testing. The data shown herein are all for a stress level of ±550 MPa (80 ksi) at a cycle rate of 1 Hz.

Fatigue data for the uncoated alpha2 and super-alpha2 specimens showed a large variability in number of cycles to failure. In the case of alpha2, the spread in data for five uncoated specimens was 10,150 to 37,100 cycles. The spread in data for super-alpha2 was 15,000 to 33,300 cycles. The arithmetic averages were 21,550 and 24,420 cycles for alpha2 and super-alpha2, respectively. Similar spreads in data were observed for the coated specimens, as is seen in Figure 41. The average value for

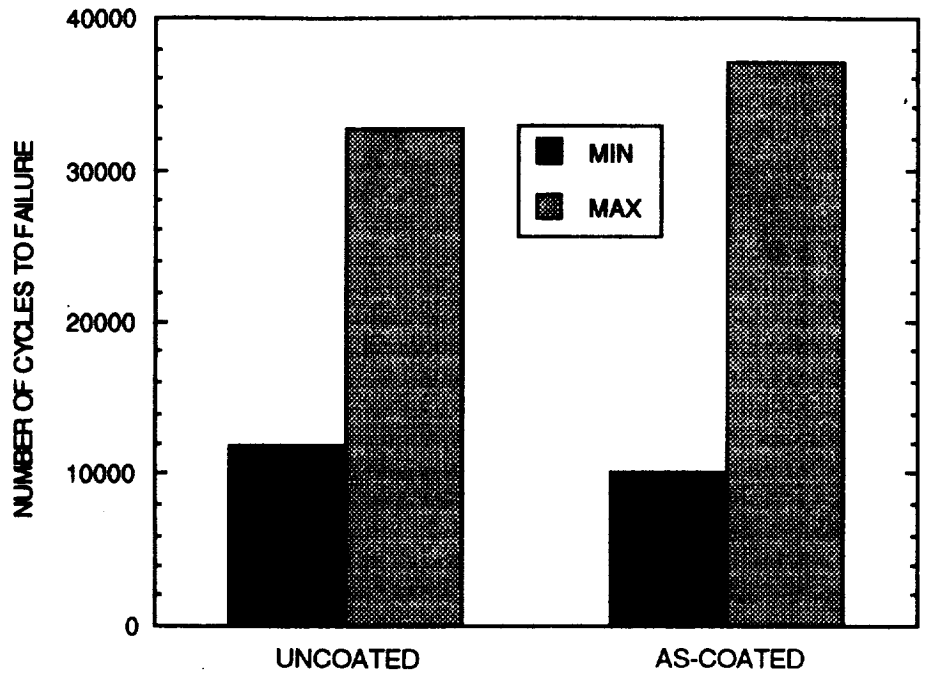

a. alpha2.

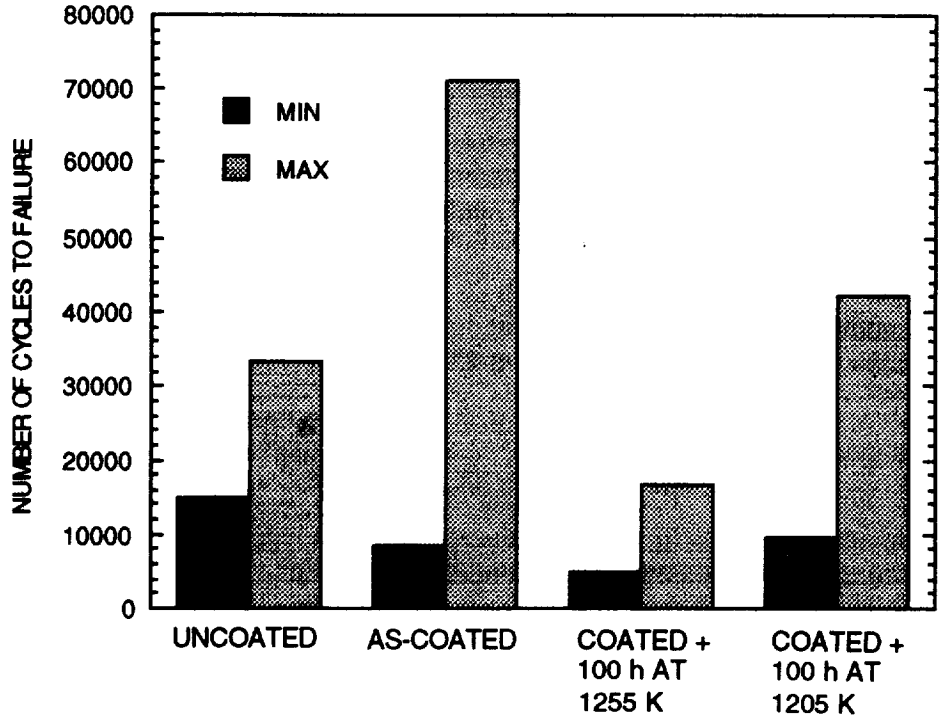

b. super-alpha2.

Figure 41. Comparison of number cycles to failure for uncoated and Type 1 coated alpha2 and super-alpha2 coated titanium-aluminides for room temperature fatigue test.

coated alpha2 was 22,900 cycles, and for super-alpha2 it was 39,600 cycles. For both materials, averages for coated specimens were equal to or greater than those for the uncoated ones.

After 100 h of static oxidation at 1255 K, the coated super-alpha2 material average of the cycles-to-failure was 11,500, a considerable reduction from the "as-coated" data. Reduction of the 100 h oxidation temperature to 1205 K resulted in an average life of 25,000 cycles.

Fatigue test results for the beta-21S alloy were inconclusive. No failure of the uncoated material was observed to 250,000 cycles, at which time the test was terminated due to funding constraints. For the coated material, one failure occurred at 205,000 cycles, and the remaining four specimens did not fail up to 250,000 cycles, at which time the test was terminated.

4.5 THERMAL SHOCK/WATER IMMERSION

Thermal shock exposures were conducted on Type 1 and Type 2 coatings on all four of the substrate materials. In no case was there any evidence of coating failure after removal from the liquid-nitrogen bath. With the exception of the beta-21S specimens, which were heated to 1089 K prior to liquid-nitrogen immersion, all of the specimens showed a small weight gain over their pretest values, 0.01 to 0.09 mg/cm^2. This is the result of coating oxidation during heating at a temperature of 1255 K before the low-temperature exposure. Post-test spectral reflectance measurements did not reveal any change in total normal emittance characteristics of any of the specimens within the measurement accuracy. HYMETS tests for a 1-h exposure did not show any increase in catalytic efficiencies. All of the coated specimens survived this severe environmental exposure test without failure or degradation in thermal control performance.

The water immersion test was conducted only on Type 1 coated specimens, because the exterior layer of both Type 1 and Type 2 coatings is of the same composition. For all specimens subjected to this test, a small weight loss was observed after the 24-h exposure. This loss ranged from 0.005 to 0.076 mg/cm^2, and it is probably due to loss of some boron oxide, which is soluble in water. Spectral reflectance data did not show any significant changes in the pretest spectra, so total emittance is essentially not affected by this exposure. Postexposure HYMETS test data for a 1-h period was within the range of recombination efficiencies seen for unexposed specimens of like coating-substrate combinations. This exposure test did not result in any significant degradation of thermal-control properties of the Type 1 coating. The behavior of the Type 2 coating is expected to be the same under these test conditions, because the outer layer compositions are equivalent.

4.6 MORPHOLOGY AND COMPOSITION

Limited studies of morphology and of surface and indepth elemental composition were conducted to obtain some insight into the recombination efficiency of coatings and

why changes occurred during HYMETS exposure. Surface topography plays an important role in the residence time, or accommodation, of a gas-phase atom on a surface. Composition as related to the electronic structure of the surface is probably the dominant factor in atom physisorption in the case of heterogeneous catalytic activity. The scanning electron microscope (SEM) was used to qualitatively examine surface topography. Composition features were semiquantitatively evaluated using energy dispersive x-ray analysis (EDAX) for both surface and indepth examinations.

Limited optical microscopy and Auger electron spectroscopy (AES) techniques were also used to characterize coating-substrate cross sections.

A summary of the coating-surface elemental analyses conducted on posttest specimens is given in Table 7. The relative intensities of the elemental lines detected are categorized from very strong (VS) to very weak (VW). Where two values are reported (as for example, VS/S) the first corresponds to one set of distinct features seen from a SEM, and the second is for a visually different region. In general, two visually different features are seen for the Types 1, 2, and 3 coatings. These are light regions on a dark background, as will be seen later.

Table 7. Summary of Coating Surface Compositional Analysis.

Spec. No.	Coating	Relative Strengths of Elements Detected on Surface of Specimen								Test	Test
	Type	Al	Si	Ti	Nb	Cu	Fe	W	Other	Type	Temp.-K
L13	3a	M	VS	S	W	ND	ND	ND	ND	HYMETS-5hr	1260
L14	3a	M	VS	W	ND	ND	ND	ND	ND	ST.OXID.-5hr	1260
L17	3a	W	VS	M	W	ND	ND	ND	ND	HYMETS-5hr	1260
L29	3	W	VS	M	W	ND	ND	ND	ND	HYMETS-5hr	1260
L31	3	VS/W	M/VS	VS/M	VW/ND	ND	ND	ND	ND	HYMETS-5hr	1260
L33	3	S/M	W/W	VS/W	W/W	ND	W	ND	ND	HYMETS-5hr	1260
L35	3b	VS	S	M	W	ND	ND	ND	ND	HYMETS-5.5hr	1260
L36	3c	VS	S	M	ND	ND	ND	ND	ND	HYMETS-5hr	1260
L37	1	W/W	W/W	S/S	W/ND	ND	ND	ND	ND	HYMETS-5hr	1260
L42	2a	ND	VS	ND	ND	ND	ND	ND	ND	HYMETS-5hr	1260
N1A	1	S/W	VW/VS	S/VW	M/ND	ND	ND	ND	ND	HYMETS-10hr	1205
N9	1	S/M	M/VS	W/W	W/TR	ND	ND	ND	Ca-Tr	HYMETS-10hr	1205
N11	1	M/VW	VS/VS	Tr/ND	Tr/ND	ND	ND	ND	ND	HYMETS-10hr	1205
NA4	1	VW/W	VS/W	Tr/VS	ND/ND	W/M	ND/W	W/M	ND	HYMETS-10hr	1094
N13	1	VS/M	W/S	M/W	ND/Tr	Tr/Tr	Tr/Tr	ND	ND	HYMETS-3.5hr	1260
N14	1	M/VW	M/VS	Tr/ND	ND	ND	ND	ND	ND	HYMETS-3.5hr	1260
R6	2	VS/ND	ND/VS	S/W	M/VW	ND	ND	ND	ND	HYMETS-10hr	1260
N6(A)	2	ND	S/VS	VS/W	VW/ND	ND	ND	ND	ND	HYMETS-1hr	1094
N7(A)	2	ND	VS/VS	VW/Tr	ND	ND	ND	ND	ND	HYMETS-5hr	1094
NG12	1	S/VW	VS/M	W/W	ND	ND	ND	ND	ND	HYMETS-10hr	1260

Note: VS = very strong, S = strong, M = medium, W = weak, VW = very weak, Tr = trace and ND = not detected.

After 5 h or more of HYMETS exposure at temperatures of 1205 K to 1260 K, aluminum is typically present at or very near the surface of the Types 1 and 3 coatings. The aluminum does not appear to be uniformly distributed over the entire surface, but is present in distinct areas, which in turn are uniformly distributed over the surface. The aluminum-rich regions show little silicon, but they include titanium and niobium. The presence of aluminum is expected in the Type 3 coating, as it is a part of the outer-layer formulation. In the Type 1 coating, the aluminum appears to migrate to the surface from the inner coating layer as well as from the substrate. Aluminum was seen at the surface of only one Type 2 coated specimen, NJSR6, and it must come from the substrate. This specimen was exposed for 10 h in HYMETS at a temperature of 1260 K. Other specimens of Type 2 coated substrates exposed in HYMETS for only 5 h or at lower temperatures did not show any evidence of aluminum at the surface. Copper and tungsten, probably from arc heater electrodes, were detected on HYMETS specimens tested at 1094 K. Apparently at the higher specimen temperatures, copper and tungsten do not form compounds on the coating surfaces that are stable at these surface temperatures and pressures. The current configuration of HYMETS does not appear to be suitable for the lower temperature testing of low-recombination-efficiency coatings because of the contamination problem.

Iron and calcium contamination was seen in several instances. The calcium is probably from contact of the coating with the water used for specimen cooling in the heated-cavity reflectance apparatus. The source of iron is not known. It does not appear to be from water, as it was not present when calcium was detected.

Elemental line scans of cross sections of the coating and the substrate for Type 1 coated alpha2 are shown in Figures 42 and 43. The as-prepared specimen is shown in Figure 42, and similar data for a specimen after 100 profiled static oxidation cycles at 1255 K are shown in Figure 43. The total coating thickness of the as-prepared specimen is nominally 5 μm, and the inner and outer layers are seen distinctly from the aluminum, boron, and silicon lines. There is some aluminum depletion in the substrate at the substrate-to-coating interface, and titanium migration from the substrate into the coating is evident. This specimen was heat treated in vacuum at 1255 K for 1/2 h and statically oxidized in air at 1255 K for 1/2 h.

After the 100-cycle static oxidation test, which corresponds to 25 h at a temperature of 1255 K, a 4- to 5-μm-thick interface region has formed, as is seen in Figure 43. Oxygen is present over a total thickness of 10 μm, and silicon is seen over a distance of approximately 17 μm. Boron appears to stay in the coating layer. Aluminum, niobium, and titanium from the substrate have moved into the coating region, but neither niobium or titanium have migrated to the surface of the coating.

Elemental profiles from AES with argon sputtering for two Type 3a coated alpha2 specimens, one after a 5-h HYMETS test and the other after 5 h of static oxidation, are shown in Figure 44. The HYMETS specimen elemental profile shows titanium has migrated to the surface of the coating and niobium is in the coating at a very low concentration. Comparable data for the static oxidation specimen show titanium in

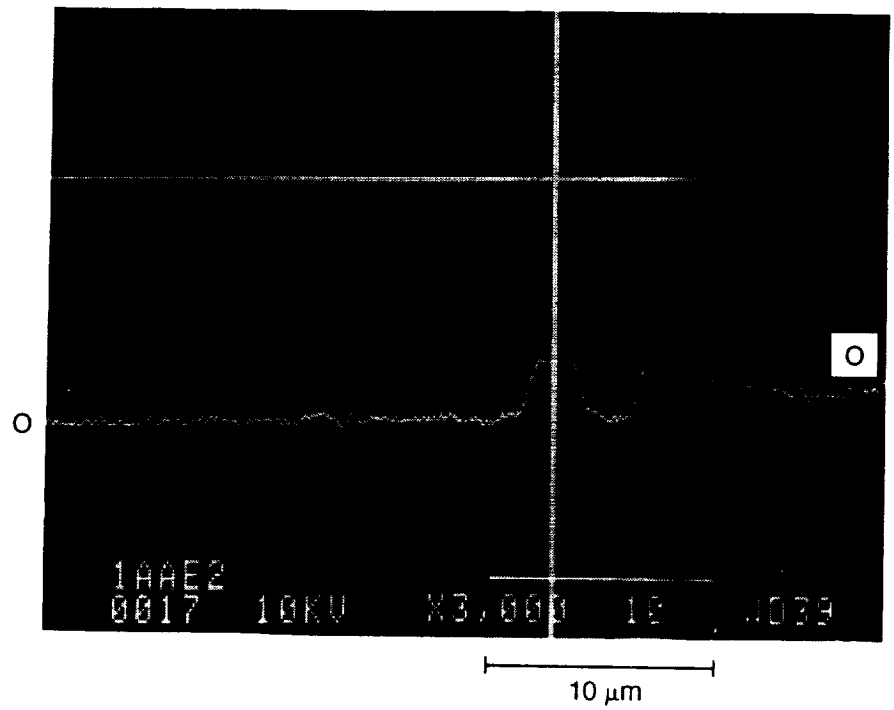

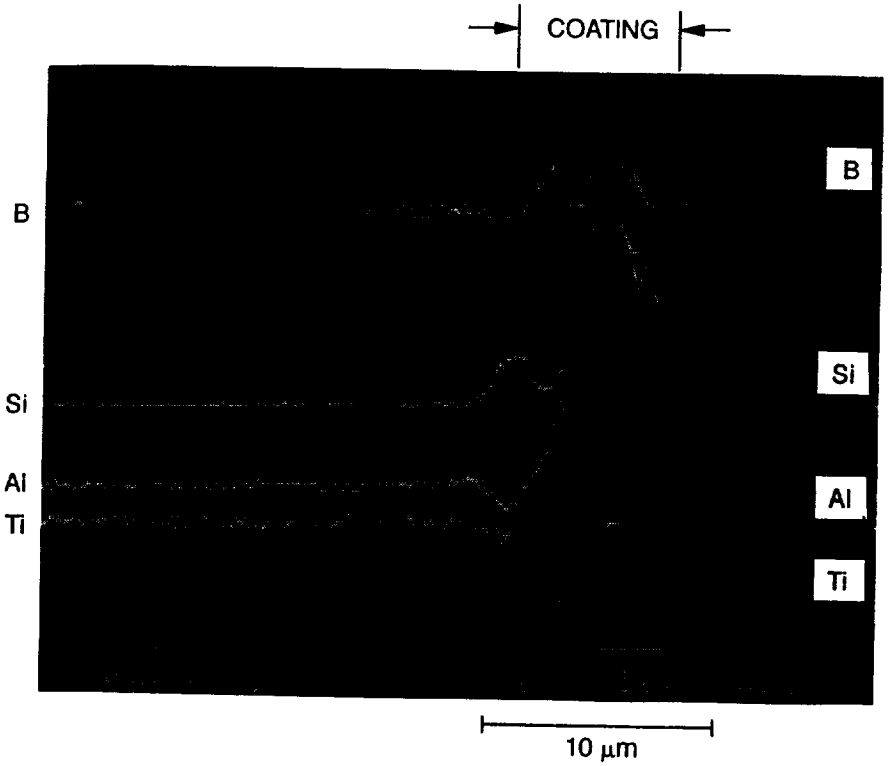

Figure 42. EDAX elemental line scan across a section of as-prepared Type 1 coated alpha2.

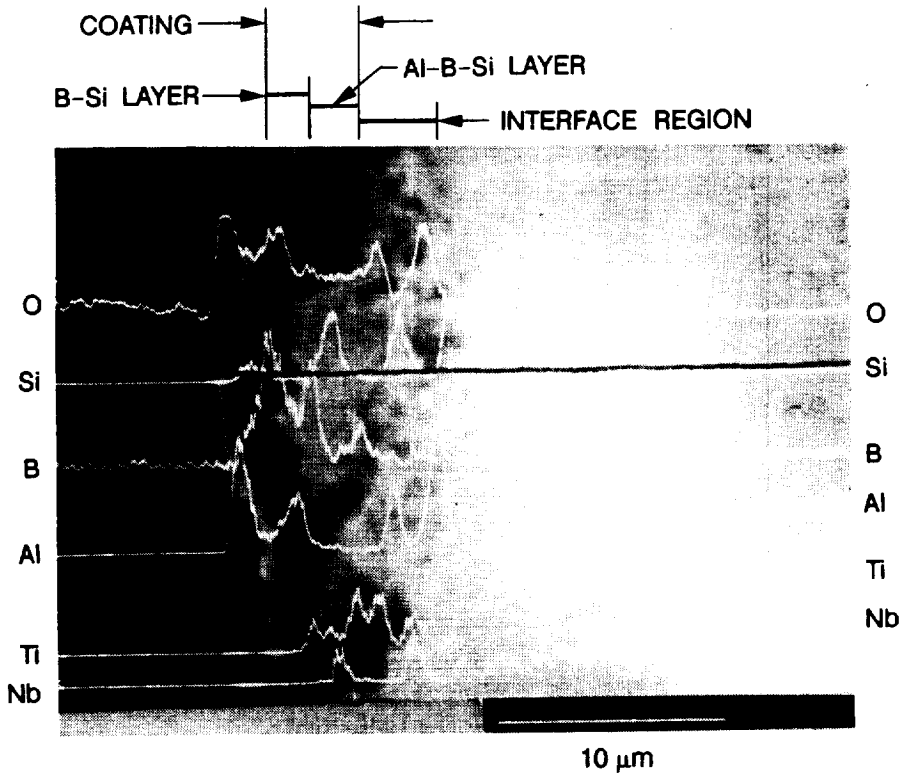

Figure 43. EDAX elemental line scans across a section of Type 1 coated alpha2 after 100-profiled-cycle oxidation test at 1255 K.

the coating but not at the surface, and no niobium is present in the coating near the surface. The sputtering time of 50 min corresponds to a depth into the coating of approximately 0.8 μm.

The elemental profile data for titanium and niobium in the two specimens suggest that the ion transport within the coating and substrate differs between the two types of exposure. The HYMETS environment appears to be the more energetic. Oxygen transport into the coating in this environment is faster, and the titanium moves to the oxygen source.

Figure 45 shows an SEM photograph of a typical surface region of the Type 1 coating after HYMETS testing. Specimen N1A was exposed in HYMETS for 10 h at a temperature of 1255 K. Surface roughness has increased significantly from the as-prepared condition. The light-colored regions are raised from the surface, and they are predominantly aluminum, niobium, and titanium, with minor amounts of silicon. The dark areas show only a trace of aluminum and titanium, with the major constituent as silicon.

An SEM photograph and an elemental map of the surface of a Type 1 coated super-alpha2 specimen, N11, tested for 10 h in HYMETS at a temperature of 1205 K, are

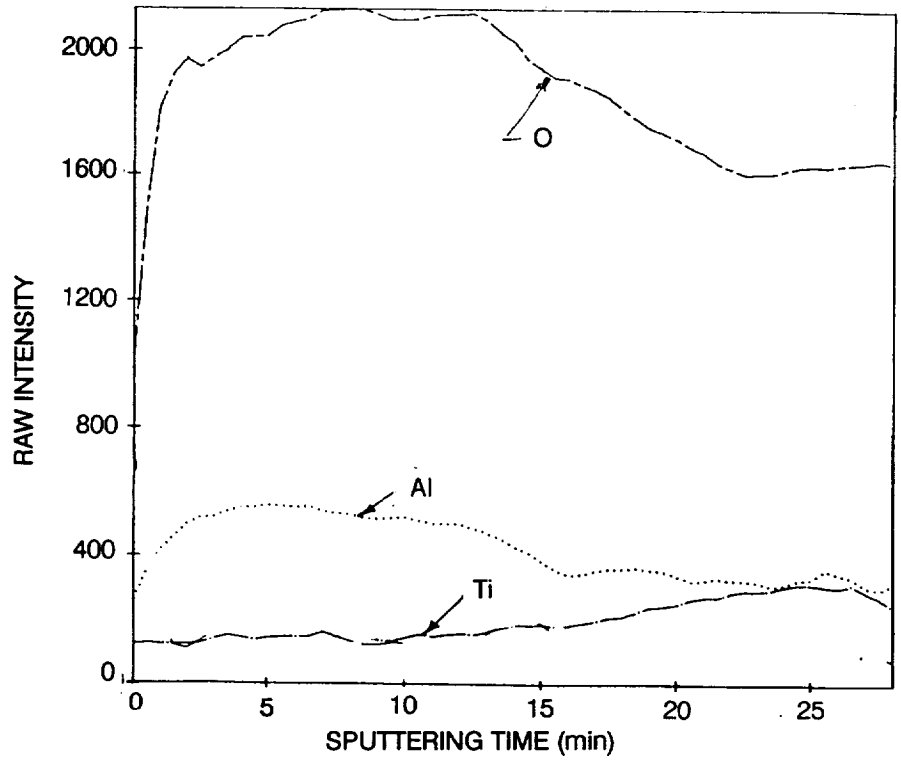

a. After 5 h static oxidation.

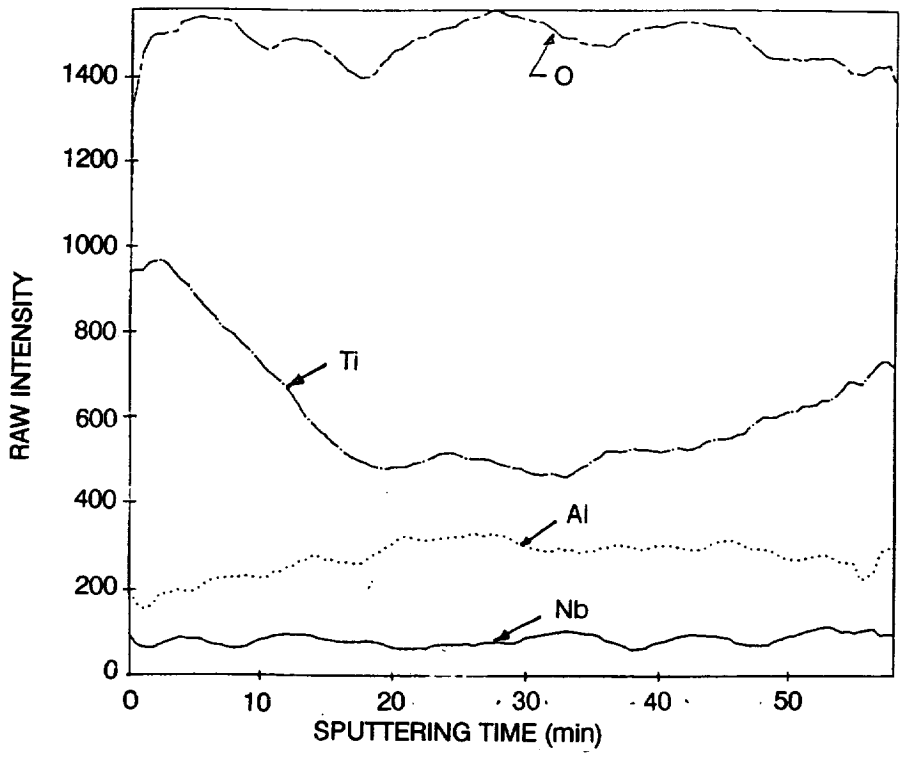

b. After 5 h HYMETS.

Figure 44. AES elemental profiles of Type 3a coated alpha2 specimens after 5 h of exposure in HYMETS and static oxidation tests at 1255 K.

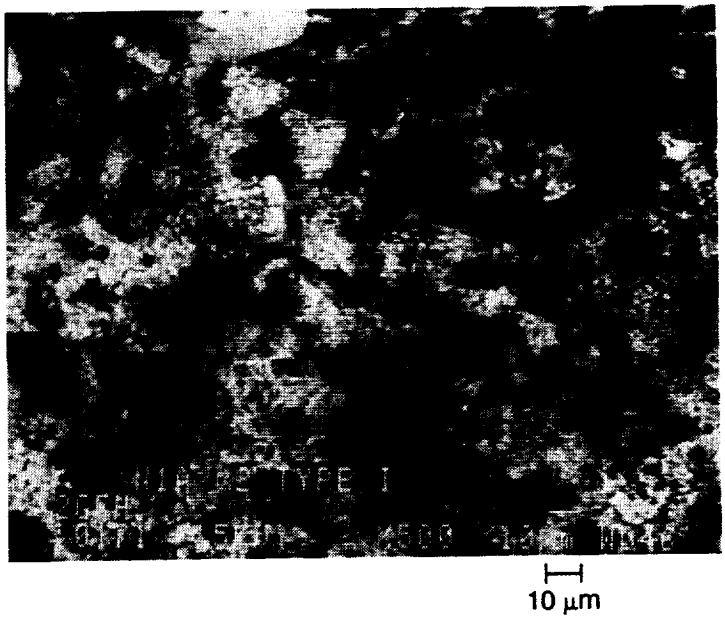

Figure 45. SEM photograph of surface of Type 1 coated alpha2 (N1A) after 10-h HYMETS test at a temperature of 1255 K.

shown in Figure 46. The light areas in the photograph showed moderate amounts of aluminum with trace amounts of niobium and titanium. The dark regions showed very small aluminum concentration and no niobium or titanium was detected. Both regions showed very strong silicon intensities. The surface roughness increased from the typical pretest appearance, and the light areas appear to be slightly raised platelets.

Figure 47 is an elemental map of a cross section of Type 1 coated super-alpha2, Specimen No. N11. Silicon migration into the substrate is seen, together with aluminum depletion of the substrate. Titanium has migrated into the coating with niobium and aluminum from the substrate. The island-like distribution of these elements is seen through the thickness of the coating.

Figure 48 shows a photomicrograph of a cross section and a SEM photograph of the surface of a Type 1 coated super-alpha2 specimen, No. N14, after a 3.5-h HYMETS test at 1260 K. The photomicrograph shows the well-defined coating region, which is light gray, and the interface region, which is dark and irregular in thickness. An EDAX scan across this region again showed the silicon penetration into the substrate and the aluminum migration from the substrate. The SEM photograph shows a needle-like surface structure. The light regions contain moderate amounts of aluminum and silicon with a trace of titanium. The dark areas are silicon with a trace of aluminum and no detectable titanium. Niobium was not found in either region.

Another example of the platelet-like structure appearing on the coating surface is seen in the SEM photograph in Figure 49. The edges of these platelets, which are 50 to 250 μm in planar dimension, appear to be sharp, and this feature would enhance gas-phase accommodation on the surface. The composition of the platelets is

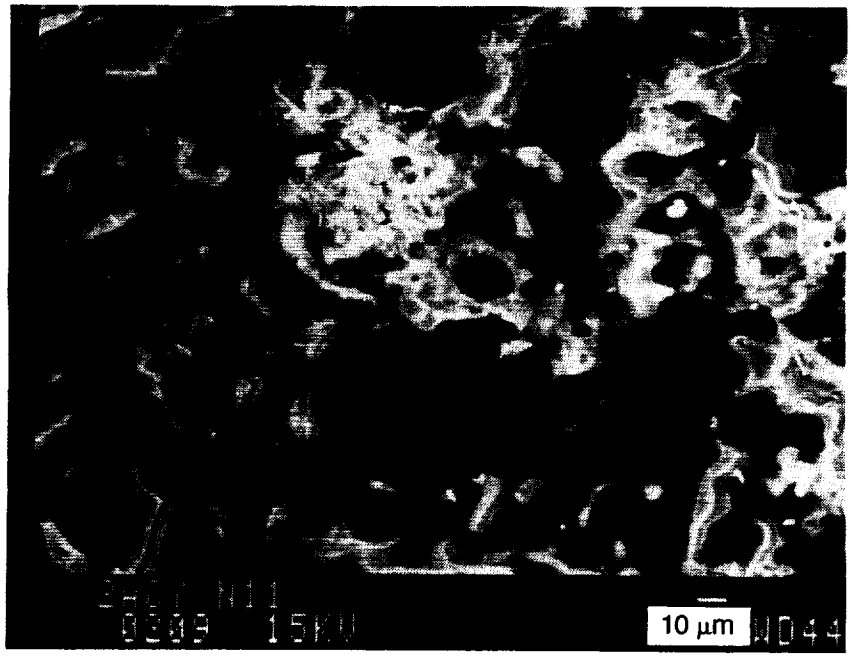

a. SEM image of surface.

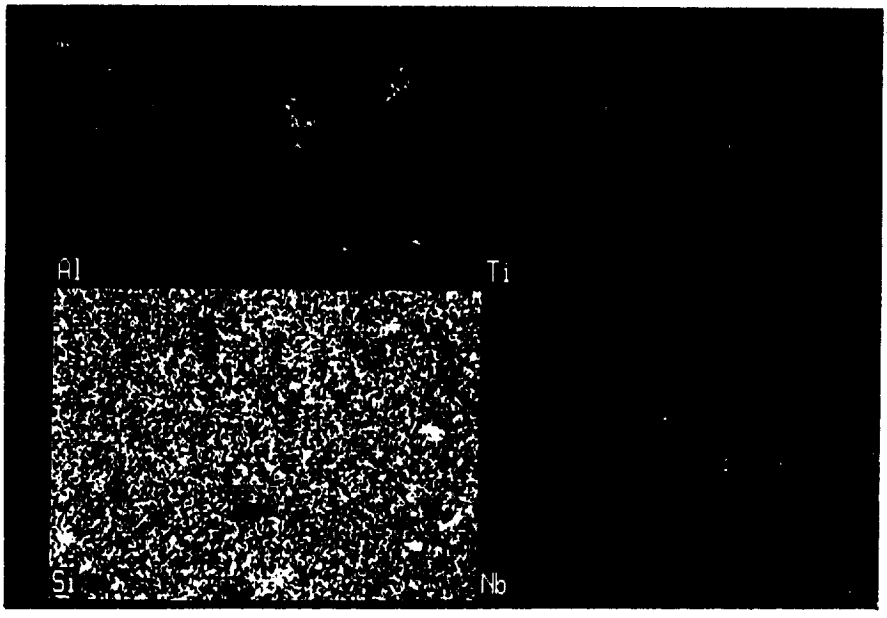

b. Elemental map of surface.

Figure 46. SEM and elemental map of surface of Type 1 coated super-alpha2, Specimen No. N11, after 10-h HYMETS test at 1205 K

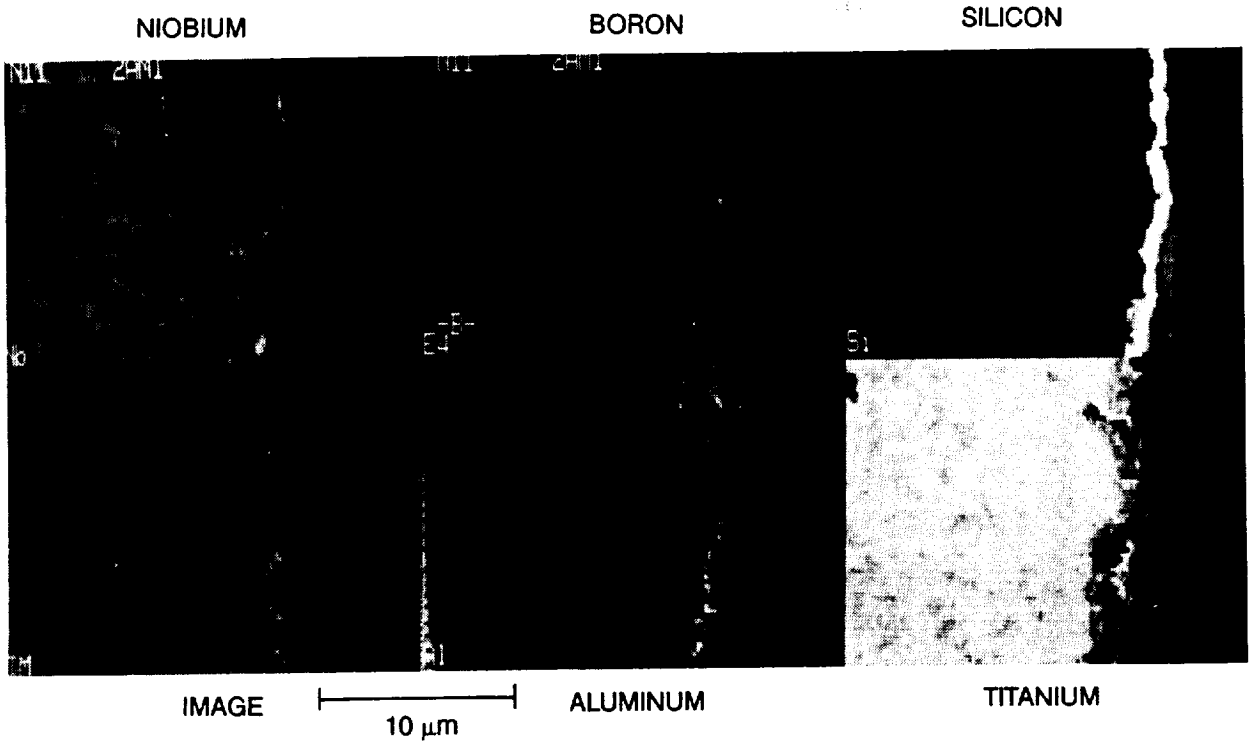

Figure 47. Elemental map of a cross section of Type 1 coated super-alpha2, Specimen No. N11, after 10-h HYMETS test at 1205 K.

aluminum as the major detected element with strong silicon intensity and a trace of titanium. For the dark regions, only silicon was detected.

A typical contamination pattern of copper and tungsten on the coating surface after HYMETS tests at 1089–1094 K is shown in the SEM photograph and elemental map of Figure 50. The contaminants are highlighted in the backscattered electron image of Figure 50a. An identical surface pattern for tungsten distribution is seen in the elemental map. One area is a mixture of titanium and tungsten. The tungsten compound masks the underlying silicon, as is seen in the silicon map in the upper left portion of Figure 50b. The types of compounds formed by these contaminants is not known, but the tungsten may be an oxide which dissociates readily in low pressures at temperatures greater than 1100 to 1200 K. Similar low-temperature–low-pressure dissociation occurs for copper oxides. The surface SEM photograph shows evidence of cracks in the outer layer of the coating. These have not been seen for this type of coating at the higher test temperatures. It is postulated that these are thermal stress cracks which occur during the rapid heatup and cooldown in HYMETS. At the higher temperatures, the layer softens and accommodates the strains without cracking.

A similar type of surface cracking is seen in the SEM photograph of a Type 2 coated beta-21S specimen in Figure 51. Again, we see the lower temperature stress cracking of the boron-silicon layer. The light regions contain silicon, titanium, and copper. A

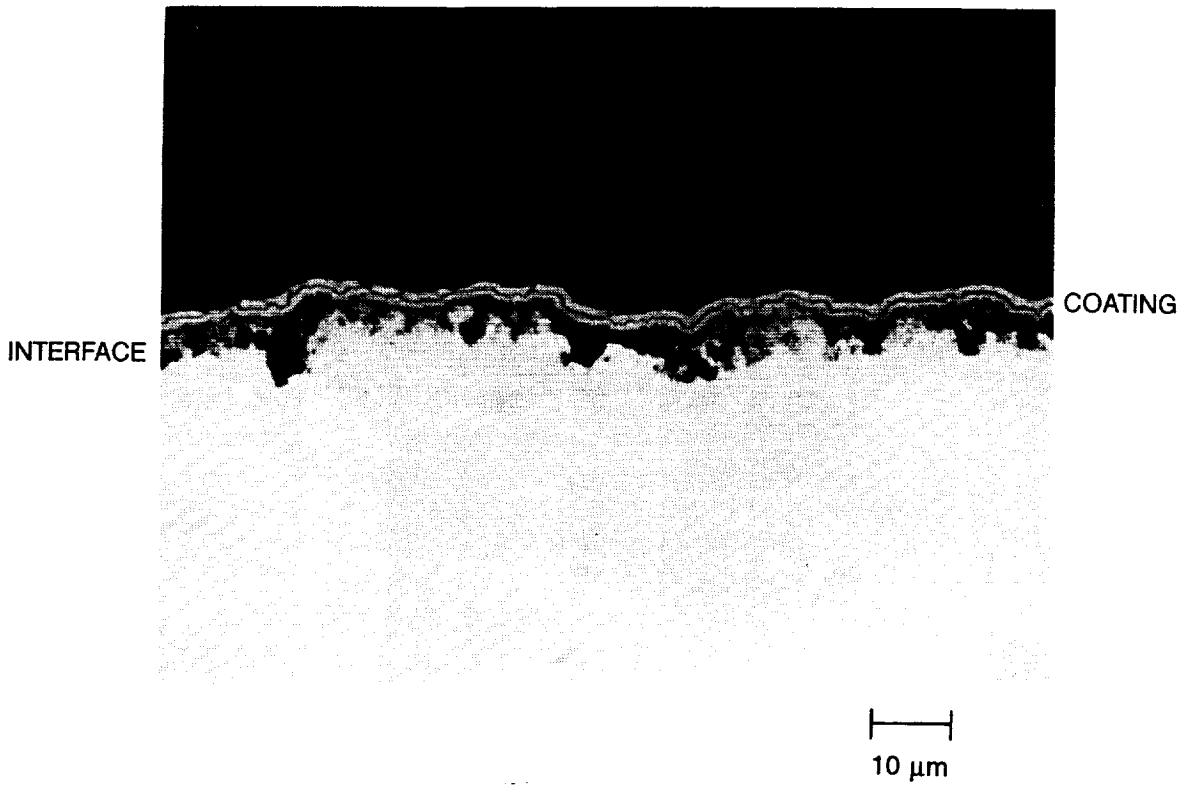

a. Photomicrograph.

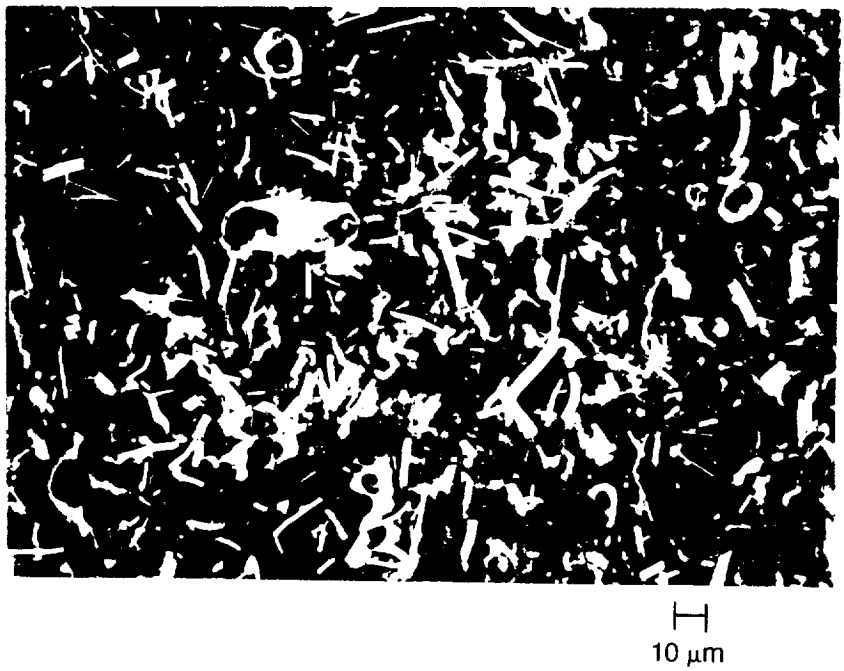

b. SEM photograph.

Figure 48. Photomicrograph of a cross section and SEM photograph of the surface of Type 1 coated super-alpha2, Specimen No. N14, after 3.5-h HYMETS test.

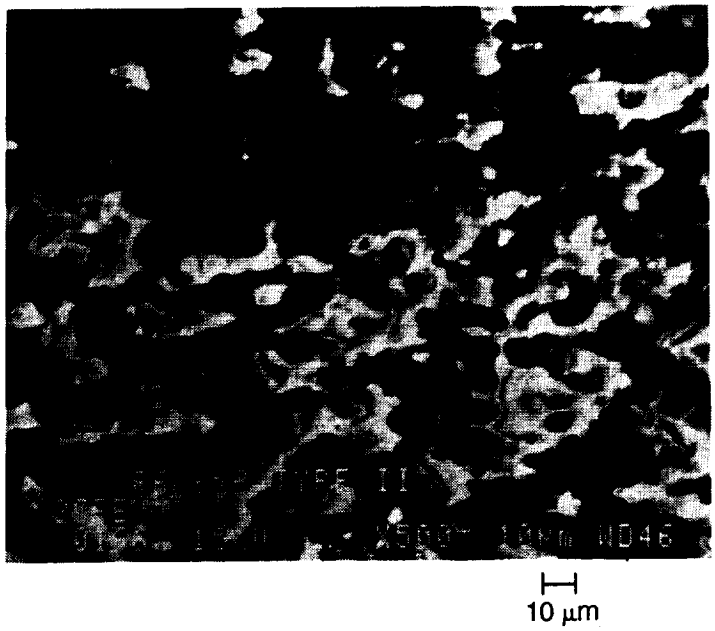

Figure 49. SEM photograph of surface of Type 1 coated gamma after 10-h HYMETS test at 1260 K, Specimen No. NG12.

trace of calcium was also detected in these regions. The dark areas showed silicon with a trace of titanium.

Figure 52 is a SEM photograph of the surface of a Type 2 coated super-alpha2 specimen after a 10-h test in HYMETS at a temperature of 1260 K. The light areas show strong intensities for aluminum, niobium, and titanium without detectable silicon. The dark regions show silicon with no detectable amount of aluminum and trace quantities of niobium and titanium. This coating does not contain aluminum as a basic constituent, therefore the aluminum detected in the light areas must come from the substrate. We do not see aluminum near the coating surface for this specimen after a 5-h HYMETS exposure. As a very rough estimate, the aluminum ion diffusion velocity in the boron-silicon layer is less than 0.7 μm/hr and greater than 0.3 μm/hr, based on the coating thicknesses for the two specimens (see Table 5) and a detection depth of EDAX of 1 μm. The effect of the two different test temperatures was not considered.

Photomicrographs of cross sections of Type 1 coated gamma and beta-21S fatigue specimens are shown in Figures 53 and 54, respectively. The gamma specimen (Figure 53) appears to have a 3- to 4-μm-thick layer which is the Al-B-Si layer and some mixing with the substrate along grain boundaries. A distinct Al-B-Si sublayer and the B-Si top layer are clearly seen in beta-21S (Figure 54). There does not appear to be mixing of layers and substrate with the lower heat treatment and static oxidation temperature of 1094 K used for the beta-21S alloy. The gamma specimen was processed at 1255 K, and we see evidence of coating reaction with the substrate.

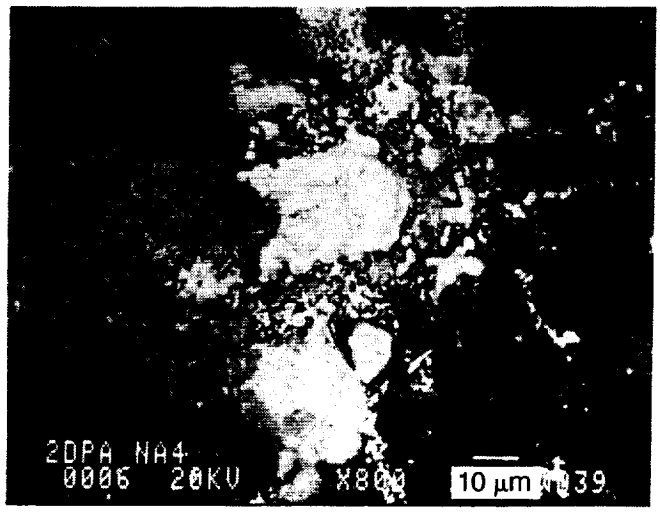

a. Backscattered electron image of surface.

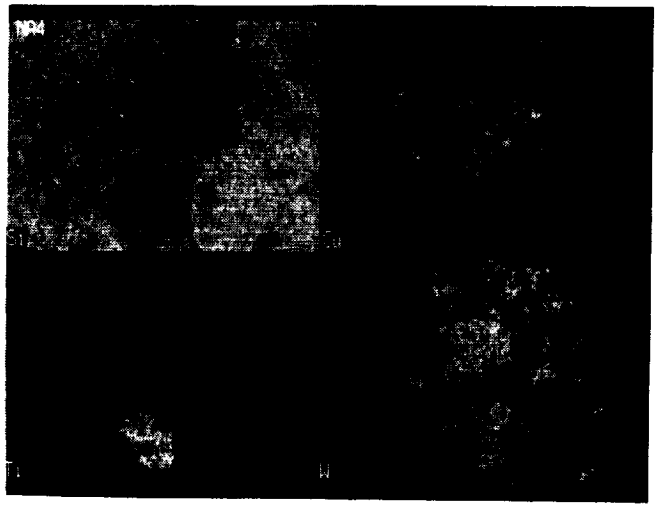

b. Elemental map of surface.

Figure 50. SEM image and elemental map showing copper and tungsten contamination on surface of Type 1 coated beta-21S alloy, Specimen No. N4A, after 10-h HYMETS test.

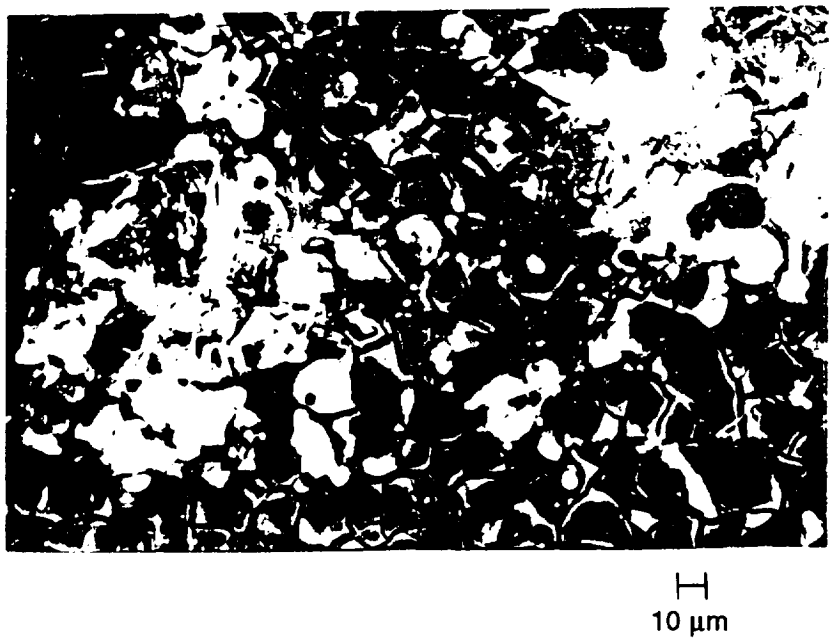

Figure 51. SEM photograph of the surface of Type 2 coated beta-21S, Specimen No. N7(A), after 5-h HYMETS test at 1094 K.

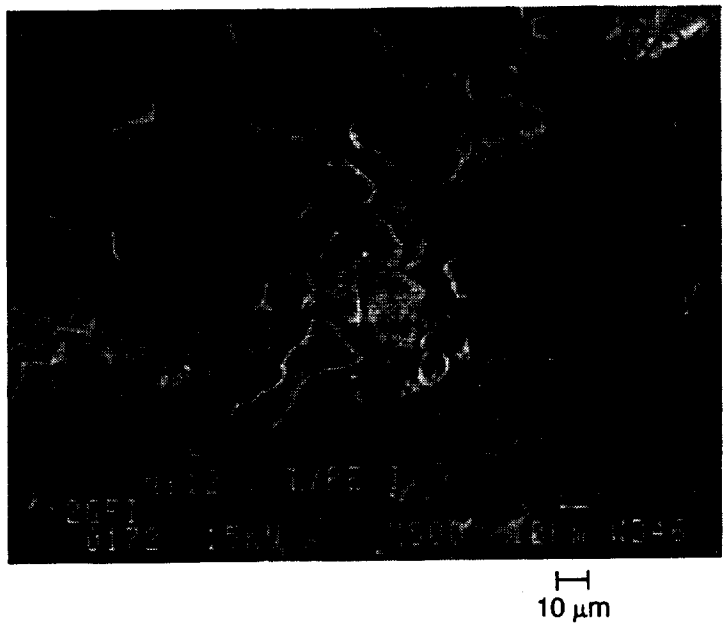

Figure 52. SEM photograph of surface of Type 2 coated super-alpha2, Specimen No. NSJR6, after 10-h HYMETS exposure at 1260 K.

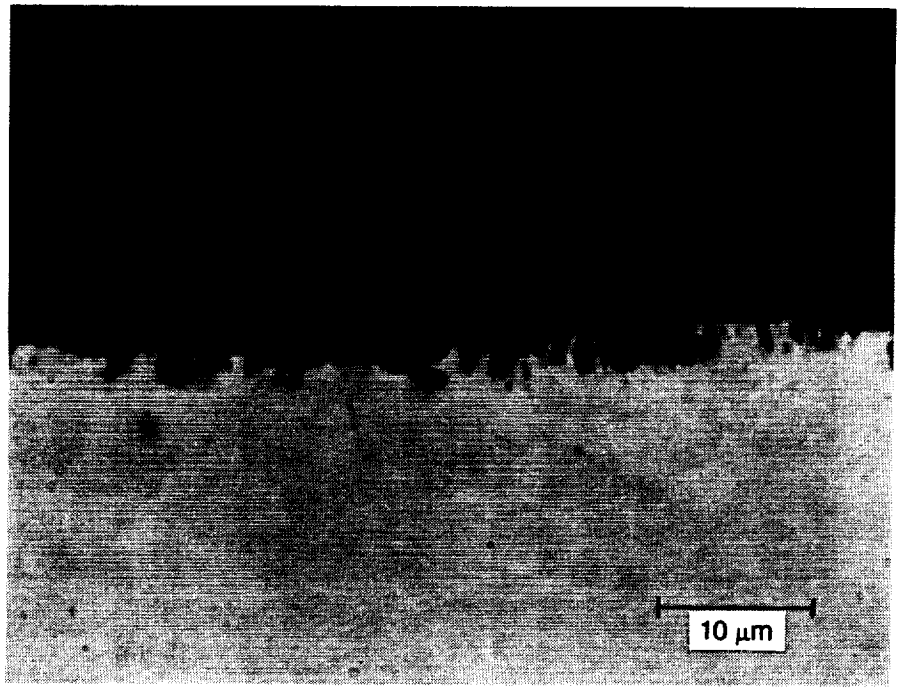

Figure 53. Photomicrograph of coating-substrate cross section of Type 1 coated gamma fatigue specimen in region of failure.

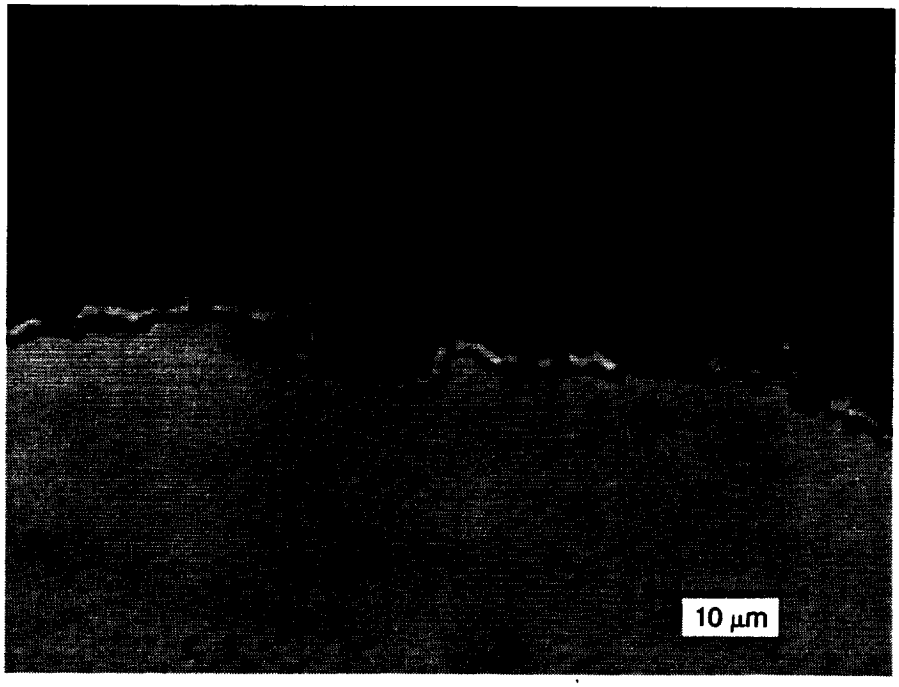

Figure 54. Photomicrograph of coating-substrate cross section of Type 1 coated beta-21S fatigue specimen in region of failure.

4.7 HYDROGEN EXPOSURE

The hydrogen pick-up of an uncoated beta-21S specimen after 24 h at 1090 K was 56 at. %, as measured by the mass of hydrogen required to maintain a constant pressure in the exposure chamber. This is considerably less than the reported value of 67 at. %. This difference is probably due to inaccuracies in the flow measurement for the low-pressure test conditions. The hydrogen pickup for a Type 1 coated specimen was zero in the same test. These data can only be viewed qualitatively, but it appears that the coating provides a good degree of protection from hydrogen intrusion into the substrate.

Section 5
DISCUSSIONS AND RECOMMENDATIONS

A comparison of the performance of the coatings with respect to the initial program goals is given in Table 8. The actual goal for recombination efficiency was to achieve as low a value as possible. The numerical value of 0.02 is not derived from any specific program requirement, but was chosen as representing the lower limit of what could be accurately determined in the HYMETS test.

Table 8. Coating Performance Summary.

Property	Goal	Test Result
Oxidation Resistance	Prevent oxidation of substrate	No evidence of substrate oxidation or coating failure. Oxygen pickup less than that required for full oxidation of coatings
Total Emittance	≥0.80 at 1255 K, for 10-h HYMETS	Type 1: 0.80 to 0.89 Type 2: 0.82 to 0.88 Type 3: 0.88 to 0.90
Recombination Efficiency	Initially ≤0.02, ≤0.03 after 10-h HYMETS at 1255 K	Type 1: ≤0.018 initially, ≤0.05 10 h Type 2: ≤0.018 initially, ≤0.03 10 h Type 3: ≤0.034 initially, ≤0.08 5 h
Mechanical Fatigue	Coating does not degrade room-temperature fatigue performance of substrate	No differences observed between uncoated and coated specimens

5.1 OXIDATION RESISTANCE

Oxidation protection provided to the three titanium-aluminides and one titanium alloy by the aluminum-boron-silicon and boron-silicon coatings applied by the LMSC low-pressure, low-temperature CVD process is excellent on the basis of the experimental investigations conducted in this program. Additional investigations of the mechanical properties of the coated materials after exposure to the simulated hypersonic flight environment are needed to confirm this. The limited mechanical-property data obtained to date are from static oxidation environments. It is believed that the kinetics of oxidation and ion transport within the coating and substrate are different in the static and molecular air environments from those in a hypersonic boundary

layer with dissociated air species and nonequilibrium chemistry. Additional testing under hypersonic flight conditions should be carried out in facilities capable of testing specimens of sufficient size for realistic mechanical properties studies.

5.2 EMITTANCE

The emittance properties of the coatings have been adequately verified with the HYMETS tests for screening and ranking purposes. However, additional tests should be conducted to directly measure total hemispherical emittance as a function of temperature. This again requires the exposure of significantly larger specimens in the simulated hypersonic environment. The high-temperature total emittance values obtained to date using room-temperature spectral near-normal reflectance measurements have an estimated uncertainty of 0.03 emittance units. More accurate emittance data are needed for analysis of actual vehicle flight data in the context of obtaining recombination efficiencies at various body stations for the overall flight environment.

5.3 RECOMBINATION EFFICIENCY

Hot-wall recombination efficiencies of the Type 2 coating are slightly less than those of the Type 1 coating under hypersonic flight simulation conditions (HYMETS exposure). The increase in recombination efficiency with increasing exposure time in HYMETS is also smaller for the Type 2 coating. The Type 3 coating has a higher recombination efficiency and exhibits a significantly greater increase with exposure time than the other coatings. The presence of aluminum at the surface of Types 1 and 3 coatings is believed to cause the increase in hot-wall recombination efficiency. Aluminum migrates to the surface from the aluminum-containing coating layer.

Recombination efficiencies of Types 1 and 2 coatings are the lowest that have been measured for coatings on titanium-aluminides and titanium alloys in HYMETS for temperatures of 1089 K to 1255 K. Comparison with data for the RCG coating of the Space Shuttle Orbiter Thermal Protection System in HYMETS tests shows that the hot-wall efficiencies of the Types 1 and 2 coatings are approximately 60% of that of RCG at 1255 K.

The absolute accuracy of hot-wall catalytic efficiency as measured by the HYMETS is estimated to be 0.007. The uncertainty in the value is driven by the individual uncertainties of specimen heat-loss terms in the energy-balance equation, total hemispherical emittance of the surface, and fully catalytic hot-wall heating rate. The precision of the measurement is estimated to be 0.004. Thus, these data provide for an excellent ranking of coatings. However, the data should not be used in the absolute sense for design purposes nor should they be applied to other boundary-layer conditions or an actual flight environment.

5.4 MECHANICAL FATIGUE

The room-temperature fatigue results are derived from a small sample population, five specimens for each condition, and they should be treated qualitatively because of the large variation in fatigue life seen within a given set. The very large data spread observed for the uncoated specimens prevents the development of a truly qualitative assessment of coating effects. A much larger sample population would be required to refine the quantitative conclusion that the coating application and/or processing does not appear to degrade substrate performance.

The effect of 100-h static oxidation at temperatures of 1205 K and 1255 K on room-temperature fatigue life was evaluated qualitatively using two five-specimen sets of Type 1 coated super-alpha2. No significant difference in fatigue life was observed between the as-coated and the 1205 K, 100-h specimens. However, for the specimens treated at 100 h at 1255 K, fatigue life was reduced to less than 50% of the as-coated value. It is not known whether this degradation was the result of substrate oxidation, a coating-substrate reaction, or, simply, thermally induced changes in the substrate microstructure.

5.5 COATING/PROCESS MODIFICATIONS

A barrier layer to prevent the diffusion and reaction of the substrate constituents with the coating is needed if stable recombination efficiencies of 0.010 to 0.015 are required. A reduction of recombination efficiency from 0.030 to 0.010 results in a 55 K decrease in adiabatic wall temperature for a surface having an emittance of 0.80 under HYMETS conditions corresponding to the 1255 K specimen temperature tests conducted in this program. This layer would impede diffusion of niobium and titanium to the surface of the coatings. It must be very thin and also not diffuse to the coating surface or into the substrate. The use of a barrier layer may degrade the coating bonding characteristics unless it provides reactive bonds with both the substrate and the coating.

Section 6
CONCLUDING REMARKS

The results of this study have demonstrated the performance in a laboratory environment of two types of CVD coatings for three titanium-aluminides and one titanium alloy which are candidate materials for use as heat-shield and structural components of hypersonic flight vehicles having multiple reuse capability. The titanium-aluminides are alpha2, super-alpha2, and gamma. The titanium alloy is beta-21S. The criteria for acceptable coating performance are: (1) prevent oxidation of the metallic materials, (2) have a high total hemispherical emittance and low recombination efficiency up to the maximum-use temperature of the metals for multiple flight cycles, and (3) do not cause degradation of the mechanical properties of the substrate materials. Both the Type 1 multilayer coating, an aluminum-boron-silicon sublayer with a boron-silicon outer layer, and the Type 2 single layer boron-silicon coatings are excellent candidates for the hypersonic vehicle application, as is shown by the following performance data:

- No evidence of oxidation of the substrate materials was found after 100 h of exposure in a static air environment to temperatures of 1255 K. The same observation was valid for specimens exposed in a simulated hypersonic flight environment for 10 h.
- Total normal emittance of the coated titanium-aluminides was 0.81 or greater for temperatures from 900 K to 1255 K throughout 10-h simulated hypersonic flight environmental simulation tests at a specimen temperature of 1255 K. Total normal emittance of the coated beta-21S alloy was 0.76 or greater for the same type of test with a surface temperature of 1089 K.
- Under the simulated hypersonic flight environment test conditions, the hot-wall recombination efficiency of the Type 2 coated titanium-aluminides was less than 0.035 throughout a 10-h test at a temperature of 1255 K. The hot-wall recombination efficiency of the Type 1 coating was 0.030 or less through 5 h of testing at 1255 K, but it increased to 0.050 at 10 h of exposure. The hot-wall recombination efficiency of both coatings on beta-21S at a test temperature of 1089 K was 0.020 or less up to 3 to 5 h of exposure, at which time contamination of the surface of the specimens with arc electrode materials resulted in a large increase in recombination efficiency and invalidated the data for longer times.
- Results of mechanical fatigue tests conducted at room temperature on both coated and uncoated specimens showed no measurable differences in fatigue life. Also, fatigue life was essentially unchanged after 100-h static oxidation at 1205 K. However, increasing the static oxidation temperature to 1255 K for 100 h resulted in a 50% reduction in fatigue life. It is not known whether this degradation is due to substrate oxidation, a coating-substrate reaction, or temperature-induced microstructural changes in the alloy.

- **The single-layer coating is the recommended choice for all of the structural materials investigated in this study because of its lower recombination efficiency and the simpler processing associated with the single-layer system.**

Section 7
REFERENCES

1. Clark, R. K.; Cunnington, G. R.; and Wiedemann, K. E.: Environmental Coatings for Titanium-Aluminide Alloys, NASP TM-1141, 1991.
2. Cunnington, G. R.; and Robinson, J. C.: Radiative Properties of Advanced Spacecraft Heat Shield Materials, NASA CR-178110, 1986.
3. Lavendel, H. W.; and Robinson, J. C.: United States Patent 4,689,104, August 25, 1987.
4. Ibid.: United States Patent 4,692,388, September 8, 1987.
5. Ibid.: United States Patent 4,778,726, October 18, 1988.
6. Ibid.: United States Patent 4,806,431, February 21, 1989.
7. Ibid.: United States Patent 4,818,625, April 4, 1989.
8. Linnett, J. W.: and Marsden, D. G. H.: The Kinetics of the Recombination of Oxygen Atoms at a Glass Surface, *Proc. of the Royal Society*, Series A, Vol. 234, March, 1956, pp. 489-504.
9. Morrison, S. R.: *Chemical Physics of Surfaces*, Plenum Press, New York, 1977.
10. Clark, R. K.; Cunnington, G. R.; and Robinson, J. C.: Vapor-Deposited Emittance-Catalysis Coatings for Superalloys in Heat-Shield Applications, *J. Thermophysics and Heat Transfer*, Vol. 1, No. 1, January 1987, pp 28-34.
11. Goulard, R.: On Catalytic Recombination Rates in Hypersonic Stagnation Heat Transfer, *J. Jet Propulsion*, Vol. 28, 1958, pp 737-745.
12. Zoby, E.: Empirical Stagnation-Point Heat-Transfer Relation in Several Gas Mixtures at High Enthalpy Levels, NASA TN D-4799, October 1968.
13. Cunnington, G. R.; Funai, A. I.; and McNab, T. K.: Radiative Properties of Advanced Spacecraft Heat Shield Materials, NASA CR-3740, 1983.
14. Cunnington, G. R.; Funai, A. I.; and Cassady, P. E.: Development of Techniques and Associated Instrumentation for High Temperature Emissivity Measurements. NASA CR-124423, 1973.
15. Dunkle, R. V.; Edwards, D. K.; Gier, J. T.; Nelson, K. E.; and Roddick, R. D.: Heated Cavity Reflectometer for Angular Reflectance Measurements, *Progress in International Research on Thermodynamic and Transport Properties*, Academic Press, New York, 1962.

Section 8
NOMENCLATURE

c_p	specific heat
d_{eff}	effective diameter of blunt body
F_{diff}	defined in Eq. (10)
H	enthalpy
k	thermal conductivity
k_w	defined in Eq. (7)
K_{air}	dimensionless stagnation point velocity gradient
L	thickness
M_{air}	molecular weight of air
P	pressure
q	heat flux
R_u	universal gas constant
t	time
T	temperature
v	velocity

Greek Symbols

γ	recombination efficiency
ε_{TH}	total hemispherical emittance
ρ	density
σ	Stefan-Boltzmann constant
ϕ	defined in Eq. (6)

Subscripts

b	back surface of insulation layer
c	convective
d	dissociation
ins	insulation
o	initial
s	specimen
w	wall

Appendix A
HYMETS TEST DATA

Results of the HYMETS arc-plasma heated hypersonic wind tunnel tests are tabulated in this appendix. The data are summarized in terms of the parameters of specimen temperature, free-stream Mach number, free-stream enthalpy, specimen surface pressure, specimen total hemispherical emittance at temperature, and the calculated values of cold-wall and hot-wall recombination efficiencies for typical time intervals of 0.25 h during the total test exposure period. Data for the uncoated alpha2, beta-21S and gamma materials are shown on page A-3. Data for the coated materials are contained on pages A-4 through A-22.

Table A-1. HYMETS Test Data for Uncoated Alpha2, Beta 21S, and Gamma Materials.

Time, Hr.	Temp., K	Mach No.	Enthalpy cal/gm	P-wall, torr	Emit. at Temp	Cat. Efficiency Cold	Hot
SPEC. NO.: Ti3Al-1	ALLOY: Ti-14Al-21Nb		THICKNESS, CM: 0.057				
0	325	4	1644	5.76		0.01	
0.25	1260	3.95	1360	5.03	0.77		0.063
0.5	1260	3.95	1385	5.07	0.78		0.06
0.5	325	3.99	1630	5.76		0.017	
0.5	325	3.98	1653	5.77		0.02	
0.75	1260	3.94	1410	5.11	0.78		0.054
1	1260	3.93	1398	5.08	0.78		0.057
SPEC. NO.: G1	ALLOY: Ti-33Al-6Nb-1.4Ta		THICKNESS, CM: 0.0465				
0	325	3.78	2385	6.26		0.021	
0	325	3.78	2385	6.26		0.011	
0.5	1260	4.07	1419	5.36			0.049
0.5	325	3.79	2419	6.3		0.02	
0.75	1260	4.06	1337	5.3			0.063
1	1260	4.06	1315	5.27			0.069
1	325	3.77	2458	6.3		0.02	
SPEC. NO.: B21S	ALLOY: BETA-21S Ti		THICKNESS, CM: 0.06383				
0	325	4.03	1949	6.19	0.2	0.006	
0.25	1094	3.91	727	4.09	0.79		0.698
0.5	1094	3.9	734	4.09	0.8		0.662
0.5	325	4.08	1849	6.2	0.43	0.029	
0.75	1094	3.91	738	4.19	0.81		0.612
1	1094	3.91	741	4.19	0.82		0.652
1	325	4.07	1837	6.21	0.66	0.028	
1	325	4.03	1946	6.19	0.66	0.025	
1.25	1094	3.93	721	4.02	0.83		1
1.5	1094	3.92	729	4.02	0.84		1
1.75	1094	3.92	738	4.11	0.85		1
2	1094	3.91	737	3.91	0.86		1
2	325	4.04	1887	6.24	0.73	0.023	
2	325	3.99	1968	6.23	0.73	0.038	
2.25	1094	3.93	740	4.11	0.88		1
2.5	1094	3.95	742	4.1	0.88		1
2.5	325	4.04	1891	6.21	0.74	0.052	
2.75	1094	3.98	749	4.28	0.88		1
3	1094	3.93	749	4.29	0.88		0.904
3	325	4.02	1970	6.17	0.75	0.045	
3.25	1094	3.98	748	4.14	0.88		1
3.5	1094	3.97	751	4.12	0.89		1
3.5	325	4.01	1960	6.29	0.76	0.053	
3.75	1094	3.91	737	4.36	0.89		1
4	1094	3.91	737	4.36	0.89		1
4	325	4.01	1941	6.22	0.77	0.042	
4.25	1094	3.97	756	4.11	0.9		1
4.5	1094	3.98	755	4.11	0.9		1
4.5	325	3.97	2007	6.21	0.78	0.043	
4.75	1094	3.96	744	3.99	0.9		1
5	1094	3.96	747	3.98	0.9		1
5	325	3.97	2018	6.19	0.79	0.04	

Table A-2. HYMETS Test Data for Type 3 Coated Alpha2 Specimens L-29 and L-33.

SPEC. NO.: L29 ALLOY: Ti-14Al-21Nb THICKNESS, CM: 0.0597

Time, Hr.	Temp., K	Mach No.	Enthalpy cal/gm	P-wall, torr	Emit. at Temp	Cat. Efficiency Cold	Hot
0.5	1260	4.09	1733	5.57			0.035
0.5	325	4.1	1716	5.52		0.008	
1	1260	4.02	1600	5.44			0.045
1	325	4.12	1710	5.62		0.014	
1	325	4.02	1861	5.45		0.004	
1.5	1260	4.18	1504	5.04			0.062
1.5	325	4.04	1830	5.44		0.011	
2	1260	4.07	1489	4.91			0.067
2	325	3.98	1794	5.3		0.011	
2.5	1260	4.09	1466	4.95			0.063
3	1260	4.06	1437	4.92			0.065
3	325	4.04	1840	5.45		0.019	
3	325	4.03	1816	5.23		0.015	
3.5	1260	4.06	1567	4.9			0.048
3.5	325	4.04	1820	5.24		0.013	
4	1260	4.15	1349	5.41			0.07
4	325	4.03	1832	5.22		0.015	
4.5	325	4.05	1803	5.26		0.004	
4.5	1260	3.94	1438	4.8			0.07
4.5	325	4.03	1840	5.31		0.007	
5	1260	4.06	1470	4.85			0.063

SPEC. NO.: L31 ALLOY: Ti-14Al-21Nb THICKNESS, CM: 0.0593

0	325	3.96	1642	5.61		0.005	
0.25	1260	3.83	1774	5.88			0.021
0.5	1260	3.93	1715	5.79			0.025
0.5	325	3.95	1664	5.63		0.003	
0.75	1260	3.87	1649	5.66			0.028
1	1260	3.87	1645	5.65			0.028
1	325	3.97	1662	5.68		0.001	
1	325	4.02	1556	5.72		0.005	
1.25	1260	3.92	1391	5.45			0.055
1.5	1260	3.92	1391	5.45			0.055
1.5	325	3.99	1636	5.84		0.005	
1.5	325	4	1670	5.87		0.003	
1.75	1260	3.9	1458	5.55			0.042
2	1260	3.9	1470	5.58			0.041
2	325	3.98	1676	5.74		0.005	
2	325	4	1637	5.75		0.004	
2.25	1260	3.91	1371	5.32			0.059
2.5	1260	3.92	1404	5.38			0.052
2.5	325	3.97	1671	5.66		0.004	
2.75	1260	3.91	1419	5.34			0.049
3	1260	3.91	1449	5.37			0.045
3	325	3.98	1638	5.7		0.004	
3	325	3.99	1649	5.7		0.004	
3.25	1260	3.9	1426	5.34			0.047
3.5	1260	3.89	1487	5.43			0.039
3.5	325	3.96	1694	5.75		0.006	
3.5	325	4	1617	5.67		0.006	
3.75	1260	3.89	1436	5.39			0.044
4	1260	3.89	1448	5.39			0.042
4	325	3.98	1639	5.68		0.005	
4.25	1260	3.96	1304	5.18			0.073
4.5	1260	3.96	1327	5.21			0.066
4.5	325	4	1702	5.72		0.006	
4.75	1260	3.97	1363	5.28			0.058
5	1260	3.89	1474	5.49			0.039
5	325	3.97	1685	5.84		0.004	

Table A-3. HYMETS Test Data for Coated Alpha2 Specimens L-33 (Type 3 Coated) and L-15 (Type 3a Coated).

SPEC. NO.: L33 ALLOY: Ti-14Al-21Nb THICKNESS, CM: 0.0565

Time, Hr.	Temp., K	Mach No.	Enthalpy cal/gm	P-wall, torr	Emit. at Temp	Cat. Efficiency Cold	Hot
0.25	1260	3.85	1719	5.84			0.023
0.5	1260	3.94	1696	5.76			0.025
0.5	325	3.95	1681	5.62		0.006	
0.75	1260	3.87	1640	5.63			0.029
1	1260	3.88	1617	5.62			0.03
1	325	3.96	1668	5.62		0.002	
1	325	4.02	1556	5.72		0.009	
1.25	1260	3.9	1315	5.29			0.071
1.5	1260	3.9	1310	5.28			0.073
1.5	325	3.99	1636	5.84		0.023	
1.5	325	4	1670	5.87		0.017	
1.75	1260	3.96	1314	5.13			0.078
2	1260	3.96	1336	5.17			0.072
2	325	3.98	1676	5.74		0.016	
2	325	4	1637	5.75		0.014	
2.25	1260	3.89	1327	4.83			0.077
2.5	1260	3.93	1355	4.83			0.075
2.5	325	3.98	1617	5.66		0.02	
2.75	1260	3.9	1312	5.18			0.072
3	1260	3.9	1310	5.18			0.073
3	325	3.98	1638	5.7		0.012	
3	325	3.99	1649	5.7		0.002	
3.25	1260	3.88	1293	5.13			0.075
3.5	1260	3.89	1314	5.15			0.069
3.5	325	3.96	1694	5.75		0.013	
3.5	325	4	1617	5.67		0.019	
3.75	1260	3.89	1249	5.11			0.085
4	1260	3.87	1353	5.27			0.055
4	325	3.98	1639	5.68		0.018	
4	325	4.01	1568	5.67		0.022	
4.25	1260	3.93	1148	5.5			0.112
4.5	1260	3.91	1145	5.44			0.118
4.5	325	4	1702	5.72		0.026	
4.75	1260	3.93	1177	5.5			0.093
5	1260	3.92	1194	5.42			0.09
5	325	3.97	1685	5.84		0.023	

SPEC. NO.: L15 ALLOY: Ti-14Al-21Nb THICKNESS, CM: 0.0597

0	325	4.02	1858	5.22	0.8	0.005	
0.5	1260	4.03	1662	4.99	0.81		0.036
0.5	325	4.03	1831	5.18	0.8	0.01	
1	1260	4.03	1658	4.98	0.81		0.036
1	325	4.04	1825	5.17	0.8	0.01	
5	325	3.93	1717	5.65	0.84	0.016	
5.5	1260	3.87	1592	5.51	0.82		0.034
5.5	325	3.94	1681	5.55	0.82	0.018	

Table A-4. HYMETS Test Data for Coated Alpha2 Specimens L-35 (Type 3b Coated) and L-15 (Type 3a Coated).

SPEC. NO.: L35 ALLOY: Ti-14Al-21Nb THICKNESS, CM: 0.0559

Time, Hr.	Temp., K	Mach No.	Enthalpy cal/gm	P-wall, torr	Emit. at Temp	Cat. Efficiency Cold	Hot
0	325	3.97	1647	5.66		0.001	
0.25	1260	3.82	1843	5.93			0.018
0.5	1260	3.85	1782	5.89			0.02
0.5	325	3.95	1705	5.71		0.005	
0.75	1260	3.87	1783	5.82			0.021
1	1260	3.88	1767	5.81			0.021
1	325	3.94	1709	5.7		0.002	
1	325	3.98	1631	5.84		0.005	
1.25	1260	3.98	1482	5.56			0.043
1.5	1260	3.98	1497	5.59			0.041
1.5	325	3.98	1582	5.8		0.01	
1.75	1260	3.97	1499	5.58			0.039
2	1260	3.97	1499	5.58			0.039
2	325	3.99	1593	5.77		0.008	
2	325	3.99	1617	5.74		0.008	
2.25	1260	3.98	1431	5.39			0.048
2.5	1260	3.98	1442	5.41			0.046
2.5	325	3.98	1610	5.77		0.01	
2.75	1260	3.98	1413	5.39			0.048
3	1260	3.98	1396	5.36			0.051
3	325	3.98	1625	5.78		0.011	
SPEC. NO.: L36 ALLOY: Ti-14Al-21Nb THICKNESS, CM: 0.061							
0	325	3.96	1670	5.66		0.003	
0.25	1260	3.88	1682	5.72			0.037
0.5	1260	3.89	1628	5.62			0.043
0.5	325	3.94	1716	5.71		0.008	
0.75	1260	3.85	1677	5.69			0.038
1	1260	3.85	1681	5.7			0.037
1	325	3.94	1710	5.71		0.006	
1	325	3.98	1631	5.84		0.01	
1.25	1260	3.98	1433	5.48			0.071
1.5	1260	3.98	1501	5.6			0.057
1.5	325	3.98	1582	5.8		0.037	
1.75	1260	3.99	1437	5.49			0.067
2	1260	4	1409	5.46			0.074
2	325	4	1590	5.8		0.053	
2	325	3.99	1611	5.8		0.028	
2.25	1260	3.98	1451	5.43			0.064
2.5	1260	3.98	1440	5.41			0.066
2.5	325	3.98	1610	5.77		0.029	
2.75	1260	3.98	1427	5.41			0.066
3	1260	3.98	1422	5.41			0.067
3	325	3.98	1625	5.78		0.019	

Table A-5. HYMETS Test Data for Type 1 Coated Alpha2 Specimens L-37 and L-58.

SPEC. NO.: L37 ALLOY: Ti-14Al-21Nb THICKNESS, CM: 0.064

Time, Hr.	Temp., K	Mach No.	Enthalpy cal/gm	P-wall, torr	Emit. at Temp	Cat. Efficiency Cold	Hot
0	325	3.91	1756	5.58		0.006	
0.25	1260	3.72	1981	5.98			0.014
0.5	1260	3.69	2020	6.02			0.013
0.5	325	3.94	1714	5.61		0.005	
0.75	1260	3.74	1961	6.07			0.014
1	1260	3.75	1938	6.03			0.014
1	325	3.92	1736	5.7		0.005	
1	325	3.97	1612	5.68		0.011	
1.25	1260	3.97	1577	5.71			0.03
1.5	1260	3.97	1535	5.59			0.034
1.5	325	3.99	1586	5.74		0.022	
1.5	325	3.98	1618	5.7		0.022	
1.75	1260	3.98	1537	5.58			0.033
2	1260	3.97	1552	5.59			0.032
2	325	3.98	1595	5.71		0.014	
2	325	3.94	1689	5.66		0.009	
2.25	1260	3.87	1642	5.67			0.026
2.5	1260	3.89	1628	5.65			0.027
2.5	325	3.94	1711	5.77		0.01	
2.75	1260	3.84	1833	6.2			0.015
3	1260	3.85	1820	6.17			0.015
3	325	3.92	1723	5.8		0.017	
3	325	3.92	1801	5.72		0.011	
3.25	1260	3.89	1600	5.55			0.029
3.5	1260	3.89	1600	5.55			0.029
3.5	325	3.93	1775	5.76		0.007	
3.75	1260	3.94	1577	5.54			0.032
4	1260	3.95	1567	5.5			0.033
4	325	3.89	1793	5.81		0.012	
4.25	1260	3.96	1584	5.55			0.031
4.5	1260	3.96	1584	5.55			0.031
4.5	325	3.91	1802	5.76		0.01	
4.75	1260	3.95	1594	5.54			0.031
5	1260	3.94	1611	5.57			0.029
5	325	3.91	1781	5.69		0.011	

SPEC. NO.: L58 ALLOY: Ti-14Al-21Nb THICKNESS, CM: 0.061

0	325	3.96	1719	5.62		0.001	
0.25	1260	3.91	1740	6.13	0.79		0.018
0.5	1260	3.92	1726	6.1	0.79		0.019
0.5	325	4	1632	5.61		0.002	
0.75	1260	3.98	1572	6.27	0.79		0.024
1	1260	3.98	1562	6.25	0.79		0.025
1	325	3.99	1639	5.55		0.002	
1	325	3.97	1677	5.45		0.001	
1.25	1260	3.89	1671	5.68	0.79		0.024
1.5	1260	3.87	1721	5.71	0.79		0.022
1.5	325	3.98	1644	5.52		0.001	
1.75	1260	3.94	1770	5.71	0.79		0.021
2	1260	3.94	1770	5.71	0.79		0.021
2	325	4.02	1685	5.55		0.001	
2.25	1260	4	1550	6.16	0.79		0.026
2.5	1260	3.96	1567	6.19	0.79		0.025
2.5	325	3.99	1654	5.63		0.001	
2.75	1260	4	1540	6.18	0.79		0.027
3	1260	3.97	1533	6.18	0.79		0.027
3	325	4	1685	5.6		0.001	
3.5	1260	3.99	1514	6.06	0.79		0.029
3.5	325	4	1660	5.61		0.002	
3.75	1260	4.02	1456	6.1	0.79		0.034
4	1260	3.99	1480	6.13	0.79		0.031
4	325	3.99	1663	5.6		0.001	
4.25	1260	3.99	1459	6.08	0.79		0.033
4.5	1260	3.98	1486	6.08	0.79		0.031
4.5	325	3.99	1628	5.54		0.001	
4.75	1260	4.01	1502	6.15	0.79		0.026
5	1260	4.01	1502	6.15	0.79		0.029
5	325	3.99	1641	5.56		0.001	

Table A-6. HYMETS Test Data for Type 1 Coated Alpha2 Specimens N-2, N-3, and N-8.

SPEC. NO.: N2 ALLOY: Ti-14Al-21Nb THICKNESS, CM: 0.0467

Time, Hr.	Temp., K	Mach No.	Enthalpy cal/gm	P-wall, torr	Emit. at Temp	Cat. Efficiency Cold	Hot
0	325	4.07	1871	6.15	0.75	0.004	
0.25	1260	3.79	2849	7.33	0.87		0.001
0.5	1260	3.79	2893	7.2	0.87		0.001
0.5	325	3.96	1988	6.06	0.75	0.009	
0.75	1260	3.77	2350	6.63	0.87		0.008
1	1260	3.77	2384	6.64	0.87		0.007
1	325	3.94	2032	6.08	0.75	0.007	
1.25	1260	3.85	2135	6.4	0.87		0.013
1.5	1260	3.86	2142	6.4	0.87		0.013
1.5	325	3.98	1972	6.06	0.75	0.005	
1.75	1260	3.94	2111	6.34	0.87		0.015
2	1260	3.94	2111	6.34	0.87		0.015
2	325	3.92	2042	6.1	0.75	0.001	
SPEC. NO.: N3 ALLOY: Ti-14Al-21Nb THICKNESS, CM: 0.0444							
0	325	3.95	2060	6.16		0.001	
0.5	1260	3.78	2350	6.32	0.85		0.009
0.5	325	3.9	2095	6.13		0.003	
0.75	1260	3.89	2098	5.87	0.85		0.016
1	1260	3.87	2155	5.98	0.86		0.015
1	325	3.94	2056	6.17		0.001	
1.25	1260	4.05	1881	5.68	0.86		0.025
1.5	1260	4.04	1924	5.73	0.86		0.023
1.5	325	3.97	2016	6.15		0.002	
SPEC. NO.: N8 ALLOY: Ti-14Al-21Nb THICKNESS, CM: 0.0527							
0	325	3.95	2060	6.16		0.001	
0.25	1260	3.78	2594	6.56	0.89		0.003
0.5	1260	3.77	2476	6.5	0.89		0.007
0.5	325	3.9	2101	6.13		0.001	
0.75	1260	3.78	2309	6.23	0.89		0.012
1	1260	3.78	2443	6.3	0.9		0.009
1	325	3.94	2056	6.17		0.001	
1.25	1260	3.84	2166	6.18	0.9		0.016
1.5	1260	3.91	2077	6.05	0.9		0.019
1.5	325	3.97	2016	6.15		0.001	

Table A-7. HYMETS Test Data for Type 1 Coated Alpha2 Specimen N1A.

SPEC. NO.: N1A ALLOY: Ti-14Al-21Nb THICKNESS, CM: 0.0549

Time, Hr.	Temp., K	Mach No.	Enthalpy cal/gm	P-wall, torr	Emit. at Temp	Cat. Efficiency Cold	Hot
0	325	3.97	2019	6.18	0.88	0.002	
0.25	1205	3.89	2114	6.22	0.81		0.004
0.5	1205	3.92	2084	6.26	0.82		0.005
0.5	325	3.93	2047	6.06	0.87	0.007	
0.75	1205	3.96	2005	6.05	0.83		0.007
1	1205	3.96	2001	6.05	0.84		0.007
1	325	3.96	2026	6.13	0.85	0.008	
1	325	3.99	2005	6.06	0.85	0.011	
1.25	1205	4.09	1767	5.63	0.84		0.014
1.5	1205	4.09	1774	5.63	0.84		0.014
1.5	325	3.99	1977	6.09	0.85	0.008	
1.75	1205	4.13	1695	5.6	0.84		0.016
2	1205	4.1	1745	5.63	0.84		0.014
2	325	3.85	2119	6.23	0.85	0.007	
2.25	1205	4.04	1874	5.81	0.84		0.01
2.5	1205	4.05	1850	5.78	0.84		0.011
2.5	325	3.87	2118	6.28	0.85	0.009	
2.75	1205	4.15	1681	5.61	0.84		0.016
3	1205	4.05	1849	5.99	0.84		0.01
3	325	4.15	1645	6.22	0.84	0.025	
3.25	1205	4.15	1645	5.6	0.84		0.018
3.5	1205	4.15	1645	5.6	0.84		0.018
3.75	1205	4.16	1663	5.58	0.84		0.017
4	1205	4.15	1691	5.68	0.84		0.016
4	325	3.91	2105	6.2	0.87	0.006	
4.25	1205	4.15	1577	5.37	0.84		0.022
4.5	1205	4.15	1540	5.33	0.84		0.025
4.5	325	3.95	2029	6.22	0.87	0.011	
4.75	1205	4.17	1516	5.41	0.84		0.025
5	1205	4.16	1633	5.55	0.84		0.018
5	325	4.04	1910	6.1	0.87	0.009	
5.25	1205	4.13	1673	5.76	0.84		0.016
5.5	1205	4.13	1677	5.76	0.84		0.015
5.5	325	3.99	1971	6.18	0.87	0.004	
5.75	1205	4.15	1649	5.62	0.84		0.017
6	1205	4.15	1656	5.6	0.84		0.017
6	325	3.95	2043	6.29	0.87	0.005	
6.25	1205	4.17	1462	5.19	0.84		0.032
6.5	1205	4.17	1425	5.14	0.84		0.035
6.5	325	4	1969	6.17	0.87	0.016	
6.75	1205	4.18	1445	5.29	0.84		0.032
7	1205	4.18	1443	5.3	0.84		0.031
7	325	3.97	2046	6.17	0.88	0.02	
7.25	1205	4.18	1507	5.29	0.84		0.027
7.5	1205	4.17	1534	5.32	0.84		0.025
7.5	325	3.99	2002	6.19	0.88	0.02	
7.75	1205	4.16	1613	5.46	0.85		0.021
8	1205	4.17	1580	5.41	0.85		0.023
8	325	3.99	2019	6.17	0.88	0.018	
8.25	1205	4.16	1625	5.51	0.85		0.02
8.5	1205	4.1	1787	5.79	0.85		0.013
8.75	1205	4.1	1738	5.46	0.85		0.016
9	1205	4.12	1741	5.51	0.85		0.016
9	325	3.95	2063	6.03	0.89	0.005	
9.25	1205	4.15	1661	5.42	0.85		0.019
9.5	1205	4.13	1698	5.47	0.85		0.018
9.5	325	3.98	2016	6.11	0.89	0.007	
9.75	1205	4.14	1672	5.51	0.85		0.018
10	1205	4.17	1589	5.38	0.85		0.023
10	325	4	2000	6.11	0.89	0.009	

Table A-8. HYMETS Test Data for Type 1 Coated Alpha2 Specimens N2A and N3A.

Time, Hr.	Temp., K	Mach No.	Enthalpy cal/gm	P-wall, torr	Emit. at Temp	Cat. Efficiency Cold	Hot
SPEC. NO.: N2A	ALLOY: Ti-14Al-21Nb		THICKNESS, CM: 0.0518				
0	325	3.97	2019	6.18	0.77	0.005	
0.25	1205	4.11	1709	5.55	0.83		0.016
0.5	1205	4.11	1722	5.56	0.83		0.015
0.5	325	3.93	2047	6.06	0.89	0.003	
0.75	1205	4.11	1725	5.52	0.83		0.015
1	1205	4.1	1713	5.5	0.83		0.016
1	325	3.96	2026	6.13	0.89	0.003	
SPEC. NO.: N3A	ALLOY: Ti-14Al-21Nb		THICKNESS, CM: 0.05174				
0	325	3.92	2083	6.04	0.68	0.005	
0.25	1205	4.03	1924	5.94	0.88		0.011
0.5	1205	3.9	2090	6.06	0.88		0.008
0.5	325	3.95	2050	6.01	0.8	0.006	
0.75	1205	3.85	2138	6.2	0.88		0.007
1	1205	3.97	1997	6	0.88		0.009
1	325	3.92	2067	6.12	0.8	0.011	

Table A-9. HYMETS Test Data for Type 1 Coated Alpha2 Specimen N4A.

SPEC. NO.: N4A ALLOY: Ti-14Al-21Nb THICKNESS, CM: 0.0525

Time, Hr.	Temp., K	Mach No.	Enthalpy cal/gm	P-wall, torr	Emit. at Temp	Cat. Efficiency Cold	Hot
0	325	3.92	2083	6.04	0.86	0.004	
0.25	1205	4.11	1711	5.5	0.81		0.015
0.5	1205	4.11	1711	5.5	0.82		0.015
0.5	325	3.95	2050	6.01	0.86	0.003	
0.75	1205	4.13	1665	5.48	0.83		0.018
1	1205	4.13	1665	5.48	0.84		0.018
1	325	3.92	2067	6.12	0.86	0.004	
1	325	3.8	2259	6.06	0.86	0.001	
1.25	1205	4.14	1632	5.44	0.84		0.02
1.5	1205	4.14	1632	5.44	0.85		0.021
1.5	325	3.99	1977	6.09	0.86	0.019	
1.75	1205	4.14	1632	5.44	0.85		0.021
2	1205	4.15	1590	5.46	0.85		0.022
2	325	3.83	2138	6.1	0.86	0.009	
2.25	1205	4.16	1588	5.43	0.85		0.023
2.5	1205	4.15	1605	5.45	0.85		0.022
2.5	325	3.87	2118	6.28	0.86	0.006	
2.75	1205	4.16	1350	4.99	0.86		0.051
3	1205	4.16	1361	4.98	0.86		0.05
3	325	3.97	2012	6.22	0.86	0.027	
3.25	1205	4.17	1354	5.01	0.86		0.05
3.5	1205	4.16	1368	5.03	0.86		0.048
3.75	1205	4.13	1209	4.65	0.86		0.1
4	1205	4.14	1222	4.65	0.86		0.094
4	325	3.91	2105	6.2	0.87	0.022	
4.25	1205	4.14	1246	4.61	0.86		0.088
4.5	1205	4.14	1246	4.61	0.86		0.088
4.5	325	3.95	2029	6.22	0.87	0.024	
4.75	1205	4.16	1392	4.9	0.86		0.048
5	1205	4.16	1406	4.91	0.86		0.046
5	325	4.04	1910	6.1	0.87	0.023	
5	325	3.96	2023	6.17	0.87	0.014	
5.25	1205	4.16	1302	4.78	0.86		0.066
5.5	1205	4.16	1364	4.83	0.86		0.053
5.5	325	4	1968	6.22	0.87	0.016	
5.75	1205	4.16	1492	4.91	0.86		0.037
6	1205	4.15	1497	4.92	0.86		0.037
6	325	3.95	2043	6.29	0.87	0.012	
6.25	1205	4.16	1409	4.88	0.86		0.046
6.5	1205	4.18	1500	5.36	0.86		0.03
6.75	1205	4.17	1553	5.44	0.86		0.025
7	1205	4.16	1581	5.47	0.86		0.024
7	325	3.97	2046	6.17	0.87	0.008	
7.25	1205	4.16	1578	5.41	0.86		0.024
7.5	1205	4.16	1610	5.46	0.87		0.023
7.5	325	3.98	2004	6.19	0.87	0.008	
7.75	1205	4.15	1605	5.44	0.87		0.024
8	1205	4.16	1594	5.43	0.87		0.024
8	325	3.97	2019	6.17	0.88	0.008	
8.25	1205	4.15	1673	5.37	0.87		0.021
8.5	1205	4.13	1692	5.37	0.87		0.021
8.5	325	3.99	2027	6.05	0.88	0.008	
8.75	1205	4.13	1715	5.4	0.87		0.02
9	1205	4.13	1703	5.37	0.87		0.02
9	325	3.95	2063	6.03	0.89	0.008	
9.25	1205	4.14	1644	5.41	0.87		0.0222
9.5	1205	3.15	1651	5.43	0.87		0.022
9.5	325	3.98	2016	6.11	0.89	0.008	
9.75	1205	4.16	1635	5.45	0.87		0.022
10	1205	4.16	1616	5.43	0.87		0.023
10	325	4	2000	6.11	0.9	0.009	

Table A-10. HYMETS Test Data for Type 1 Coated Super-Alpha2 Specimen N9.

SPEC. NO.: N9 ALLOY: Ti-14Al-19Nb-2V-2Mo THICKNESS, CM: 0.0984

Time, Hr.	Temp., K	Mach No.	Enthalpy cal/gm	P-wall, torr	Emit. at Temp	Cat. Efficiency Cold	Hot
0	325	4.07	1874	5.98	0.77	0.033	
0.25	1205	5.99	1828	5.99	0.87		0.015
0.5	1205	4.08	1834	6.02	0.87		0.015
0.5	325	4.12	1762	5.93	0.78	0.01	
0.75	1205	4.16	1632	5.78	0.87		0.023
1	1205	4.13	1682	5.76	0.87		0.021
1	325	4.05	1867	5.98	0.78	0.003	
1.25	1205	4.14	1635	5.69	0.87		0.024
1.5	1205	4.06	1767	5.88	0.87		0.017
1.5	325	4.01	1948	5.99	0.78	0.003	
1.75	1205	4.14	1664	5.58	0.88		0.025
2	1205	4.14	1691	5.6	0.88		0.023
2	325	4.08	1829	5.94	0.79	0.01	
2.25	1205	4.09	1765	5.8	0.88		0.019
2.5	1205	4.08	1784	5.81	0.88		0.018
2.5	325	4.04	1887	6.11	0.79	0.008	
2.75	1205	4.1	1774	5.78	0.88		0.019
3	1205	4.09	1753	5.72	0.88		0.02
3	325	4.05	1896	6.06	0.8	0.006	
3.25	1205	4.09	1742	5.73	0.89		0.021
3.5	1205	4.09	1747	5.74	0.89		0.021
3.5	325	4.01	1924	6.03	0.81	0.005	
3.75	1205	4.09	1728	5.71	0.89		0.022
4	1205	4.09	1742	5.72	0.89		0.021
4	325	4.08	1876	5.96	0.81	0.006	
4.25	1205	4.15	1701	5.68	0.89		0.023
4.5	1205	4.15	1691	5.63	0.89		0.024
4.5	325	4.07	1869	5.98	0.82	0.004	
4.75	1205	4.18	1606	5.56	0.89		0.029
5	1205	4019	1602	5.51	0.89		0.029
5	325	4.07	1887	5.97	0.83	0.006	
5.25	1205	4.2	1542	5.44	0.9		0.035
5.5	1205	4.21	1529	5.41	0.9		0.037
5.5	325	4.05	1911	6	0.84	0.014	
5.75	1205	4.21	1501	5.4	0.9		0.039
6	1205	4.21	1511	5.39	0.9		0.039
6	325	3.9	1769	6.23	0.84	0.011	
6.25	1205	4.17	1366	5.29	0.9		0.058
6.5	1205	4.18	1358	5.29	0.9		0.059
6.5	325	3.9	1774	6.24	0.84	0.02	
6.75	1205	4.17	1347	5.28	0.9		0.062
7	1205	4.18	1339	5.25	0.9		0.064
7	325	3.98	1725	6.21	0.85	0.021	
7.25	1205	4.18	1296	5.28	0.9		0.072
7.5	1205	4.18	1308	5.29	0.9		0.069
7.5	325	4.02	1674	6.23	0.85	0.022	
7.75	1205	4.21	1296	5.29	0.9		0.073
8	1205	4.16	1287	5.29	0.9		0.074
8	325	4.02	1684	6.2	0.86	0.022	
8.25	1205	4.16	1263	5.36	0.91		0.078
8.5	1205	4.16	1255	5.34	0.91		0.082
8.5	325	4.03	1632	6.24	0.86	0.024	
8.75	1205	4.15	1208	535	0.91		0.098
9	1205	4.15	1194	5.34	0.91		0.105
9	325	4.01	1673	6.22	0.87	0.025	
9.25	1205	4.19	1274	5.31	0.91		0.007
9.5	1205	4.18	1295	5.32	0.91		0.072
9.5	325	4.06	1633	6.21	0.87	0.026	
9.75	1205	4.19	1286	5.34	0.91		0.074
10	1205	4.18	1289	5.33	0.91		0.073
10	325	4.08	1604	6.23	0.88	0.026	

Table A-11. HYMETS Test Data for Type 1 Coated Super-Alpha2 Specimens N12, N13, N14, N15, and N16.

SPEC. NO.: N12* ALLOY: Ti-14Al-19Nb-2V-2Mo THICKNESS, CM: 0.09748
*SPECIMEN SUBJECTED TO THERMAL SHOCK: LIQUID N2 TO FURNACE IN 2 SEC

Time, Hr.	Temp., K	Mach No.	Enthalpy cal/gm	P-wall, torr	Emit. at Temp	Cat. Efficiency Cold	Hot
0	325	4.07	1867	5.92	0.77	0.006	
0.25	1260	3.77	2296	6.39	0.85		0.011
0.5	1260	3.78	2268	6.36	0.86		0.012
0.5	325	3.98	1984	6.08	0.78	0.004	
0.75	1260	3.8	2238	6.29	0.87		0.014
1	1260	3.8	2228	6.29	0.88		0.015
1	325	4.04	1929	5.92	0.78	0.005	

SPEC. NO.: N13 ALLOY: Ti-14Al-19Nb-2V-2Mo THICKNESS, CM: 0.0986

0	325	4.14	1779	5.94	0.72	0.108	
0.25	1260	3.99	2008	6.25	0.86		0.019
0.5	1260	3.98	2012	6.21	0.87		0.02
0.75	1260	3.97	2012	6.1	0.88		0.021
1	1260	3.96	2031	6.14	0.89		0.021
1	325	4.08	1807	6.02	0.77	0.024	
1.25	1260	4.08	1670	5.96	0.89		0.039
1.5	1260	4.1	1675	5.96	0.89		0.039
1.5	325	4.07	1824	6	0.72	0.039	
1.75	1260	4.16	1560	5.6	0.89		0.055
2	1260	4.16	1560	5.6	0.89		0.055
2	325	4.07	1833	6	0.81	0.042	
2.25	1260	4.17	1561	5.6	0.88		0.053
2.5	1260	4.16	1598	5.61	0.88		0.049
2.5	325	4.05	1858	6.02	0.82	0.036	
2.75	1260	4.16	1623	5.66	0.88		0.046
3	1260	4.16	1616	5.7	0.88		0.046
3	325	4.05	1867	6.01	0.83	0.043	
3.25	1260	4.14	1665	5.74	0.89		0.043
3.5	1260	4.13	1668	5.65	0.89		0.044

NOTE: SPEC. N13 COATING SHOWS EVIDENCE OF FAILURE AT 2.5 HR--
FOUR-TENTHS DIAM. SPOT AT EDGE FRONT AND BACK SURFACES
IN AREA OF ALUMINA PINS THAT HOLD SPECIMEN DURING HYMETS TEST.

SPEC. NO.: N15* ALLOY: Ti-14Al-19Nb-2V-2Mo THICKNESS, CM: 0.1003
*SPECIMEN SUBJECTED TO 24 HR WATER BOIL BEFORE HYMETS EXPOSURE

0	325	4.13	1789	6.91	0.82	0.001	
0.25	1260	3.99	1975	6.05	0.89		0.023
0.5	1260	4.01	1952	5.96	0.89		0.025
0.5	325	4.04	1910	5.92	0.83	0.001	
0.75	1260	4.04	1895	6.1	0.9		0.027
1	1260	4.06	1879	6.06	0.91		0.029
1	325	3.99	1976	6.09	0.84	0.001	

SPEC. NO.: N16* ALLOY: Ti-14Al-19Nb-2V-2Mo THICKNESS, CM: 0.0927
*SPECIMEN SUBJECTED TO 24 HR WATER BOIL BEFORE HYMETS EXPOSURE

0	325	4.07	1867	5.92	0.77	0.009	
0.25	1260	4.06	1849	5.9	0.88		0.029
0.5	1260	4.09	1812	5.86	0.88		0.031
0.5	325	3.98	1993	6.08	0.77	0.008	
0.75	1260	4	1951	6.05	0.88		0.024
1	1260	3.98	1981	6.07	0.88		0.023
1	325	4.04	1929	5.92	0.77	0.01	

Table A-12. HYMETS Test Data for Type 1 Coated Gamma Specimens PG1 and PG2.

SPEC. NO.: PG1 ALLOY: Ti-33Al-6Nb-1.4Ta THICKNESS, CM: 0.0489

Time, Hr.	Temp., K	Mach No.	Enthalpy cal/gm	P-wall, torr	Emit. at Temp	Cat. Efficiency Cold	Hot
0	325	3.78	2416	6.08	0.84	0.004	
0.25	1255	3.78	2135	5.96	0.84		0.014
0.5	1255	3.82	2086	5.9	0.85		0.015
0.5	325	3.79	2316	6.05	0.84	0.005	
0.75	1255	3.72	2231	5.99	0.85		0.011
1	1255	3.71	2225	5.99	0.85		0.012
1	325	3.78	2350	6.05	0.84	0.004	

SPEC. NO.: PG2 ALLOY: Ti-33Al-6Nb-1.4Ta THICKNESS, CM: 0.04783

0	325	3.8	2394	6.17		0.002	
0.25	1255	3.74	2471	6.37	0.84		0.004
0.5	1255	3.81	2139	5.92	0.84		0.014
0.5	325	3.79	2404	6.15		0.003	
0.75	1255	3.84	2100	5.9	0.85		0.016
1	1255	3.83	2120	5.9	0.85		0.015
1	325	3.86	2231	6.16		0.005	
1.25	1255	3.9	2043	5.96	0.85		0.017
1.5	1255	3.88	2062	5.95	0.85		0.016
1.5	325	3.79	2348	6.17		0.003	
1.75	1255	3.89	2037	5.92	0.85		0.017
2	1255	3.98	1927	5.93	0.85		0.02
2	325	3.8	2354	6.09		0.005	
2.25	1255	3.87	2074	5.93	0.86		0.016
2.5	1255	3.87	2050	5.92	0.86		0.017
2.5	325	3.79	2382	6.12		0.004	
2.75	1255	3.88	2015	5.88	0.86		0.018
3	1255	3.9	2030	5.89	0.86		0.018
3	325	3.8	2334	6.12		0.004	
3.25	1255	3.92	1995	5.85	0.86		0.019
3.5	1255	3.88	2031	5.88	0.86		0.018
3.5	325	4.06	1933	5.92		0.004	
3.75	1255	3.88	2071	6.16	0.86		0.015
4	1255	3.92	2013	6.1	0.86		0.017
4	325	3.94	2088	6.1		0.003	
4.25	1255	3.94	1976	6.05	0.86		0.018
4.5	1255	3.93	2001	6.06	0.86		0.018
4.5	325	3.96	2062	6.13		0.004	
4.75	1255	3.91	1958	6.08	0.86		0.018
5	1255	3.8	2088	6.23	0.86		0.014
5	325	4	2021	6.07		0.004	

Table A-13. HYMETS Test Data for Type 1 Coated Gamma Specimen NGAMMA12.

SPEC. NO.: NGAMMA12 ALLOY: Ti-33Al-6Nb-1.4Ta THICKNESS, CM: 0.0767

Time, Hr.	Temp., K	Mach No.	Enthalpy cal/gm	P-wall, torr	Emit. at Temp	Cat. Efficiency Cold	Hot
0	325	3.94	2070	6.11	0.76	0.013	
0.25	1260	4.01	1966	6.07	0.79		0.016
0.5	1260	4.09	1846	5.85	0.8		0.021
0.5	325	3.97	2041	6.13	0.77	0.013	
0.75	1260	4.15	1702	5.59	0.81		0.03
1	1260	4.15	1702	5.59	0.81		0.03
1	325	4	2007	6.12	0.79	0.017	
1.25	1260	4.16	1660	5.55	0.82		0.034
1.5	1260	4.17	1663	5.55	0.83		0.035
1.5	325	3.99	2013	6.12	0.81	0.018	
1.75	1260	4.16	1661	5.5	0.83		0.036
2	1260	4.16	1668	5.5	0.84		0.037
2.25	1260	4.14	1712	5.63	0.84		0.033
2.5	1260	4.11	1770	5.69	0.84		0.029
2.75	1260	4.14	1710	5.65	0.84		0.032
3	1260	4.15	1675	5.58	0.84		0.035
3.25	1260	4.15	1691	5.59	0.84		0.034
3.5	1260	4.13	1717	5.62	0.85		0.034
3.75	1260	4.16	1656	5.54	0.85		0.039
4	1260	4.15	1670	5.55	0.85		0.038
4.25	1260	4.16	1662	5.55	0.85		0.038
4.5	1260	4.16	1662	5.55	0.85		0.038
4.75	1260	4.16	1653	5.55	0.85		0.039
5	1260	4.16	1653	5.55	0.85		0.039
5	325	3.99	2000	6.14	0.86	0.01	
5.25	1260	4.15	1601	5.55	0.85		0.043
5.5	1260	4.15	1636	5.6	0.85		0.039
5.5	325	3.97	2018	6.16	0.86	0.018	
5.75	1260	4.19	1523	5.37	0.85		0.054
6	1260	4.16	1583	5.48	0.85		0.045
6	325	4	1969	6.17	0.86	0.026	
6.25	1260	4.18	1581	5.55	0.85		0.045
6.5	1260	4.17	1596	5.57	0.85		0.043
6.5	325	4.03	1941	6.13	0.87	0.017	
6.75	1260	4.18	1579	5.5	0.86		0.047
7	1260	4.18	1579	5.5	0.86		0.047
7	325	4.04	1914	6.12	0.87	0.025	
7.25	1260	4.19	1469	5.34	0.86		0.065
7.5	1260	4.2	1482	5.35	0.86		0.063
7.75	1260	4.21	1419	5.2	0.86		0.079
8	1260	4.21	1464	5.27	0.86		0.068
8	325	3.88	2133	6.06	0.88	0.015	
8.25	1260	4.13	1682	5.49	0.86		0.04
8.5	1260	4.12	1695	5.53	0.86		0.037
8.75	1260	4.16	1603	5.43	0.86		0.046
9	1260	4.15	1617	5.45	0.86		0.044
9.25	1260	4.15	1613	5.42	0.87		0.047
9.5	1260	4.14	1643	5.44	0.87		0.044
9.75	1260	4.18	1508	5.3	0.87		0.062
10	1260	4.16	1604	5.4	0.87		0.048

A-2

Table A-14. HYMETS Test Data for Type 1 Coated Beta-21S Specimen NA4.

SPEC. NO.: NA4 ALLOY: BETA-21S Ti THICKNESS, CM: 0.0678

Time, Hr.	Temp., K	Mach No.	Enthalpy cal/gm	P-wall, torr	Emit. at Temp	Cat. Efficiency Cold	Hot
0	325	4.05	1921	6.09	0.85	0.009	
0.25	1094	4.16	1163	5.05	0.76		0.014
0.5	1094	4.16	1307	5.04	0.76		0.005
0.5	325	4.06	1908	6.09	0.85	0.01	
0.75	1094	4.16	1307	5.04	0.76		0.005
1	1094	4.16	1292	5.02	0.76		0.006
1	325	4.06	1911	6.09	0.85	0.01	
1.25	1094	4.16	1421	4.94	0.76		0.002
1.5	1094	4.15	1335	4.77	0.76		0.006
1.5	325	3.99	1978	6.17	0.85	0.019	
1.75	1094	4.14	1246	4.8	0.76		0.01
2	1094	4.14	1246	4.8	0.76		0.01
2	325	4.01	1935	6.16	0.85	0.02	
2	325	3.99	2013	6.06	0.85	0.01	
2.25	1094	4.14	1234	4.57	0.76		0.012
2.5	1094	4.15	1233	4.57	0.76		0.012
2.5	325	3.89	2133	6.1	0.85	0.015	
2.75	1094	4.17	1296	4.62	0.76		0.009
3	1094	4.17	1289	4.62	0.76		0.009
3	325	3.96	2038	6.11	0.85	0.015	
3.25	1094	4.17	1261	4.61	0.77		0.011
3.5	1094	4.17	1261	4.61	0.77		0.011
3.5	325	3.97	2035	6.11	0.86	0.016	
3.75	1094	4.16	1246	4.61	0.77		0.012
4	1094	4.16	1232	4.6	0.77		0.013
4	325	3.99	2015	6.1	0.86	0.017	
4.25	1094	4.16	1215	4.59	0.77		0.014
4.5	1094	4.15	1169	4.55	0.77		0.019
4.5	325	3.99	2017	6.12	0.86	0.018	
4.75	1094	4.15	1200	4.56	0.77		0.016
5	1094	4.14	1128	4.46	0.77		0.025
5	325	3.98	2012	6.11	0.86	0.019	
5.25	1094	4.14	1128	4.46	0.77		0.025
5.5	1094	4.13	1125	4.44	0.77		0.025
5.5	325	3.96	2056	6.1	0.86	0.025	
5.75	1094	4.15	1220	4.48	0.77		0.015
6	1094	4.15	1220	4.48	0.77		0.015
6	325	3.97	2032	6.13	0.86	0.02	
6	325	4	2003	6.1	0.86	0.005	
6.25	1094	4.17	1225	4.52	0.77		0.014
6.5	1094	4.15	1136	4.39	0.77		0.024
6.5	325	4	2000	6.1	0.86	0.021	
6.75	1094	4.14	1113	4.39	0.77		0.028
7	1094	4.13	1032	4.28	0.77		0.045
7	325	4.02	1970	6.09	0.86	0.023	
7.25	1094	4.13	1059	4.3	0.77		0.039
7.5	1094	4.13	1021	4.28	0.77		0.048
7.5	325	4.02	1974	6.12	0.86	0.024	
7.75	1094	4.12	978	4.24	0.77		0.063
8	1094	4.14	868	4.1	0.77		0.134
8	325	4	2013	6.11	0.85	0.025	
8.25	1094	4.13	947	4.14	0.77		0.08
8.5	1094	4.13	947	4.14	0.77		0.08
8.5	325	3.99	2007	6.11	0.85	0.023	
8.75	1094	4.12	973	4.2	0.77		0.067
9	1094	4.12	973	4.2	0.77		0.067
9	325	4	1996	6.14	0.85	0.031	
9.25	1094	4.12	955	4.19	0.77		0.074
9.5	1094	4.12	955	4.19	0.77		0.074
9.5	325	4.01	1983	6.14	0.85	0.029	
9.75	1094	4.12	963	4.21	0.77		0.07
10	1094	4.12	877	4.17	0.77		0.122
10	325	4.02	1967	6.14	0.85	0.032	

Table A-15. HYMETS Test Data for Type 2a Coated Alpha2 Specimens L-42 and L-47.

SPEC. NO.: L42 ALLOY: Ti-14Al-21Nb THICKNESS, CM: 0.06426

Time, Hr.	Temp., K	Mach No.	Enthalpy cal/gm	P-wall, torr	Emit. at Temp	Cat. Efficiency Cold	Hot
0	325	3.91	1756	5.58		0.005	
0.25	1260	3.74	1931	5.94			0.024
0.5	1260	3.76	1898	5.84			0.026
0.5	325	3.94	1714	5.61		0.013	
0.75	1260	3.76	1903	5.99			0.024
1	1260	3.76	1904	5.99			0.024
1	325	3.92	1736	5.7		0.008	
1	325	3.97	1612	5.68		0.017	
1.25	1260	3.98	1528	5.64			0.056
1.5	1260	3.97	1569	5.72			0.05
1.5	325	3.98	1618	5.7		0.014	
1.75	1260	3.97	1594	5.78			0.038
2	1260	3.96	1606	5.79			0.037
2	325	3.98	1595	5.71		0.012	
2	325	3.94	1689	5.66		0.011	
2.25	1260	3.92	1669	5.78			0.032
2.5	1260	3.9	1697	5.76			0.031
2.5	325	3.94	1711	5.77		0.018	
2.75	1260	3.91	1684	5.72			0.031
3	1260	3.91	1685	5.69			0.031
5	1260	3.87	1840	5.78			0.023
5	325	3.97	1689	5.62		0.009	

SPEC. NO.: L47 ALLOY: Ti-14Al-21Nb THICKNESS, CM: 0.0622

0	325	3.8	2286	6.28		0.001	
0.5	1260	3.71	2778	6.8	0.9		0.001
0.5	325	3.79	2448	6.23		0.001	
0.75	1260	3.71	2735	6.52	0.91		0.001
1	1260	3.71	2791	6.09	0.92		0.001
1	325	3.79	2466	6.09		0.001	
1.25	1260	3.69	2650	6.42	0.92		0.001
1.5	1260	3.69	2645	6.42	0.92		0.001
1.5	325	3.78	2317	6.06		0.001	
1.75	1260	3.68	2583	6.38	0.92		0.003
2	1260	3.69	2630	6.4	0.92		0.002
2.25	1260	3.72	2543	6.39	0.92		0.005
2.5	1260	3.71	2525	6.38	0.92		0.006
2.5	325	3.79	2438	6.12		0.002	
2.75	1260	3.7	2630	6.42	0.92		0.002
3	1260	3.7	2630	6.42	0.92		0.002
3	325	3.79	2361	6.16		0.001	
3.25	1260	3.72	2577	6.41	0.93		0.004
3.5	1260	3.72	2556	6.38	0.93		0.005
3.5	325	3.8	2355	6.15		0.002	
3.75	1260	3.72	2587	6.41	0.93		0.004
4	1260	3.71	2540	6.39	0.93		0.006
4	325	3.79	2422	6.09		0.001	
4.25	1260	3.71	2577	6.31	0.93		0.004
4.5	1260	3.71	2605	6.44	0.93		0.003
4.5	325	3.82	2265	6.03		0.002	
4.75	1260	3.72	2781	6.44	0.93		0.001
5	1260	3.71	2718	6.4	0.93		0.001
5	325	3.79	2408	6.16		0.001	

Table A-16. HYMETS Test Data for Coated Alpha2 Specimens L-48 (Type 2a Coated) and L-59 (Type 2b Coated).

SPEC. NO.: L48 ALLOY: Ti-14Al-21Nb THICKNESS, CM: 0.0579

Time, Hr.	Temp., K	Mach No.	Enthalpy cal/gm	P-wall, torr	Emit.	Cat. Efficiency Cold	Hot
0	325	3.8	2286	6.28	0.82	0.001	
0.25	1260	3.71	2505	6.54	0.84		0.003
0.5	1260	3.71	2492	6.47	0.86		0.004
0.5	325	3.78	2471	6.08	0.86	0.001	
0.75	1260	3.73	2200	6.03	0.87		0.013
1	1260	3.72	2201	6.09	0.88		0.014
1	325	3.78	2430	6.05	0.84	0.001	
1.25	1260	3.94	2019	5.78	0.87		0.02
1.5	1260	3.92	2043	5.77	0.87		0.02
1.5	325	3.78	2317	6.06	0.87	0.004	
1.75	1260	3.93	2015	5.8	0.87		0.02
2	1260	3.72	2236	6.15	0.87		0.012
2	325	3.79	2389	6.16	0.87	0.004	
2.25	1260	3.94	1953	5.76	0.86		0.021
2.5	1260	3.93	1961	5.75	0.86		0.021
2.5	325	3.79	2439	6.12	0.86	0.002	
2.75	1260	3.77	2154	5.99	0.86		0.014
3	1260	3.77	2095	5.94	0.86		0.016
3	325	3.79	2361	6.16	0.86	0.005	
3.25	1260	3.84	2048	5.87	0.85		0.017
3.5	1260	3.84	2041	5.85	0.85		0.017
3.5	325	3.79	2356	6.15	0.85	0.006	
3.75	1260	4.03	1853	5.62	0.85		0.025
4	1260	4.01	1878	5.64	0.85		0.024
4	325	3.79	2422	6.09	0.85	0.004	
4.25	1260	4.01	1897	5.66	0.84		0.023
4.5	1260	4.01	1889	5.65	0.84		0.023
4.5	325	3.82	2265	6.03	0.84	0.006	
4.75	1260	4.02	1870	5.65	0.84		0.024
5	1260	4.01	1892	5.65	0.84		0.023
5	325	3.79	2408	6.16	0.84	0.005	

SPEC. NO.: L59 ALLOY: Ti-14Al-21Nb THICKNESS, CM: 0.0635

0.25	1260	3.98	1593	6.2	0.82		0.026
0.5	1260	3.99	1568	6.2	0.82		0.028
0.5	325	4	1632	5.61		0.003	
0.75	1260	3.97	1642	6.31	0.82		0.023
1	1260	4	1612	6.28	0.82		0.025
1	325	4	1642	5.57		0.002	
1	325	3.97	1677	5.45		0.001	
1.25	1260	3.95	1726	5.74	0.83		0.026
1.5	1260	3.96	1702	5.73	0.83		0.027
1.5	325	3.98	1650	5.52		0.001	
1.75	1260	3.92	1714	5.72	0.84		0.027
2	1260	3.92	1721	5.75	0.84		0.027
2	325	4.02	1685	5.55		0.001	
2.25	1260	3.97	1693	5.69	0.85		0.03
2.5	1260	3.98	1681	5.63	0.85		0.032
2.5	325	4	1652	5.67		0.001	
2.75	1260	3.97	1683	5.73	0.86		0.031
3	1260	3.98	1649	5.66	0.86		0.034
3	325	4	1685	5.6		0.001	
3.25	1260	4.02	1605	5.55	0.87		0.04
3.5	1260	4.01	1625	5.59	0.87		0.038
3.5	325	4	1660	5.61		0.001	
3.75	1260	4.01	1622	5.59	0.88		0.04
4	1260	4.01	1622	5.59	0.88		0.04
4	325	3.99	1663	5.6		0.001	
4.25	1260	4	1604	5.51	0.89		0.044
4.5	1260	4	1604	5.51	0.89		0.044
4.5	325	4	1625	5.6		0.002	
4.75	1260	4.02	1600	5.58	0.9		0.045
5	1260	4.01	1601	5.58	0.9		0.045
5	325	3.99	1641	5.56		0.002	

Table A-17. HYMETS Test Data for Type 2 Coated Super-Alpha2 Specimen NSJR6.

SPEC. NO.: NSJR6 ALLOY: Ti-14Al-19Nb-2V-2Mo THICKNESS, CM: 0.09075

Time, Hr.	Temp., K	Mach No.	Enthalpy cal/gm	P-wall, torr	Emit. at Temp	Cat. Efficiency Cold	Hot
0	300	3.88	2164	6.17		0.007	
0.25	1260	4.07	1883	5.85	0.82		0.022
0.5	1260	3.97	2051	6.05	0.82		0.016
0.5	300	3.89	2145	6.16		0.003	
0.75	1260	3.96	2050	6.05	0.82		0.016
1	1260	3.94	2073	6.13	0.83		0.016
1	300	3.86	2180	6.2		0.004	
1.25	1260	4.1	1848	5.79	0.83		0.025
1.5	1260	3.98	2028	6.06	0.83		0.017
1.5	300	3.89	2140	6.19		0.003	
1.75	1260	3.99	2019	6.06	0.84		0.018
2	1260	3.99	2019	6.06	0.84		0.018
2	300	3.89	2139	6.19		0.003	
2	300	3.86	2172	6.22		0.005	
2.25	1260	4.11	1805	5.76	0.84		0.027
2.5	1260	4.02	1960	6.03	0.84		0.02
2.5	300	3.91	2113	6.19		0.003	
2.75	1260	3.99	1992	6.09	0.84		0.018
3	1260	3.98	2015	6.12	0.85		0.018
3	300	3.88	2145	6.19		0.001	
3.25	1260	4.01	1981	6.05	0.85		0.02
3.5	1260	4	1989	6.05	0.85		0.02
3.75	1260	4.02	1968	6.01	0.86		0.021
4	1260	4.01	1988	6.05	0.86		0.02
4	300	3.91	2139	6.18		0.002	
4.25	1260	4.04	1950	6	0.86		0.022
4.5	1260	4.03	1968	6.02	0.86		0.021
4.5	300	3.93	2105	6.18		0.002	
4.75	1260	4.03	1964	6.04	0.86		0.021
5	1260	4.03	1964	6.04	0.86		0.021
5	300	3.93	2099	6.18		0.003	
5	300	3.92	2111	6.19		0.003	
5.25	1260	4.13	1790	5.73	0.86		0.03
5.5	1260	4.14	1771	5.7	0.86		0.032
5.5	300	3.93	2093	6.21		0.003	
5.75	1260	4.13	1788	5.78	0.86		0.031
6	1260	4.12	1810	5.81	0.86		0.03
6	300	3.92	2104	6.2		0.002	
6.25	1260	4.13	1794	5.73	0.86		0.03
6.5	1260	4.12	1806	5.76	0.86		0.029
6.5	300	3.95	2077	6.19		0.002	
6.75	1260	4.13	1792	5.76	0.86		0.03
7	1260	4.12	1797	5.78	0.86		0.03
7	300	3.95	2072	6.2		0.002	
7.25	1260	4.12	1812	5.72	0.86		0.03
7.5	1260	4.12	1815	5.67	0.86		0.03
7.5	300	3.94	2096	6.15		0.003	
7.75	1260	4.15	1759	5.66	0.86		0.033
8	1260	4.14	1775	5.68	0.86		0.032
8	300	3.95	2089	6.15		0.003	
8.25	1260	4.15	1751	5.66	0.86		0.033
8.5	1260	4.15	1760	5.68	0.86		0.033
8.5	300	3.96	2077	6.17		0.003	
8.75	1260	4.16	1742	5.66	0.87		0.035
9	1260	4.16	1754	5.68	0.87		0.034
9	300	3.96	2074	6.16		0.003	
9.25	1260	4.15	1747	5.68	0.87		0.035
9.5	1260	4.15	1767	5.7	0.87		0.033
9.75	1260	4.16	1748	5.7	0.87		0.034
10	1260	4.15	1768	5.74	0.87		0.033

Table A-18. HYMETS Test Data for Type 2 Coated Gamma Specimens NG2, NG3, and NGAMMA6.

Time, Hr.	Temp., K	Mach No.	Enthalpy cal/gm	P-wall, torr	Emit. at Temp	Cat. Efficiency Cold	Hot
SPEC. NO.: NG2	ALLOY: Ti-33Al-6Nb-1.4Ta			THICKNESS, CM: 0.079991			
0	300	3.86	2176	6.13	0.8	0.005	
0.25	1260	4.14	1748	5.5	0.86		0.035
0.5	1260	4.09	1842	5.66	0.85		0.027
0.5	300	3.9	2140	6.12	0.85	0.016	
0.75	1260	4.14	1741	5.47	0.84		0.033
1	1260	4.12	1760	5.5	0.84		0.032
1	300	3.9	2127	6.13	0.84	0.018	
SPEC. NO.: NG3	ALLOY: Ti-33Al-6Nb-1.4Ta			THICKNESS, CM: 0.07717			
0	300	3.86	2176	6.13	0.76	0.012	
0.25	1260	4.15	1703	5.44	0.71		0.021
0.5	1260	4.15	1674	5.39	0.74		0.026
0.5	300	3.9	2140	6.12	0.8	0.012	
0.75	1260	4.17	1567	5.27	0.8		0.043
1	1260	4.12	1569	5.29	0.84		0.048
1	300	3.9	2127	6.13	0.84	0.023	
SPEC. NO.: NGAMMA6	ALLOY: Ti-33Al-6Nb-1.4Ta			THICKNESS, CM: 0.0767			
0	325	3.94	2070	6.11	0.86	0.008	
0.25	1260	4.04	1939	5.99	0.83		0.019
0.5	1260	4.04	1931	5.94	0.83		0.02
0.5	325	3.97	2041	6.13	0.86	0.009	
0.75	1260	4.08	1868	5.88	0.83		0.022
1	1260	4.08	1864	5.85	0.83		0.023
1	325	4	2007	6.12	0.86	0.011	
1.25	1260	4.13	1780	5.74	0.82		0.026
1.5	1260	4.12	1791	5.78	0.82		0.024
1.5	325	3.99	2013	6.12	0.86	0.011	
1.75	1260	4.12	1781	5.74	0.82		0.026
2	1260	4.12	1785	5.76	0.82		0.026
2	325	3.99	2016	6.13	0.86	0.011	
2.25	1260	4.1	1785	5.73	0.82		0.026
2.5	1260	4.1	1785	5.73	0.82		0.026
2.75	1260	4.15	1669	5.53	0.82		0.034
3	1260	4.15	1669	5.53	0.82		0.034
3.25	1260	4.16	1668	5.56	0.82		0.034
3.5	1260	4.15	1676	5.59	0.83		0.034
3.75	1260	4.14	1690	5.59	0.83		0.033
4	1260	4.15	1681	5.57	0.83		0.034
4.25	1260	4.15	1680	5.5	0.83		0.035
4.5	1260	4.12	1769	5.73	0.83		0.028
4.75	1260	4.16	1676	5.56	0.83		0.034
5	1260	4.16	1662	5.55	0.83		0.035
5	325	4.01	1955	6.16	0.86	0.003	
5.5	325	3.97	2018	6.16	0.86	0.008	
5.75	1260	4.01	1941	6.09	0.83		0.019
6	1260	4.01	1941	6.09	0.83		0.019
6.25	325	3.97	2041	6.08	0.83	0.009	
6.25	1260	4.06	1876	6.08	0.83		0.02
6.5	1260	4.06	1876	6.08	0.83		0.02
6.5	325	4.03	1941	6.13	0.86	0.008	
6.75	1260	4.04	1920	6.1	0.84		0.02
7	1260	4.04	1920	6.1	0.84		0.02
7	325	4.04	1914	6.12	0.86	0.009	
7.25	1260	4.08	1837	6.01	0.84		0.023
7.5	1260	4.08	1837	6.01	0.84		0.023
7.5	325	4.03	1937	6.1	0.86	0.007	
7.75	1260	4.08	1843	5.96	0.84		0.023
8	1260	4.08	1843	5.96	0.84		0.023
8	325	3.88	2133	6.06	0.86	0.006	
8.25	1260	3.97	1981	5.99	0.84		0.019
8.5	1260	3.95	2026	5.98	0.84		0.018
8.5	325	3.9	2093	6.15	0.86	0.01	
8.75	1260	4.02	1928	5.92	0.85		0.022
9	1260	4.02	1917	5.95	0.85		0.022
9.25	1260	4.01	1930	5.91	0.86		0.022
9.5	1260	4.01	1930	5.91	0.86		0.022
9.75	1260	3.99	1977	6.05	0.86		0.02
10	1260	3.99	1977	6.05	0.86		0.02

Table A-19. HYMETS Test Data for Type 2 Coated Beta-21S Specimens N6(A), N7(A), and N8(A).

SPEC. NO.: N6(A) ALLOY: BETA-21S Ti THICKNESS, CM: 0.0647

Time, Hr.	Temp., K	Mach No.	Enthalpy cal/gm	P-wall, torr	Emit. at Temp	Cat. Efficiency Cold	Hot
0	325	3.81	2258	6.07		0.001	
0.25	1094	3.9	924	4.12	0.8		0.099
0.5	1094	3.99	958	4.17	0.79		0.078
0.5	325	3.81	2274	6.09		0.004	
0.75	1094	4	931	4.16	0.78		0.089
1	1094	4.03	953	4.19	0.77		0.074
1	325	3.8	2268	6.1		0.004	

SPEC. NO.: N7(A) ALLOY: BETA-21S Ti THICKNESS, CM: 0.064

1	325	3.8	2268	6.17		0.004	
1	325	3.9	2102	6.17		0.007	
1.25	1094	4.15	1225	4.47	0.75		0.014
1.5	1094	4.16	1299	4.51	0.76		0.01
1.5	325	3.92	2043	6.19		0.012	
1.75	1094	4.15	1247	4.59	0.77		0.013
2	1094	4.15	1247	4.59	0.77		0.013
2	325	3.97	1981	6.17		0.013	
2.25	1094	4.17	1313	4.82	0.77		0.008
2.5	1094	4.18	1322	4.82	0.77		0.007
2.5	325	3.9	2066	6.19		0.014	
2.75	1094	4.17	1292	4.81	0.77		0.009
3	1094	4.18	1318	4.84	0.77		0.007
3	325	3.95	2025	6.24		0.014	
3	325	3.99	1999	6.15		0.001	
3.25	1094	4.14	870	4.25	0.77		0.126
3.5	1094	4.13	884	4.22	0.77		0.117
3.5	325	3.97	2017	6.14		0.011	
3.75	1094	4.14	853	4.23	0.77		0.144
4	1094	4.14	850	4.21	0.77		0.149
4	325	3.99	2001	6.2		0.009	
4.25	1094	4.16	778	4.36	0.77		0.25
4.5	1094	4.14	789	4.3	0.77		0.236
4.5	325	4.02	1944	6.21		0.009	
4.75	1094	4.14	770	4.23	0.77		0.291
5	1094	4.14	764	4.2	0.77		0.317

SPEC. NO.: N8(A) ALLOY: BETA-21S Ti THICKNESS, CM: 0.0644

0	325	3.99	1999	6.15		0.001	
0.25	1094	4.15	1065	4.49	0.79		0.038
0.5	1094	4.15	1149	4.54	0.78		0.023
0.5	325	3.97	2017	6.14		0.006	
0.75	1094	4.16	1107	4.51	0.77		0.028
1	1094	4.15	1039	4.45	0.76		0.04
1	325	3.99	2001	6.2		0.003	
1.25	1094	4.14	955	4.44	0.75		0.063
1.5	1094	4.14	925	4.42	0.74		0.066
1.5	325	4.02	1944	6.21		0.006	
1.75	1094	4.15	797	4.48	0.73		0.162
2	1094	4.15	797	4.48	0.73		0.162

Table A-20. HYMETS Test Data for RCG Coating at Six Temperatures.

SPEC. NO.: RCG ALLOY: LI2200 WITH RCG COAT THICKNESS, CM: 0.0381

Temp., K	Time, hr	Mach No.	Enthalpy cal/gm	P-wall, torr	Emit. at Temp	Cat. Efficiency Cold	Hot
1198	0.5	4.14	1295	3.82	0.88		0.088
1243	1	4.19	1457	4.03	0.88		0.084
1272	1.5	4.14	1600	4.5	0.88		0.069
1301	2	4.11	1707	4.85	0.88		0.067
1337	2.5	3.93	2006	4.85	0.88		0.059
1374	3	3.78	2236	5.07	0.88		0.056

SURFACE TEMPERATURE DETERMINED BY MICRO-OPTICAL PYROMETER.
BRIGHTNESS TEMPERATURE CORRECTED TO TRUE TEMPERATURE USING
EFFECTIVE EMITTANCE OF 0.846 (0.92 x 0.92)

Appendix B
SPECTRAL EMITTANCE DATA

Spectral near normal room temperature emittance data derived from spectral near-normal reflectance measurements made at a specimen temperature of 295 to 300 K for the oxidation and HYMETS test specimens are tabulated in this appendix. Figures B-1 through B-33 present the data for pre- and post-HYMETS tests. Data for coated alpha2 titanium aluminide are shown in Figures B-1 through B-13 and B-24 through B-27. Figures B-14 through B-20 and Figure B-26 show data for the coated super-alpha2 titanium aluminide. Data for the gamma titanium aluminide are given in Figures B-21, B-22, B-29, B-30 and B-31. Figures B-23, B-32 and B-33 present data for the beta-21S titanium alloy. Data for oxidation tests are shown in Figures B-34 through B-39.

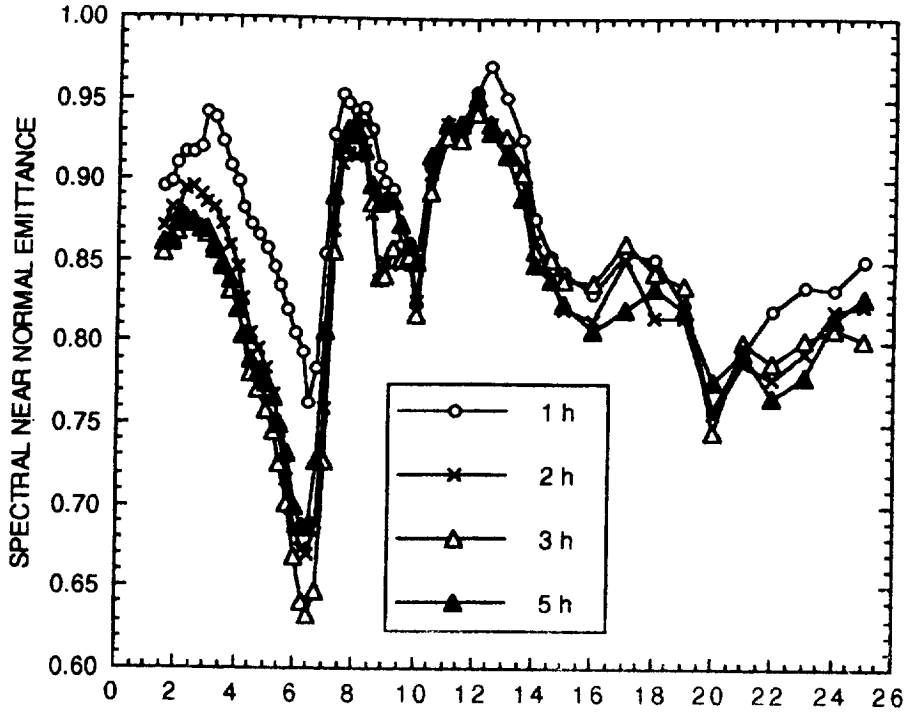

(b) Specimen L-29.

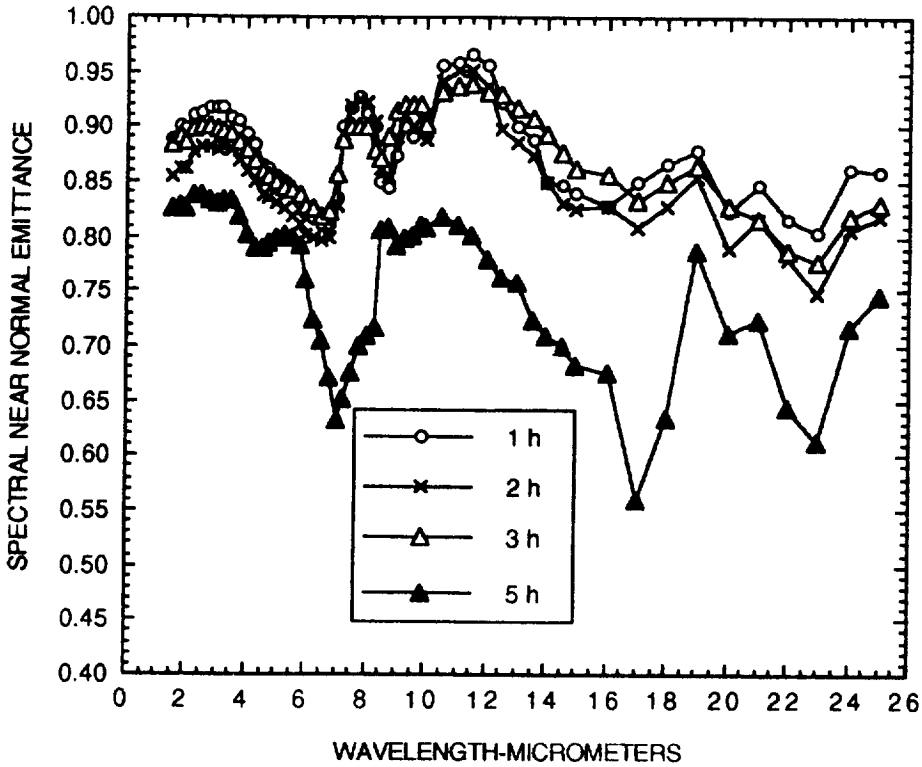

(a) Specimen L-17, statically oxidized 5 hr before HYMETS test.

Figure B-1. Spectral near normal emittance of two Type 3 coated Alpha2 alloy specimens (L-17 and L-29) as a function of HYMETS exposure time at 1260 K.

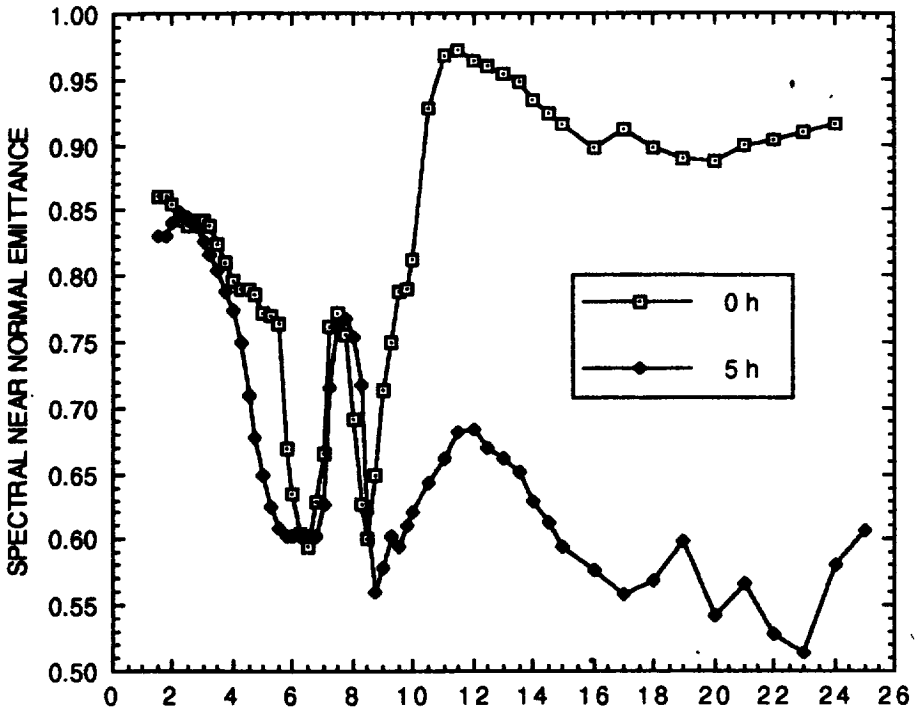

(b) Specimen L-33.

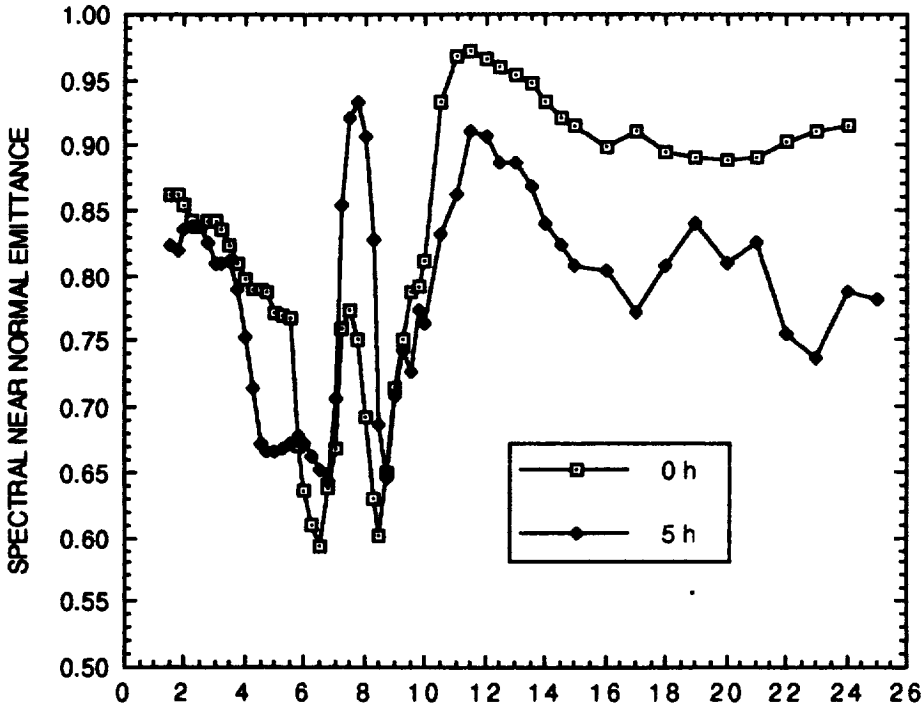

(a) Specimen L-31

Figure B-2. Spectral near normal emittance of two Type 3 coated Alpha2 alloy specimens (L-31 and L-33) as a function of HYMETS exposure time at 1260 K.

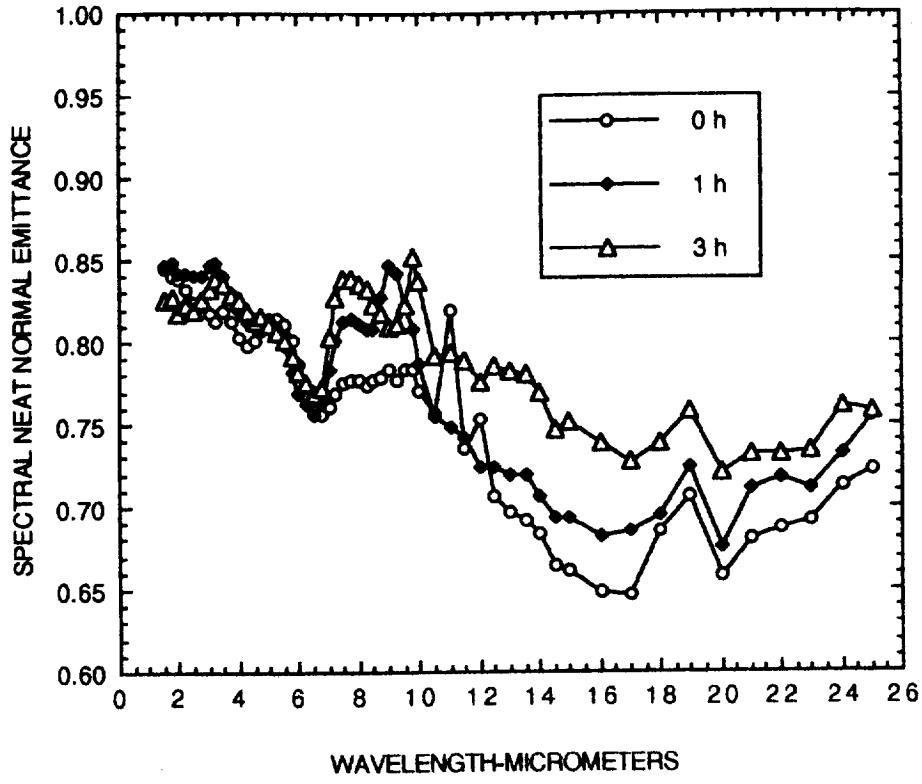

Figure B-4. Spectral near normal emittance of Specimen L-15, Type 3a coated Alpha2 substrate, as a function of HYMETS exposure time at 1260 K.

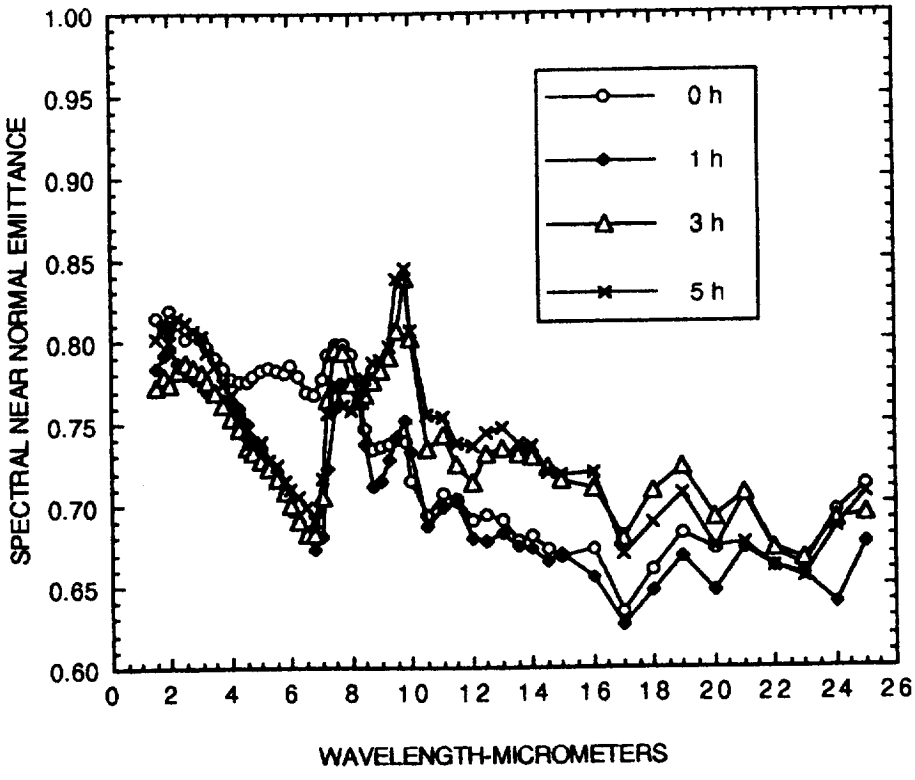

Figure B-3. Spectral near normal emittance of Specimen L-13, Type 3a coated Alpha2 substrate, as a function of HYMETS exposure time at 1260 K.

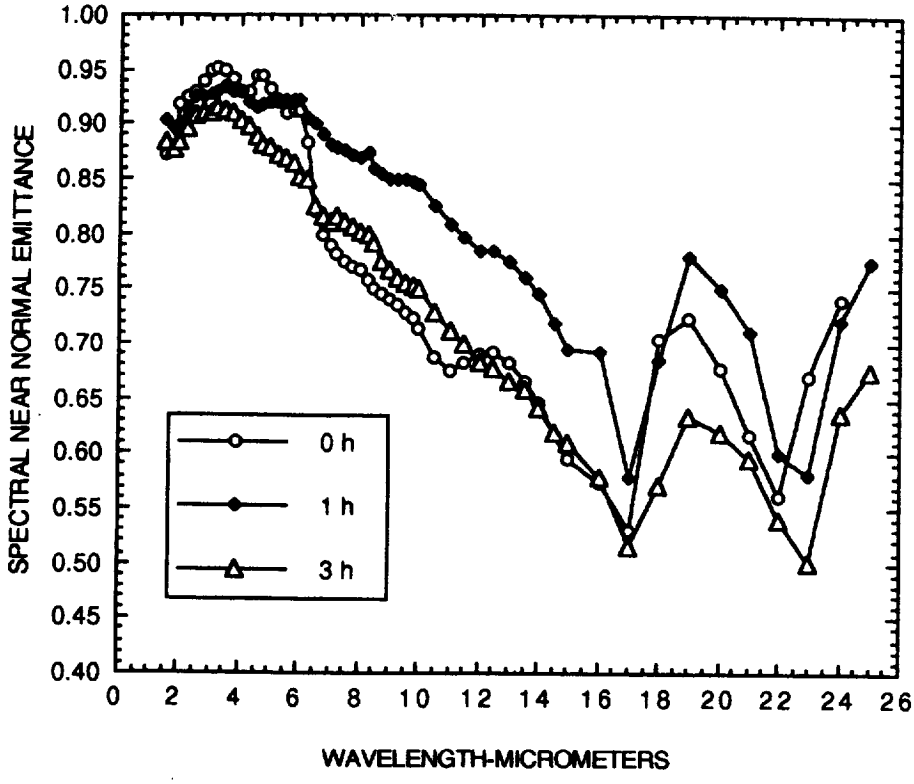

Figure B-6. Spectral near normal emittance of Specimen L-36, Type 3c coating on Alpha2 substrate, as a function of HYMETS exposure time at 1260 K.

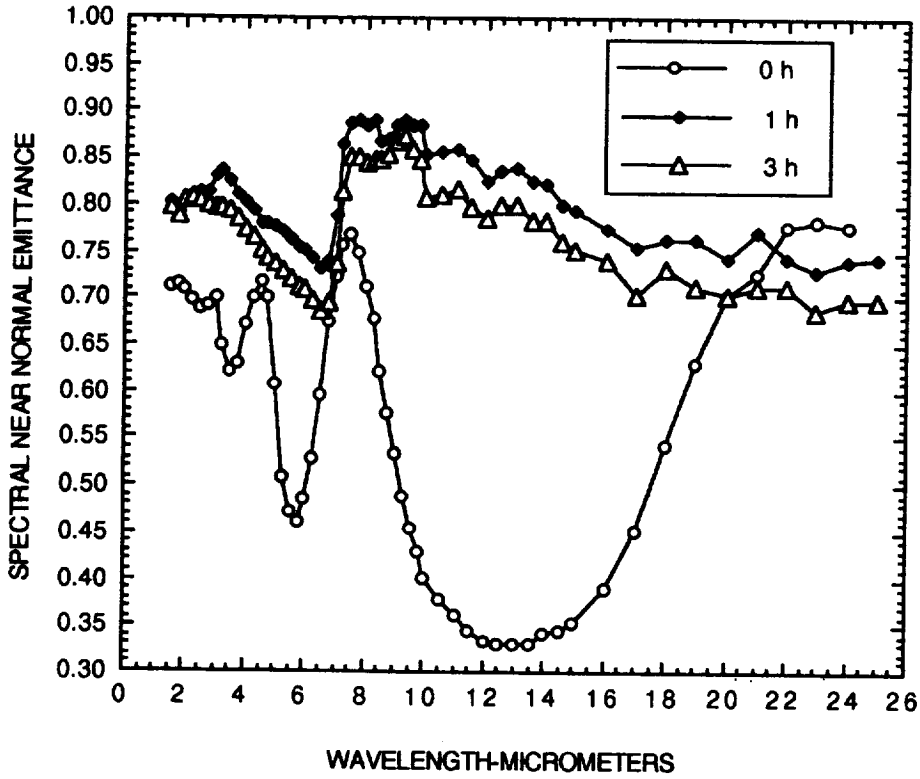

Figure B-5. Spectral near normal emittance of Specimen L-35, Type 3b coated Alpha2 substrate, as a function of HYMETS exposure time at 1260 K.

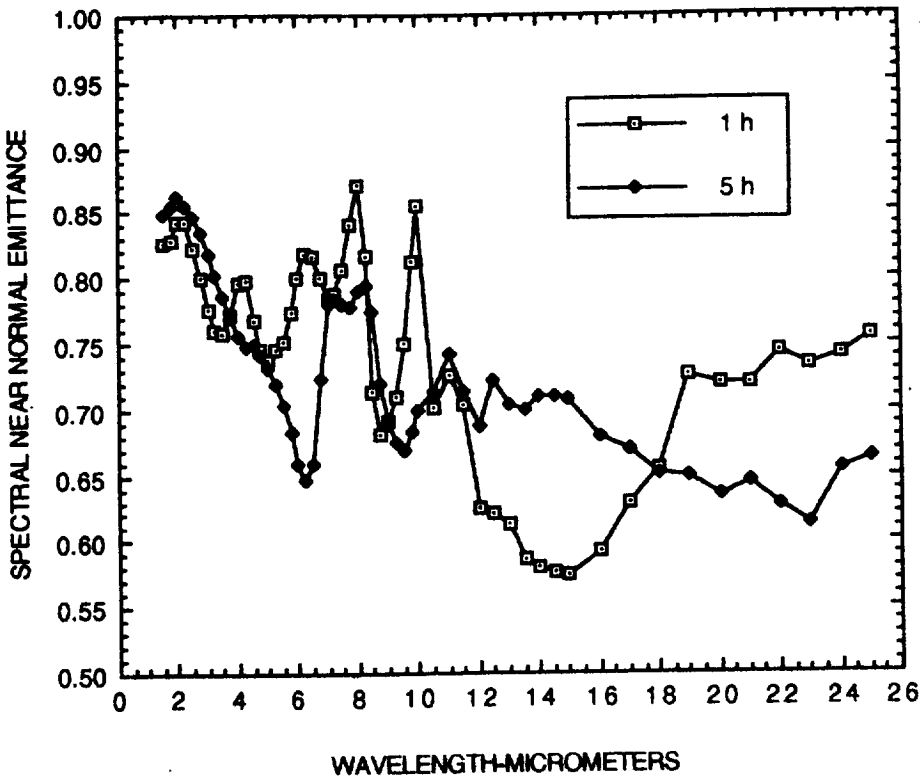

Figure B-8. Spectral near normal emittance of Specimen L-58, Type 1 coated Alpha2 substrate, as a function of HYMETS exposure time at 1260 K.

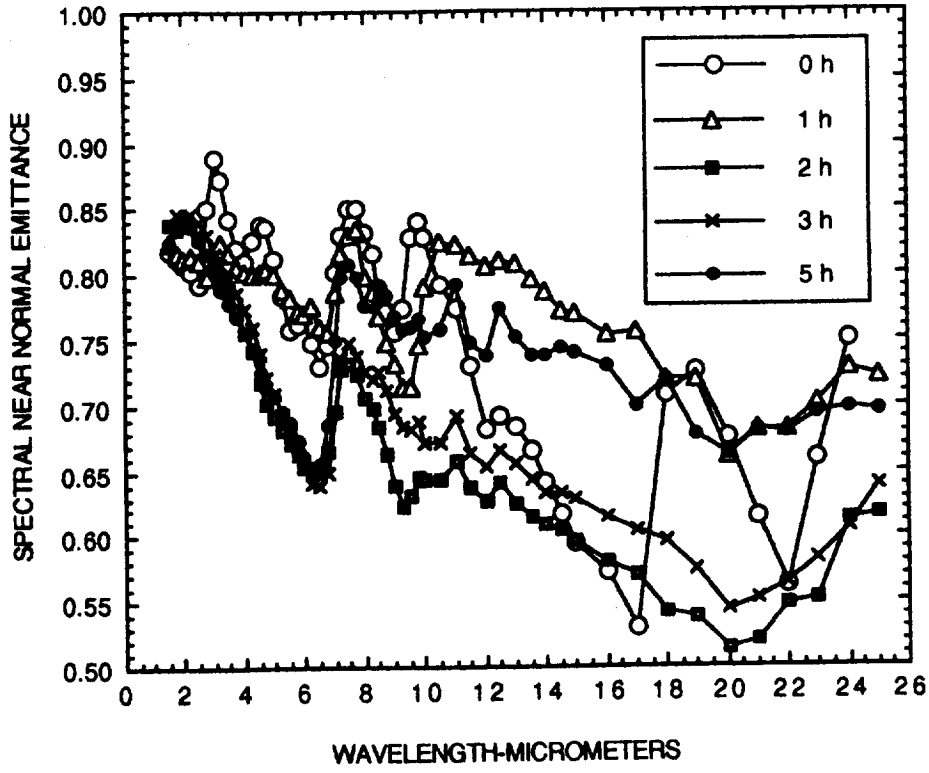

Figure B-7. Spectral near normal emittance of Specimen L-37, Type 1 coated Alpha2 substrate, as a function of HYMETS exposure time at 1260 K.

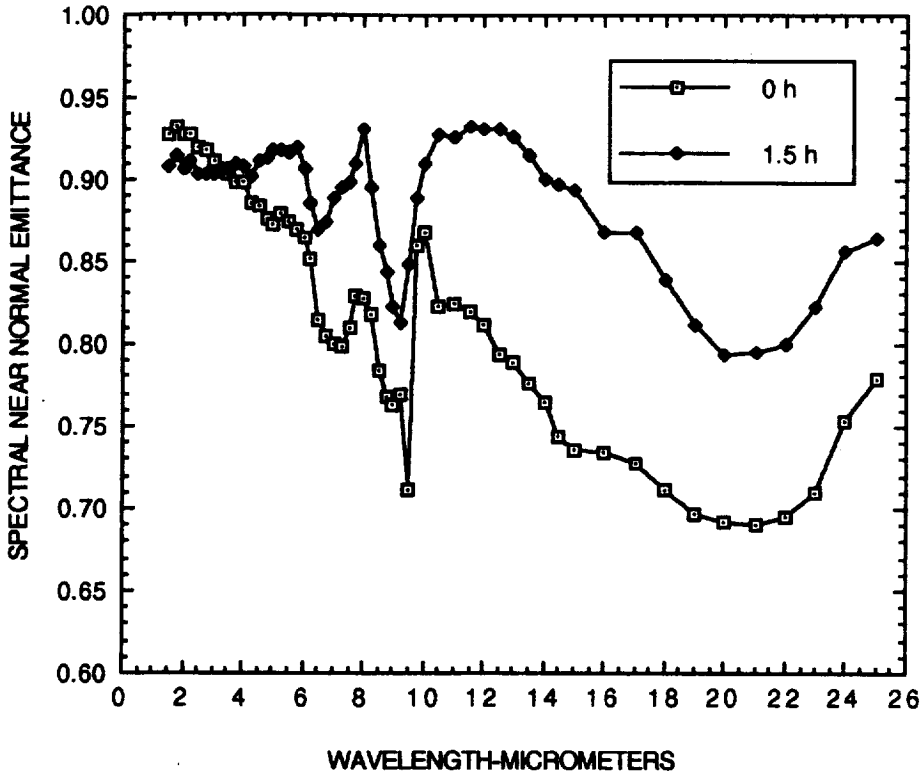

Figure B-10. Spectral near normal emittance of Specimen N8, Type 1 coated Alpha2 substrate, after thermal shock and 1.5 hr HYMETS exposure at 1260 K.

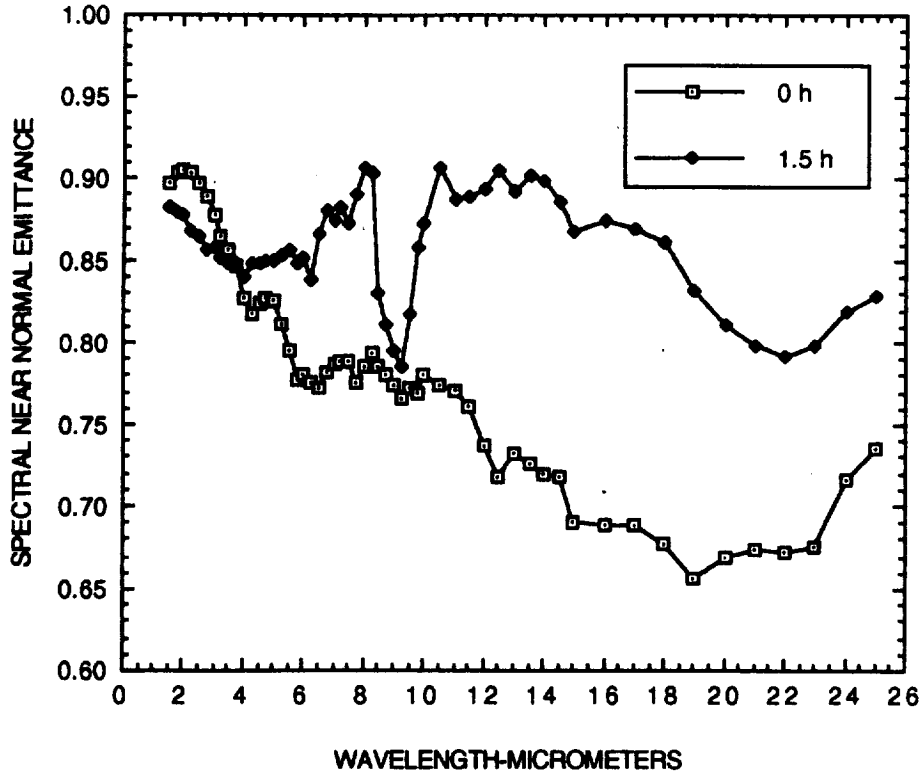

Figure B-9. Spectral near normal emittance of Specimen N3, Type 1 coated Alpha2 substrate, after water immersion and 1.5 hr HYMETs exposure at 1260 K.

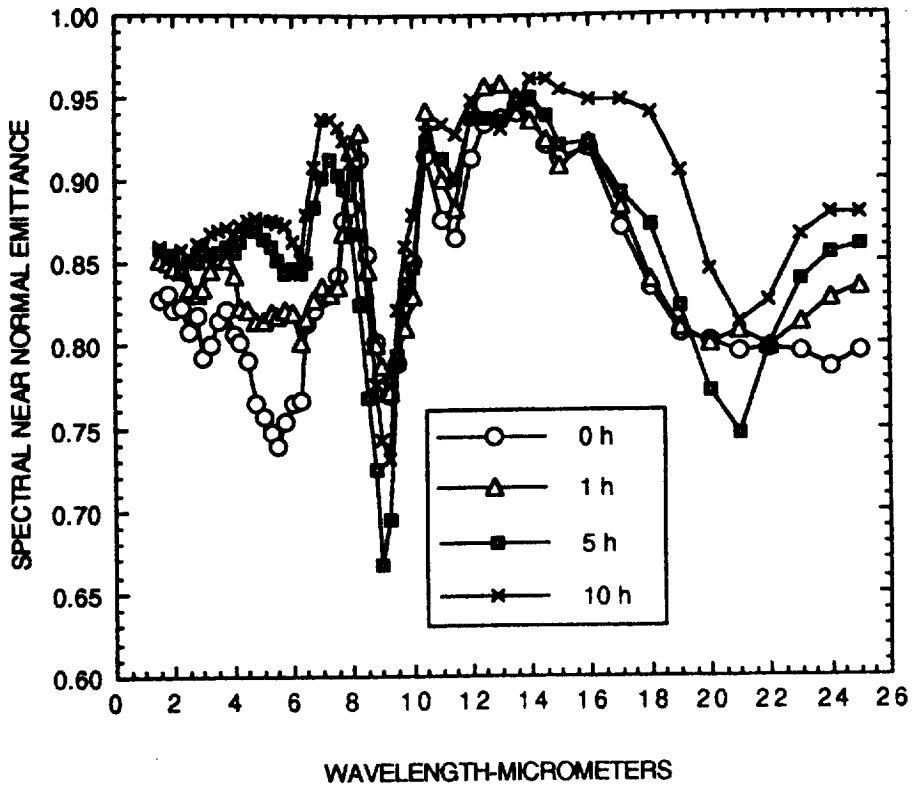

(b) Specimen N4A.

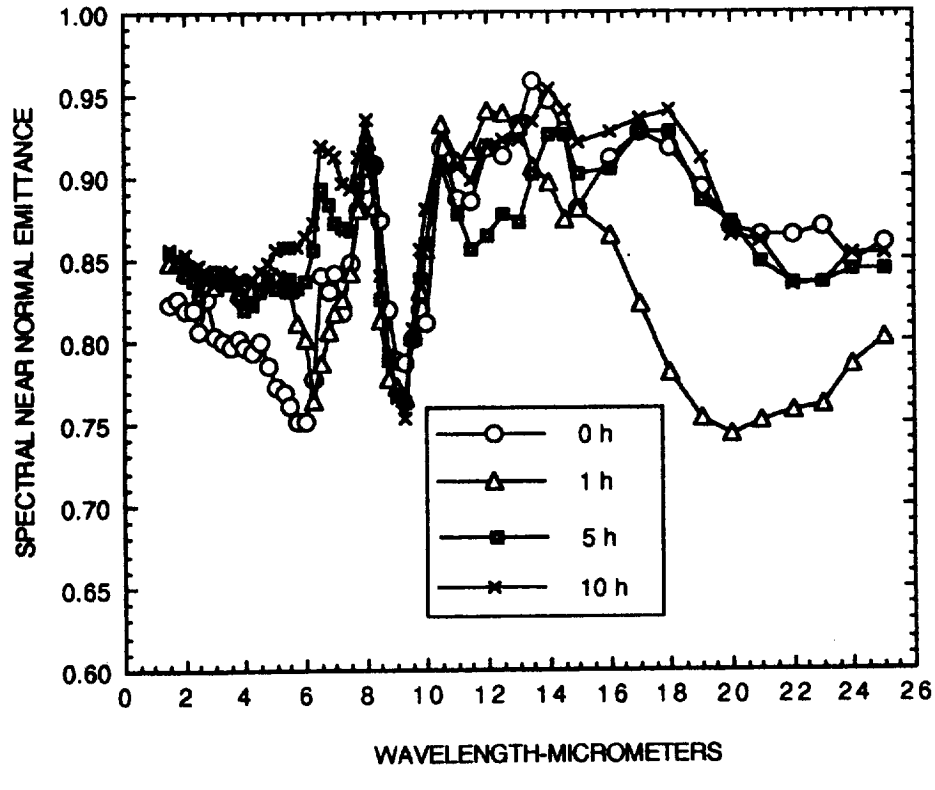

(a) Specimen N1A.

Figure B-11. Spectral near normal emittance of Specimens N1A and N4A, Type 1 coated Alpha2 substrates, as a function of HYMETS exposure time at 1205 K.

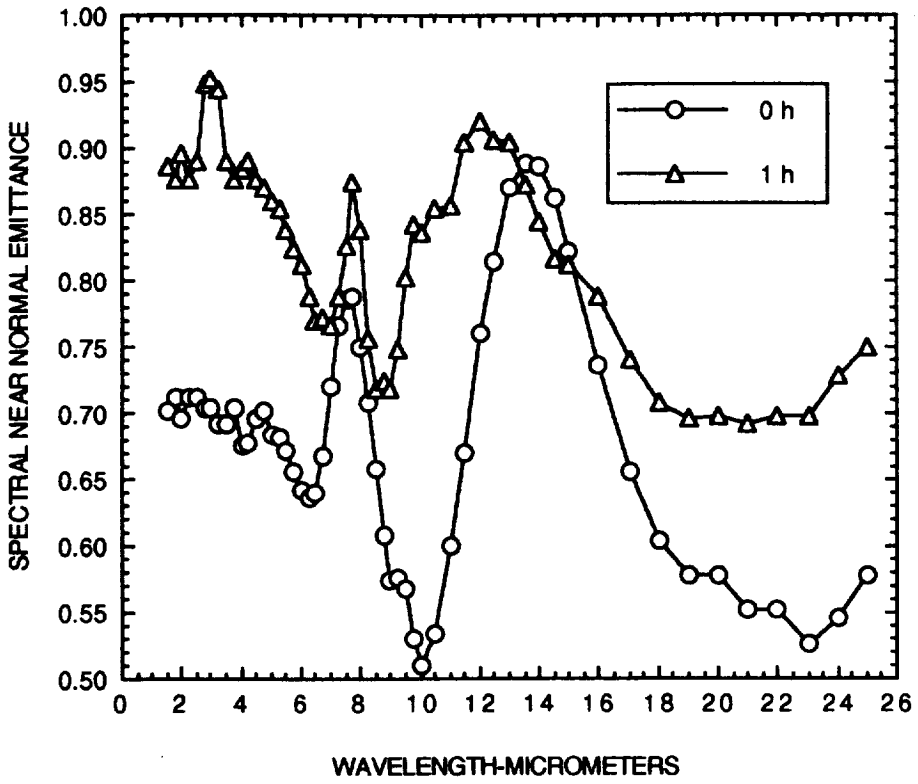

Figure B-13. Spectral near normal emittance of Specimen N3A, Type 1 coated Alpha2 substrate, before and after 1 hr HYMETS exposure at 1205 K.

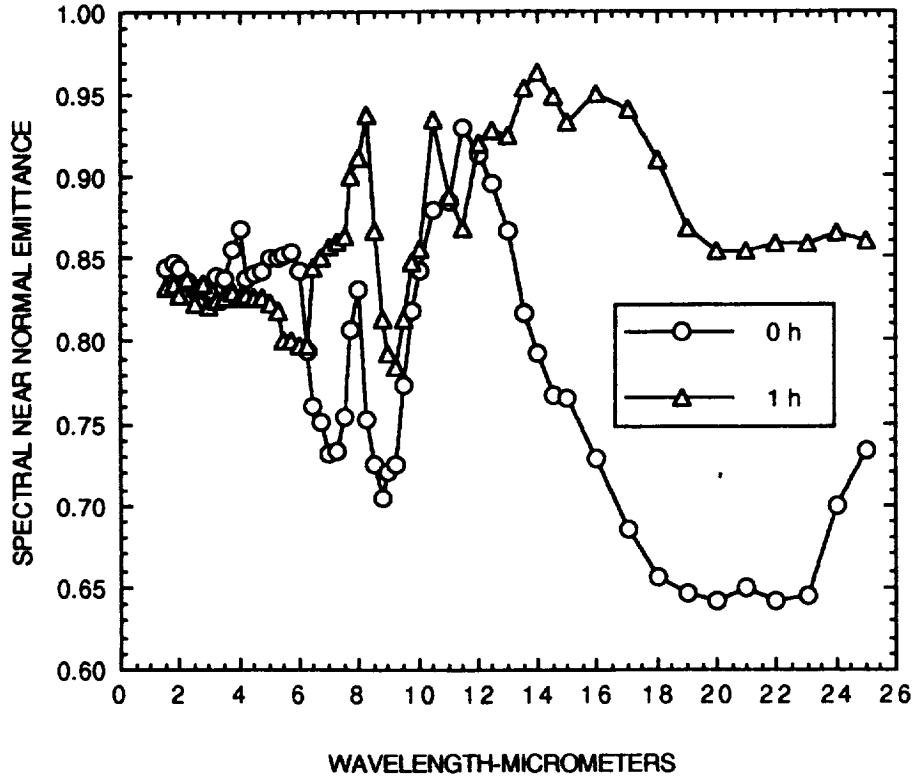

Figure B-12. Spectral near normal emittance of Specimen N2A, Type 1 coated Alpha2 substrate, before and after 1 hr HYMETS Exposure at 1205 K.

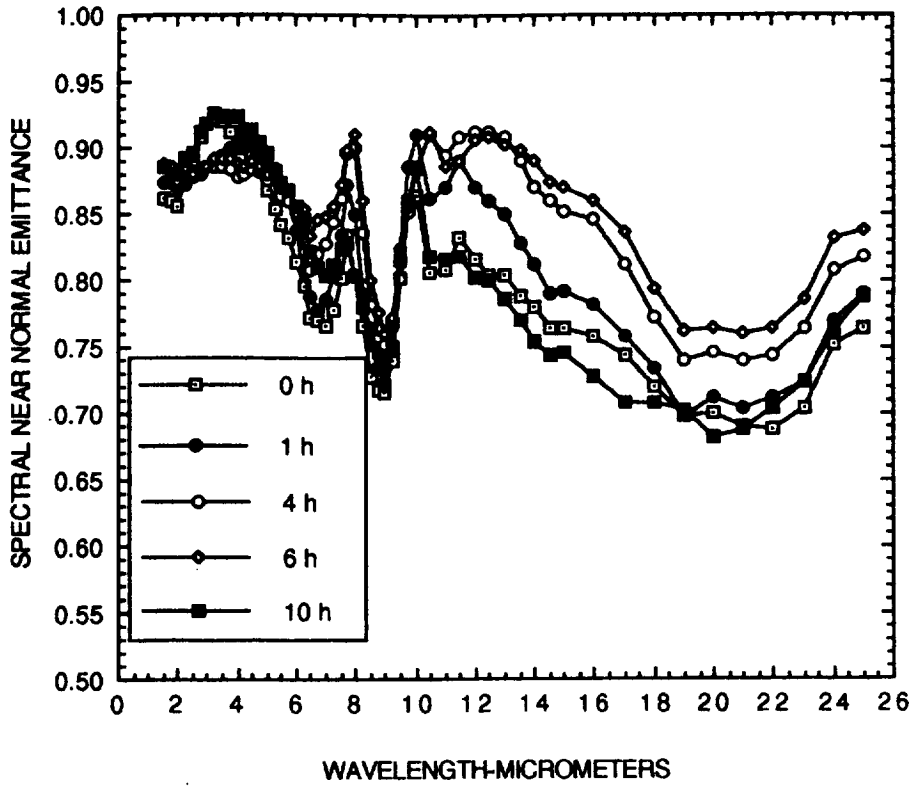

Figure B-15. Spectral near normal emittance of Specimen N11, Type 1 coated Super-Alpha2 substrate, as a function of HYMETS exposure time at 1205 K.

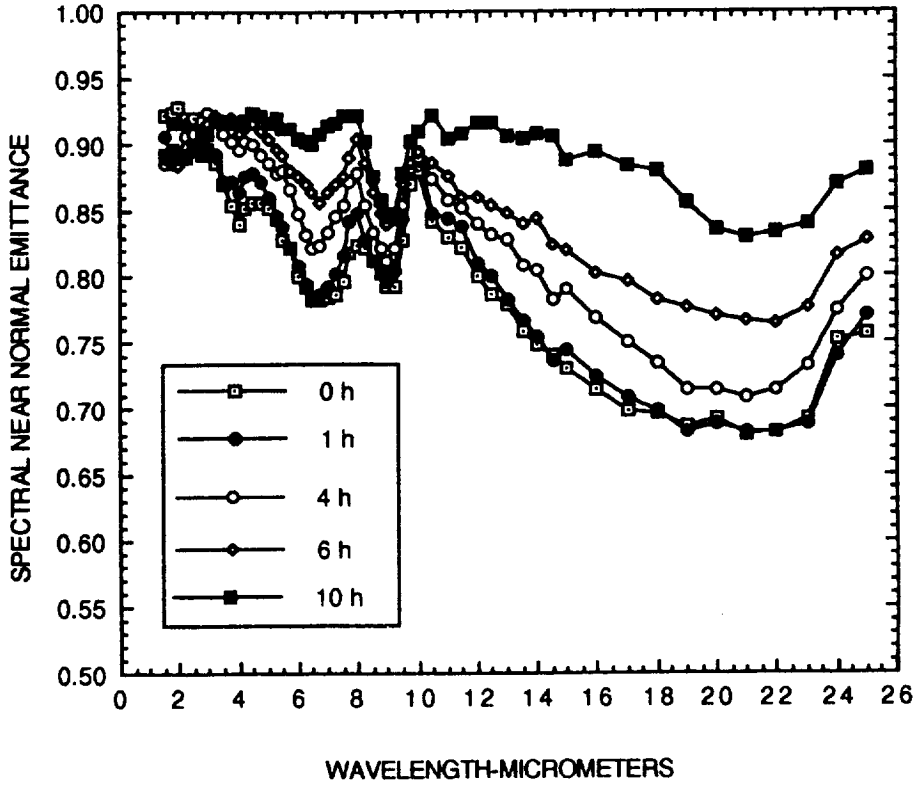

Figure B-14. Spectral near normal emittance of Specimen N9, Type 1 coated Super-Alpha2 substrate as a function of HYMETS exposure time at 1205 K.

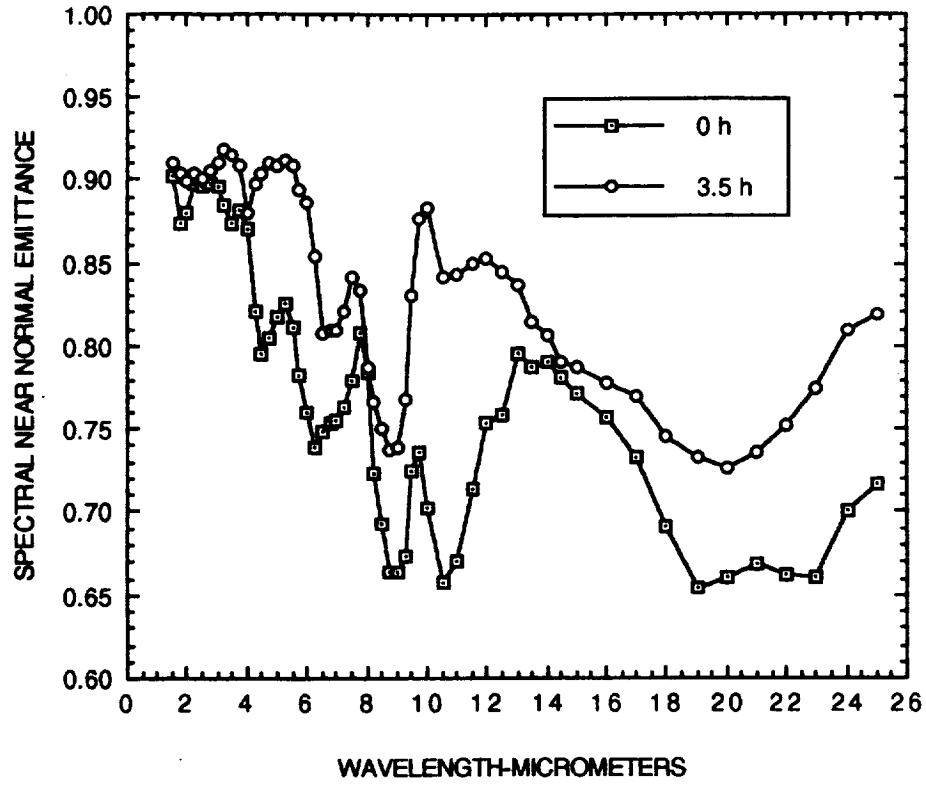

Figure B-17. Spectral near normal emittance for Specimen N14, Type 1 coated Super-Alpha2 substrate, as a function of HYMETS exposure time.

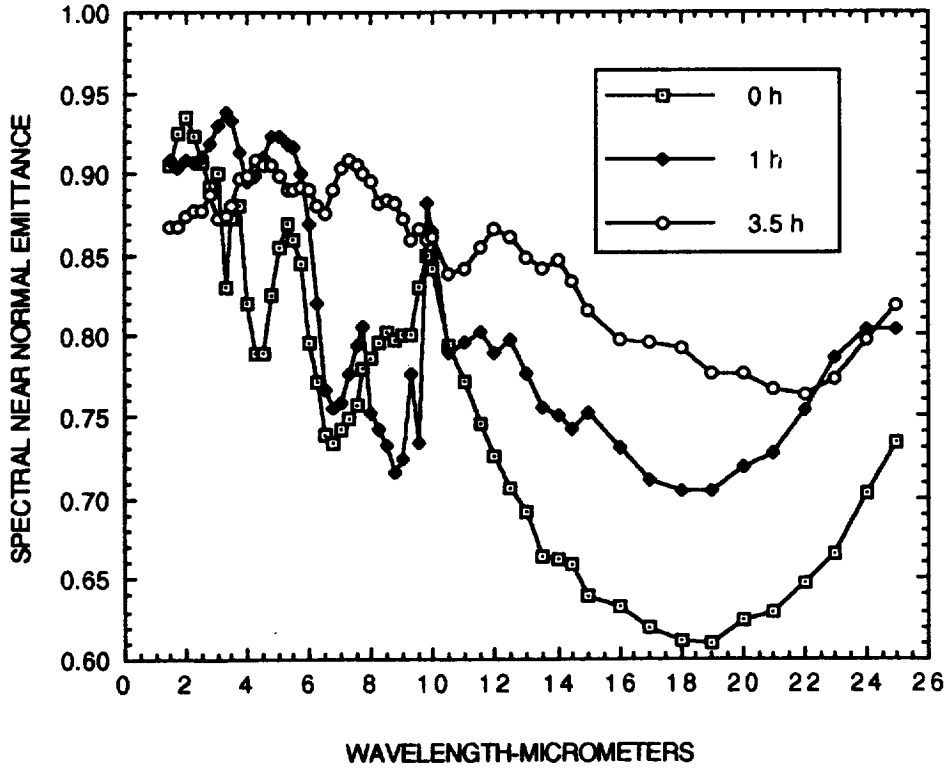

Figure B-16. Spectral near normal emittance for Specimen N13, Type 1 coated Super-Alpha2 substrate, as a function of HYMETS exposure time.

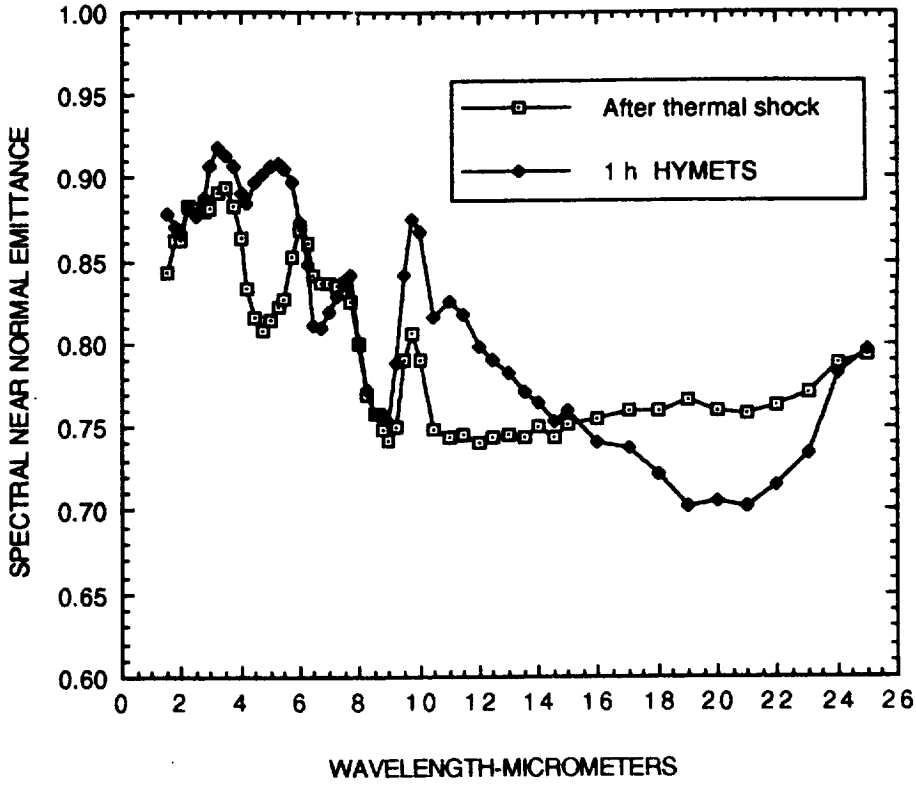

Figure B-19 . Spectral near normal emittance for Specimen N12, Type 1 coated Super-Alpha2 substrate, after thermal shock and after 1 h HYMETS exposure.

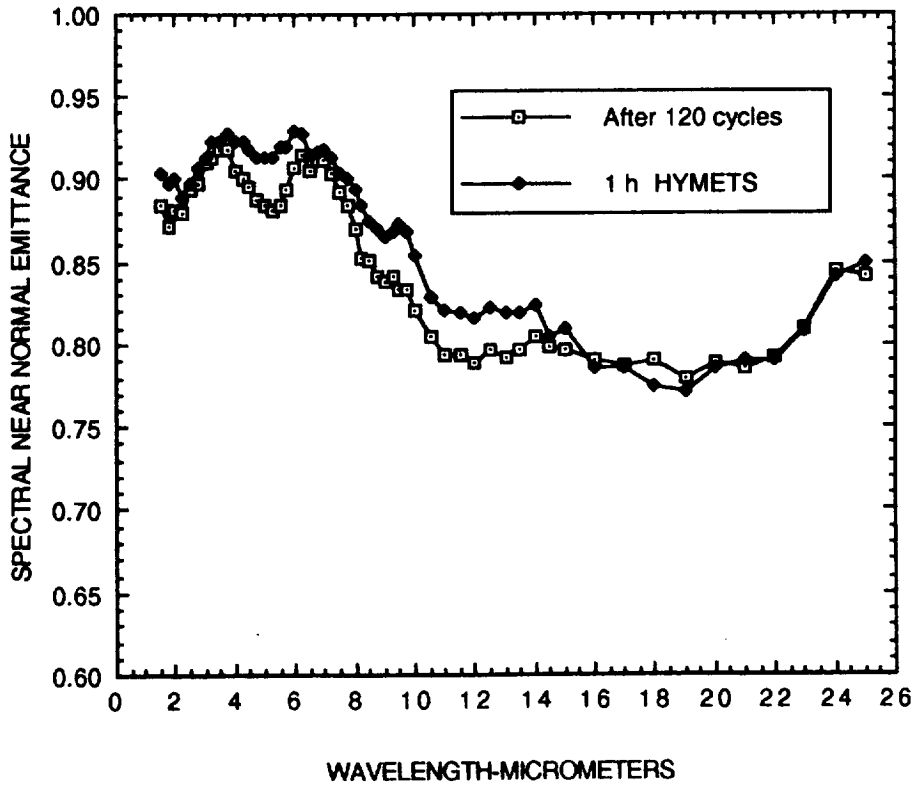

Figure B-18. Spectral near normal emittance of Specimen N15, Type 1 coated Super-Alpha2 substrate, after 120 cyclic oxidation exposures and then a 1 h HYMETS exposure.

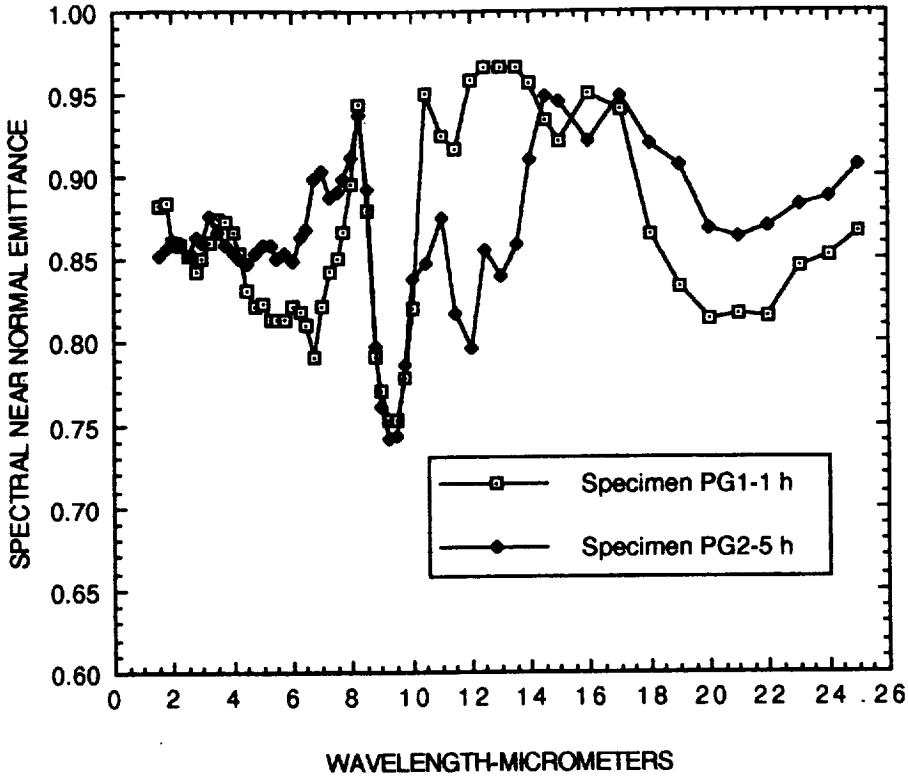

Figure B-21. Spectral near normal emittance of Type 1 coated Gamma specimens PG1 and PG2 after 1 h and 5 h , respectively, of HYMETS exposure at 1260 K.

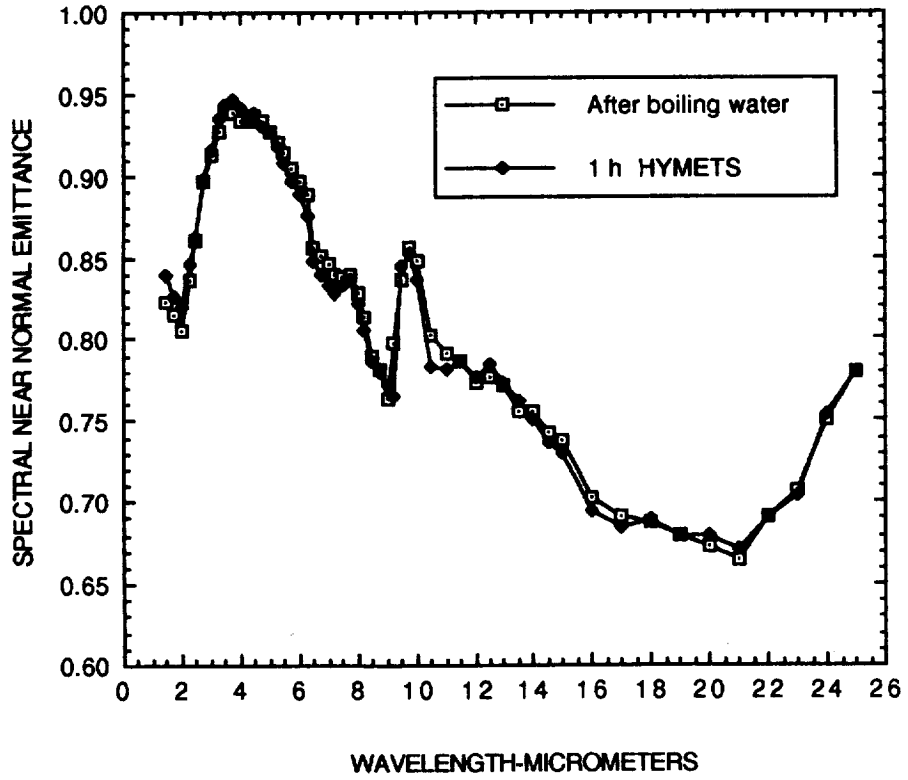

Figure B-20. Spectral near normal emittance of Specimen N16, Type 1 coated Super-Alpha2 substrate, after 24 h boiling water immersion and then after 1 h HYMETS exposure.

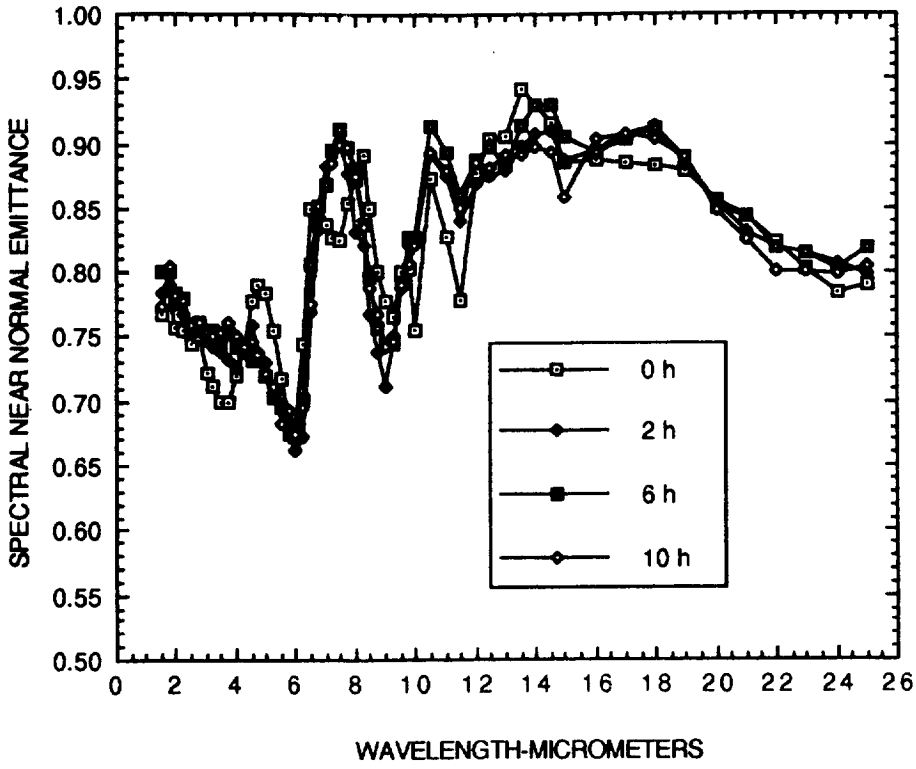

Figure B-23. Spectral near normal emittance of Specimen NA4, Type 1 coated Beta-21S substrate, as a function of HYMETS exposure time at 1094 K.

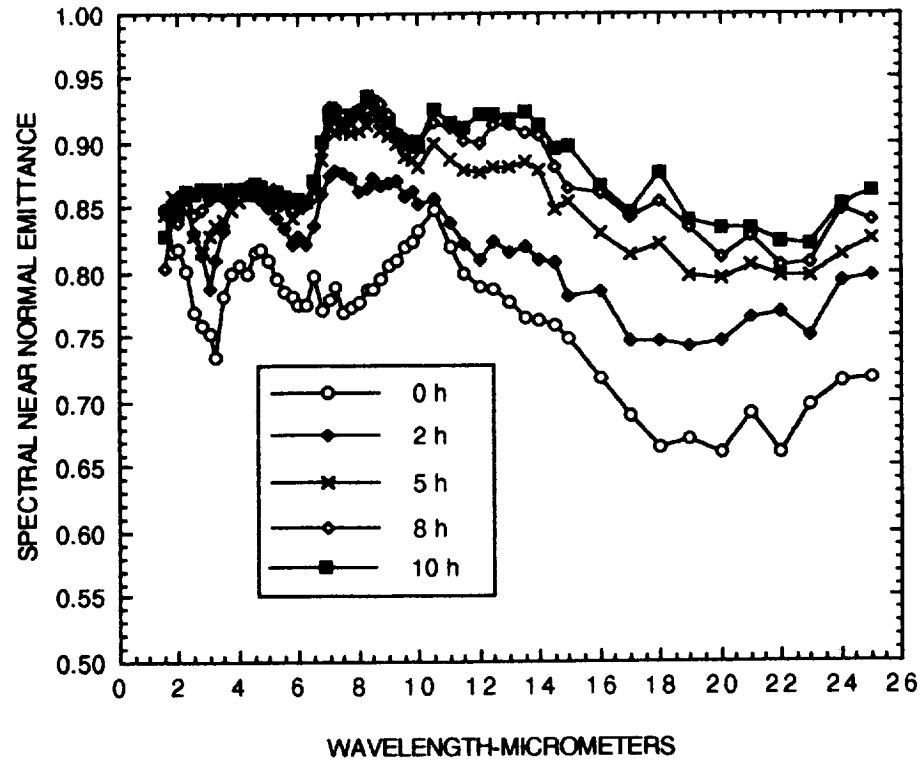

Figure B-22. Spectral near normal emittance of Specimen NG12, Type 1 coated Gamma substrate, as a function of HYMETS exposure time at 1260 K.

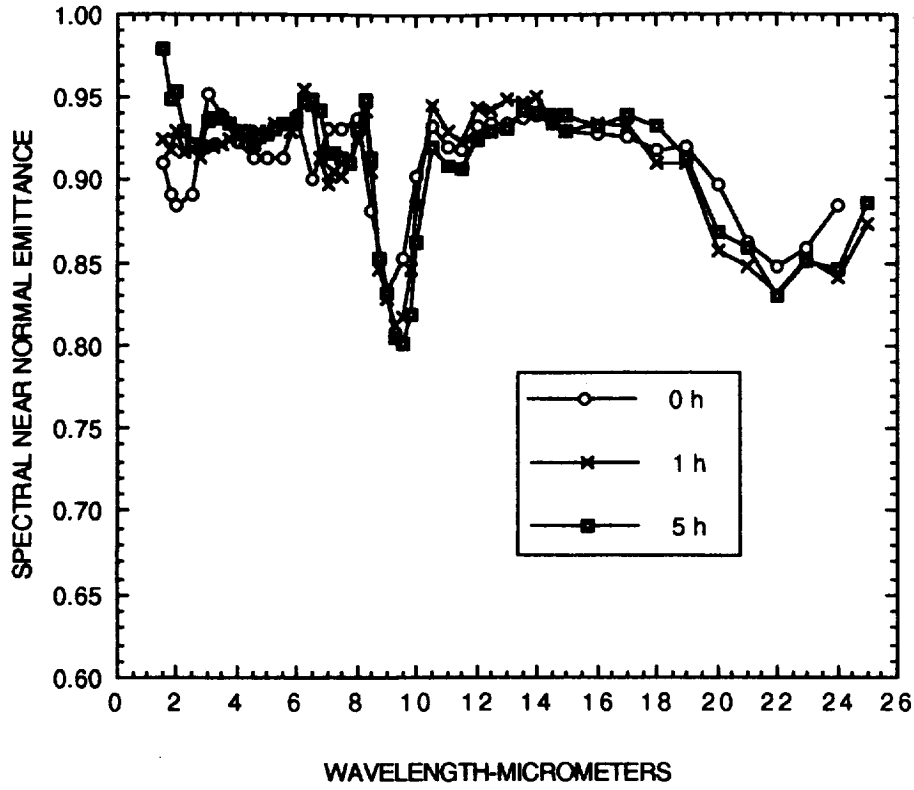

Figure B-25. Spectral near normal emittance of Specimen L-47, Type 2a coated Alpha2 substrate, as a function of HYMETS exposure time at 1260 K.

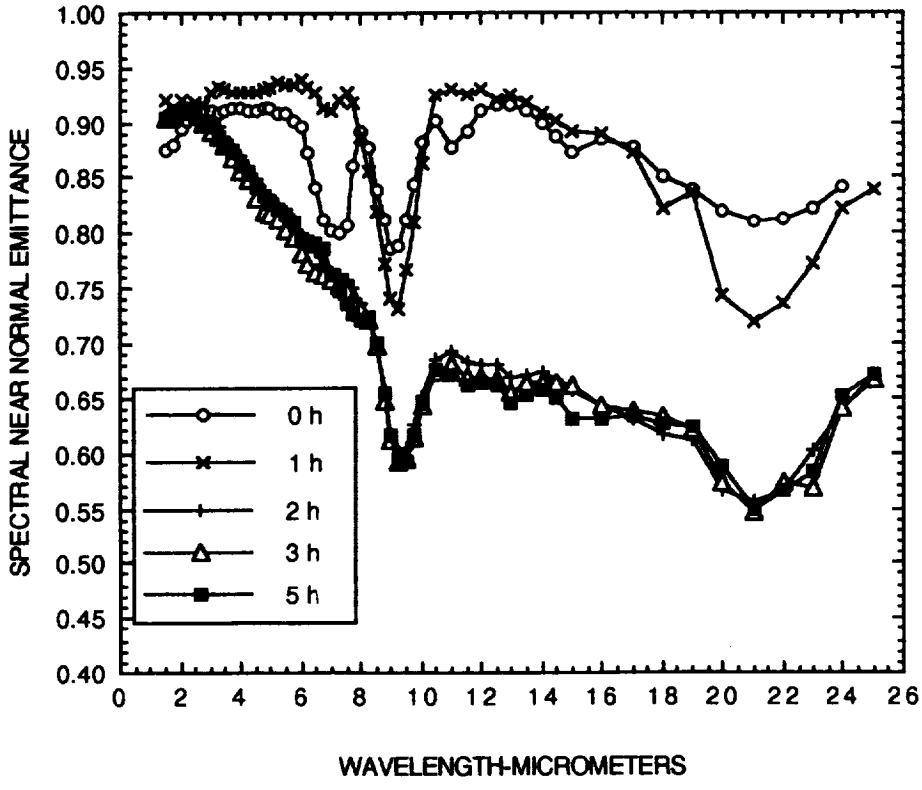

Figure B-24. Spectral near normal emittance of Specimen L-42, Type 2a coated Alpha2 substrate, as a function of HYMETS exposure time at 1260 K.

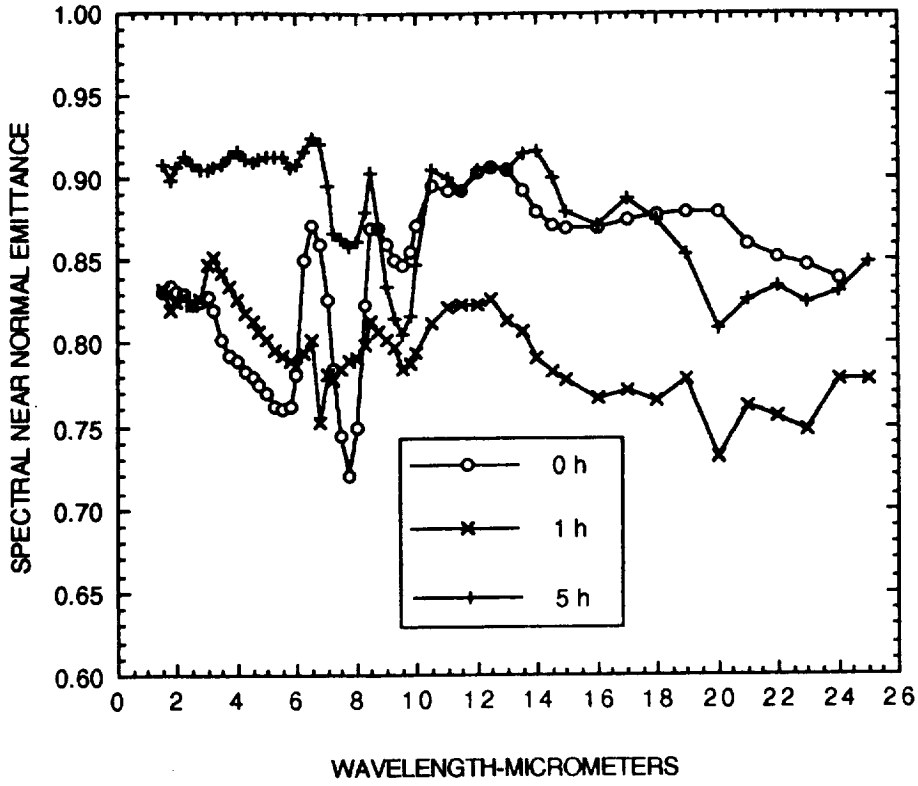

Figure B-27. Spectral near normal emittance of Specimen L-59, Type 2b coated Alpha2 substrate, as a function of HYMETS exposure time at 1260 K.

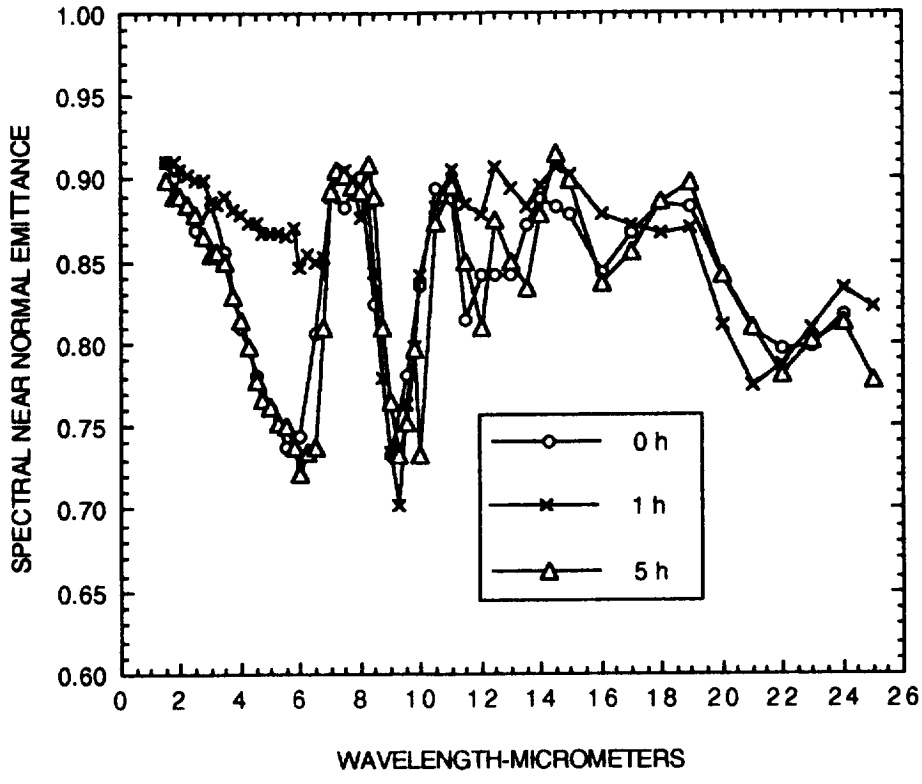

Figure B-26. Spectral near normal emittance of Specimen L-48, Type 2a coated Alpha2 substrate, as a function of HYMETS exposure time at 1260 K.

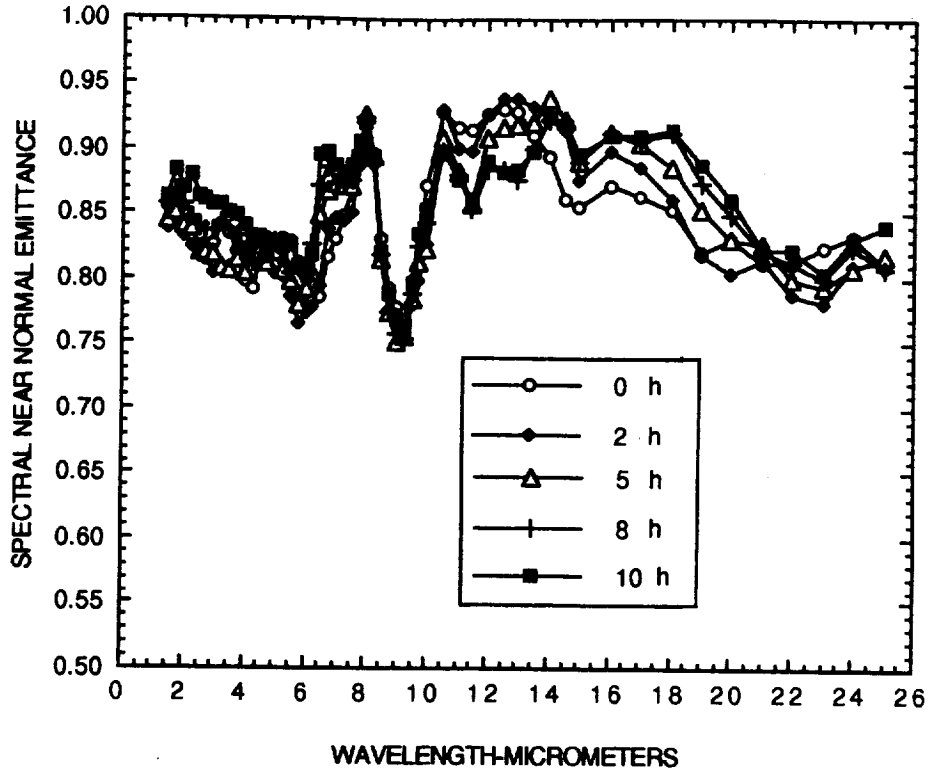

Figure B-29. Spectral near normal emittance of Specimen NG6, Type 2 coated Gamma substrate, as a function of HYMETS exposure time at 1260 K.

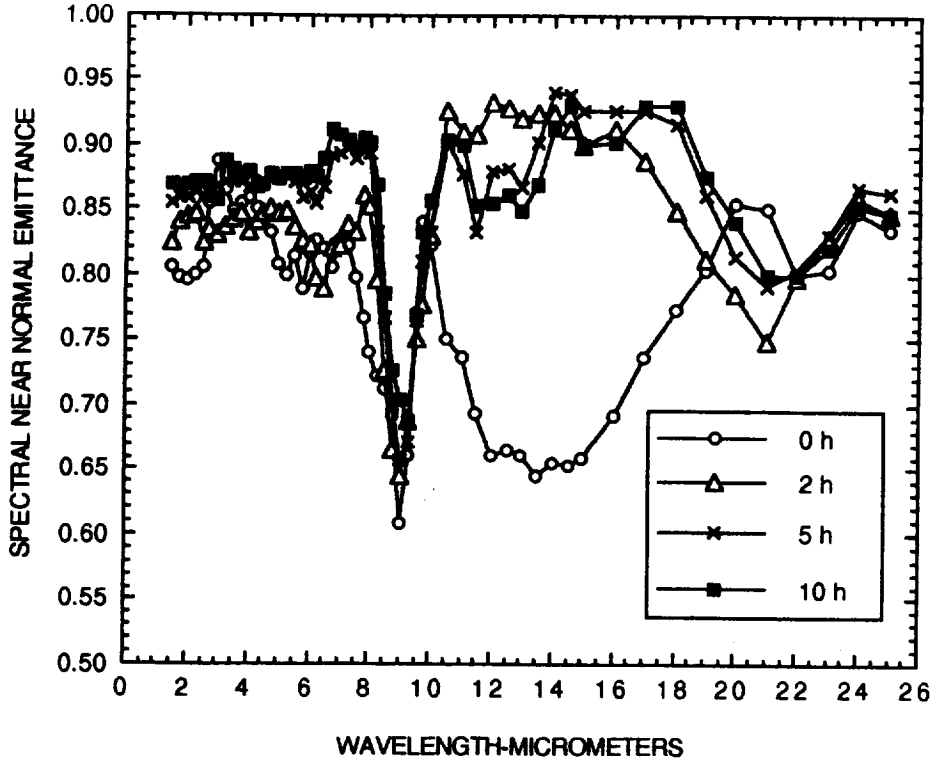

Figure B-28. Spectral near normal emittance of Specimen NSJR6, Type 2 coated Super-Alpha2 substrate, as a function of HYMETS exposure time at 1260 K.

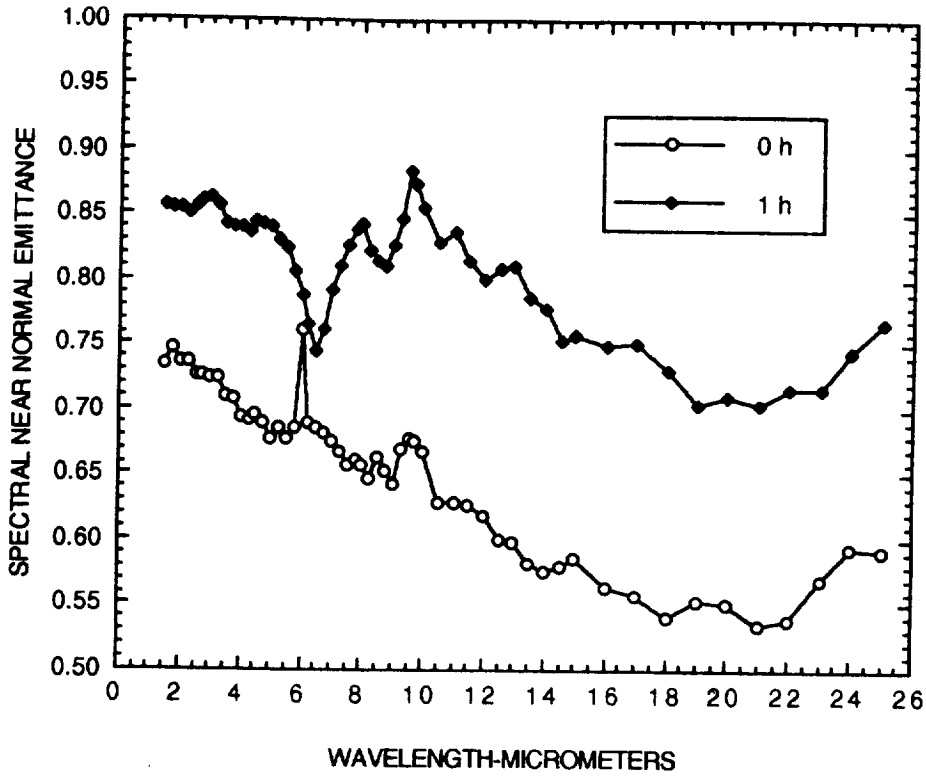

Figure B-31. Spectral near normal emittance of Specimen NG3, Type 2 coated Gamma substrate, as a function of HYMETS exposure time at 1260 K.

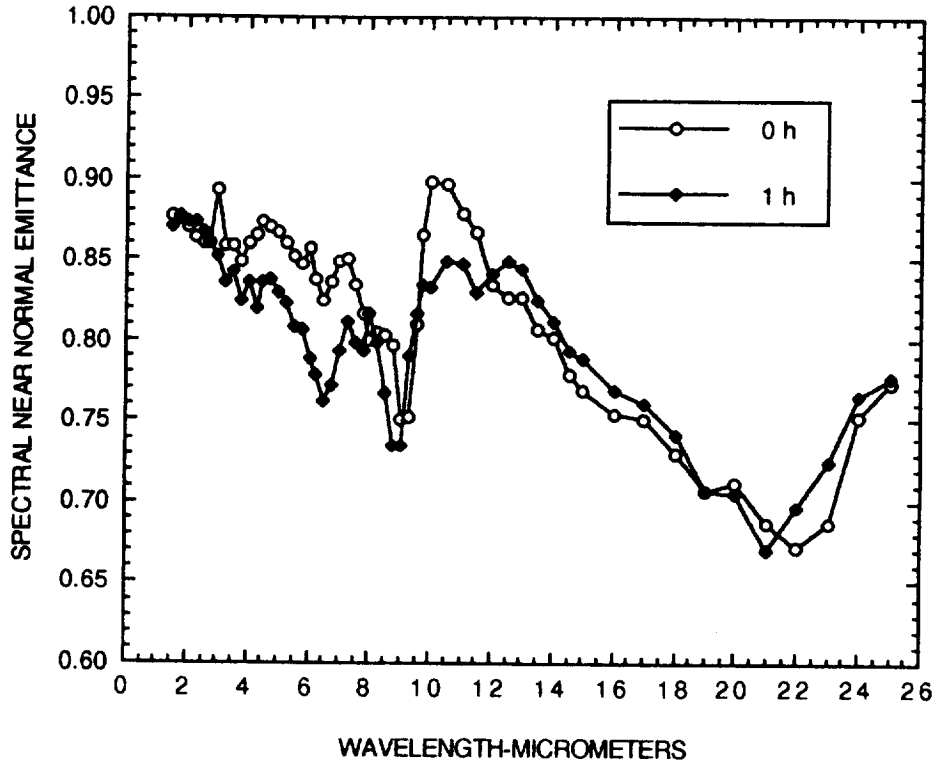

Figure B-30. Spectral near normal emittance of Specimen NG2, Type 2 coated Gamma substrate, as a function of HYMETS exposure time at 1260 K.

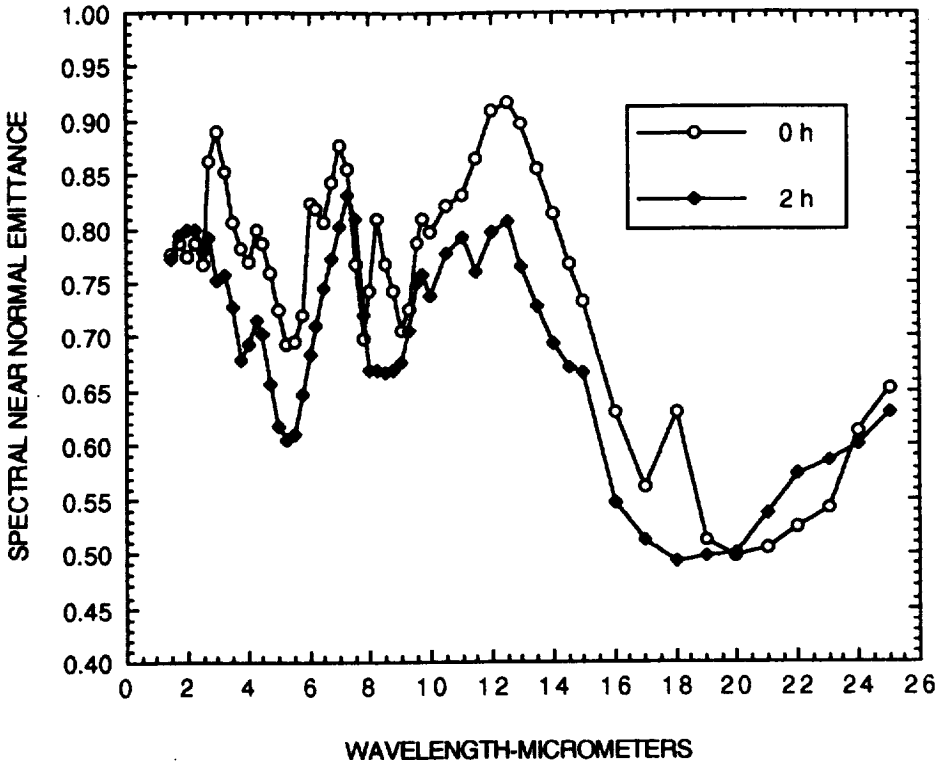

Figure B-33. Spectral near normal emittance of Specimen N8(A), Type 2 coated Beta-21S substrate, as a function of HYMETS exposure time at 1094 K.

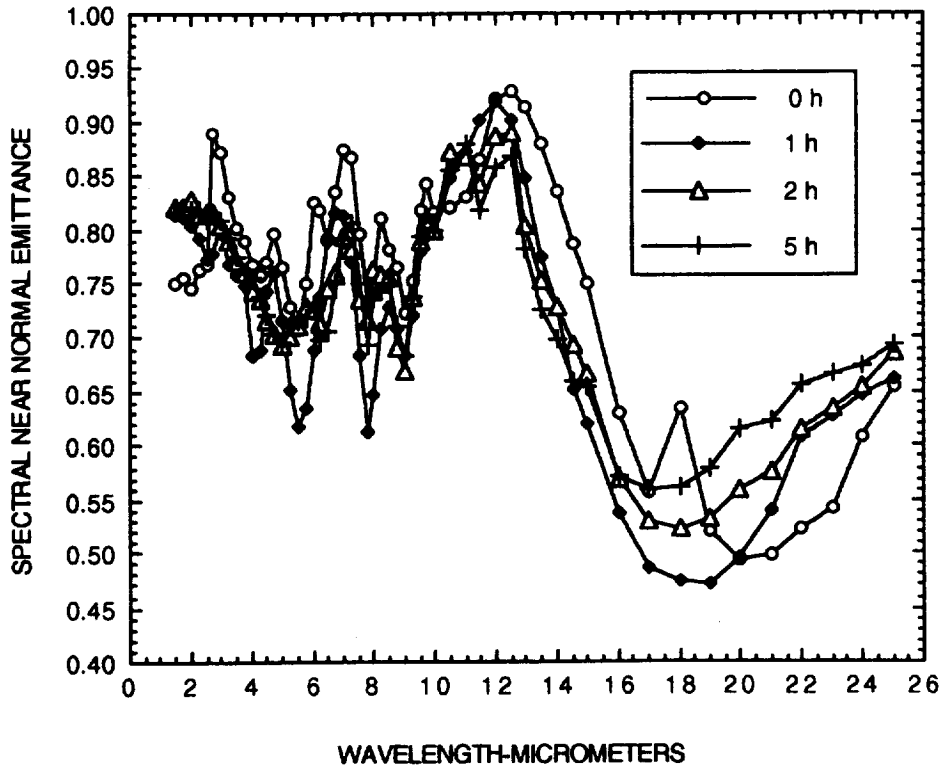

Figure B-32. Spectral near normal emittance of Specimen N7(A), Type 2 coated Beta-21S substrate, as a function of HYMETS exposure time at 1094 K.

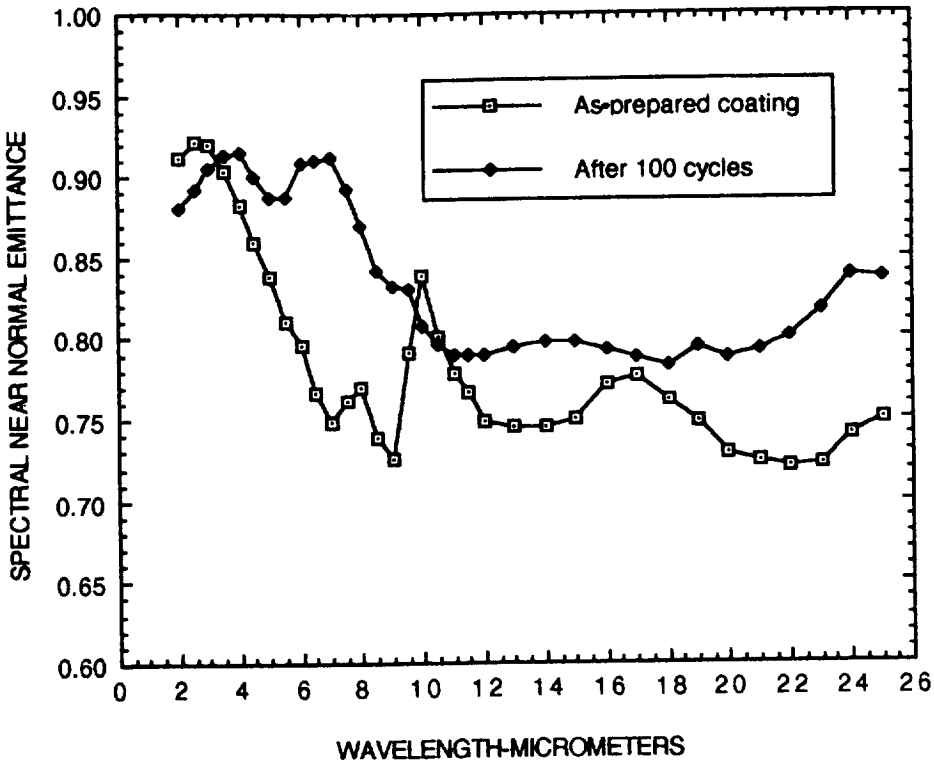

Figure B-35. Change in spectral near normal emittance of Type 1 coated Super Alpha2 substrate with 100 cyclic oxidation cycles at 1260 K.

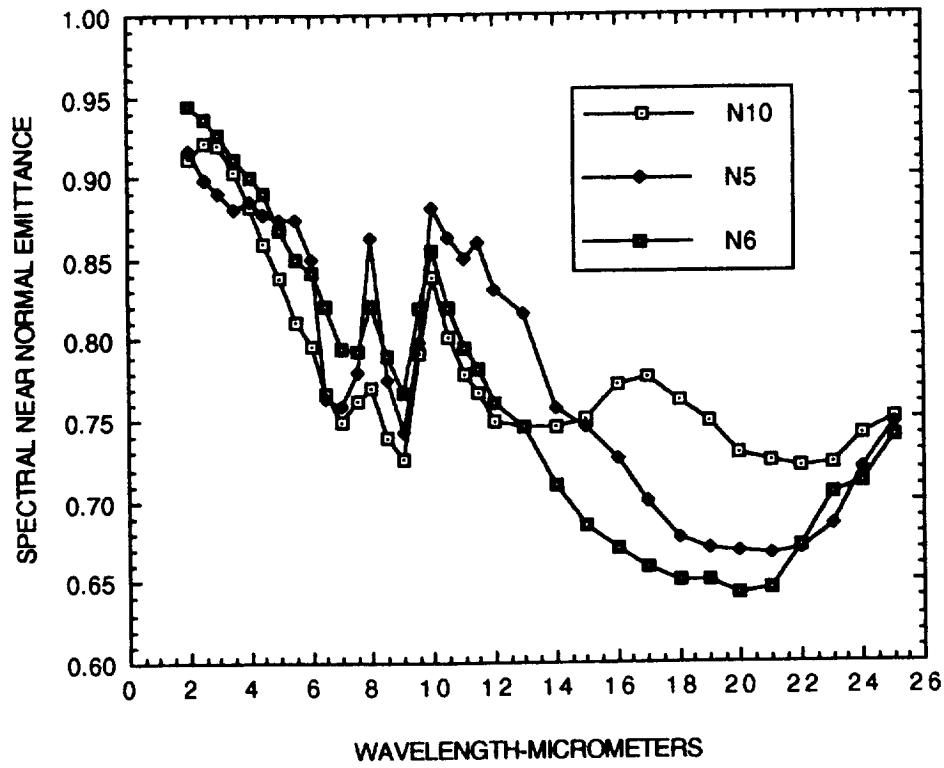

Figure B-34. Spectral near normal emittance of three as prepared specimens of Type 1 coating on Alpha2 (N5 and N6) and Super-Alpha2 (N10) substrates.

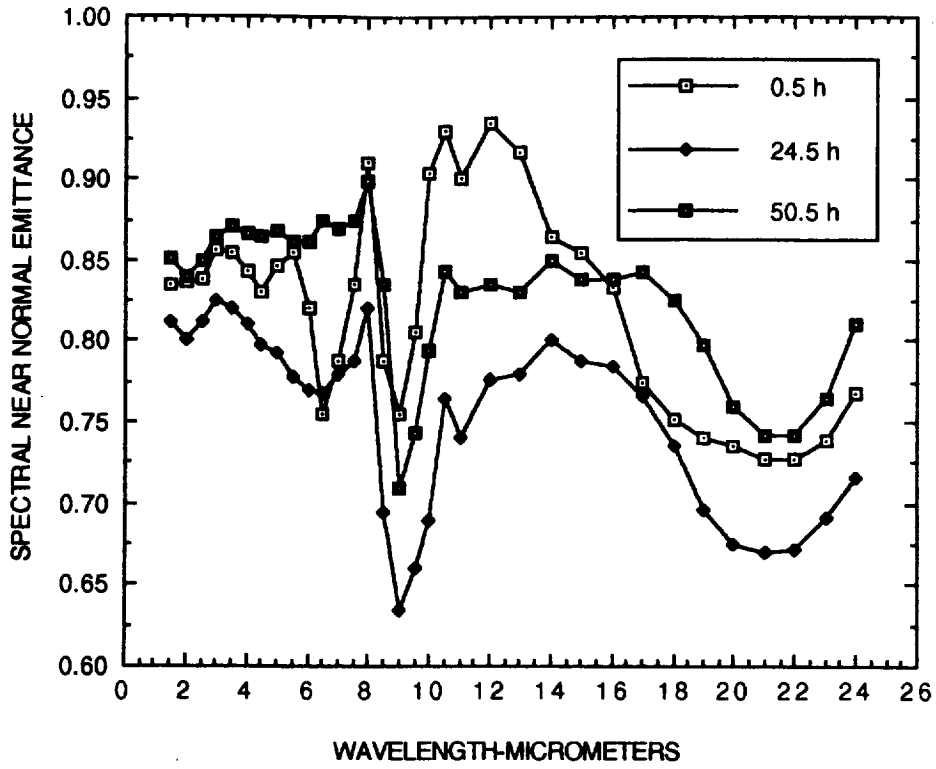

Figure B-37 . Effect of isothermal static oxidation time at 1260 K on spectral near normal emittance of Type 1 coated Alpha2 substrate.

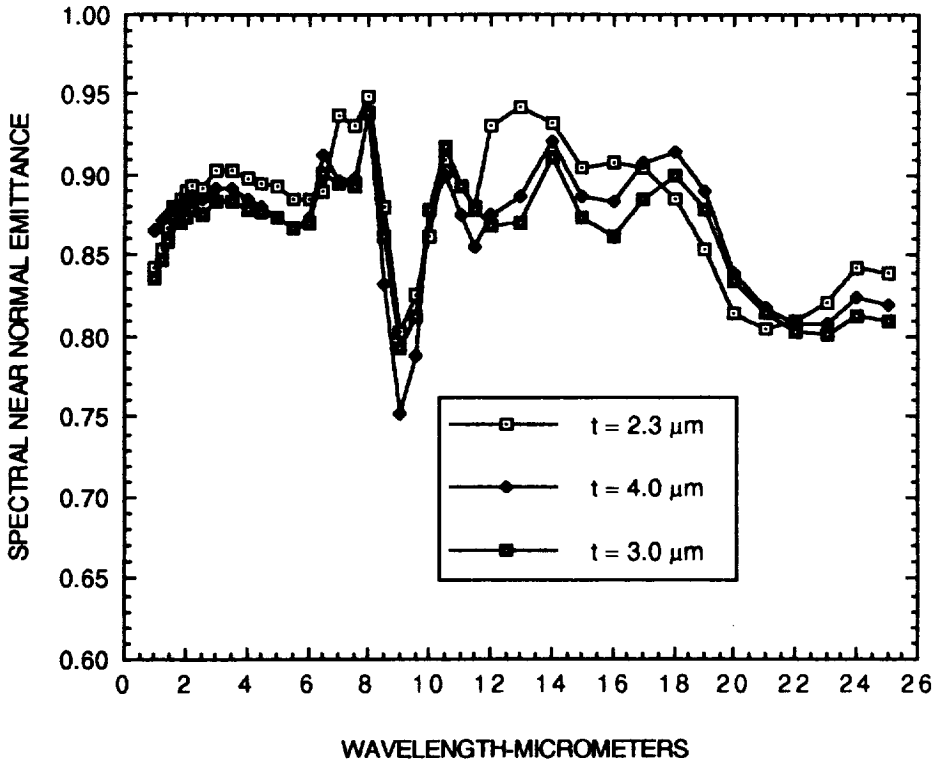

Figure B-36. Effect of Type 2 coating thickness on spectral near normal emittance of coated Super-Alpha2 substrates.

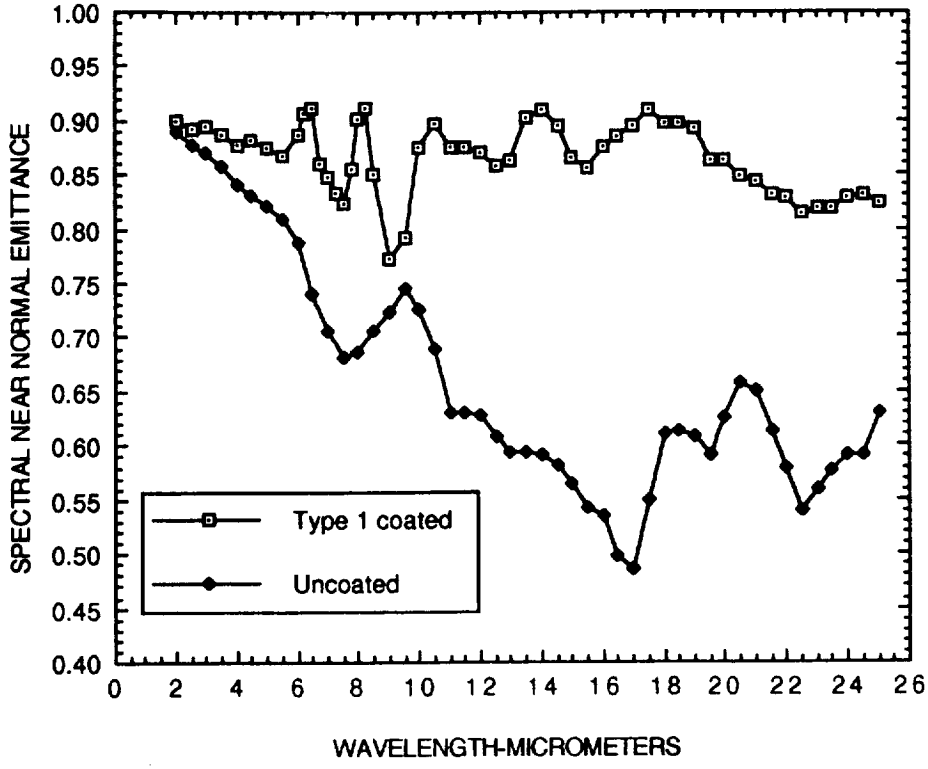

Figure B-39. Spectral near normal emittance of uncoated and Type 1 coated Beta-21S substrates after profiled cyclic oxidation exposure at 1094 K, 25 cycles for uncoated and 100 cycles for coated specimens.

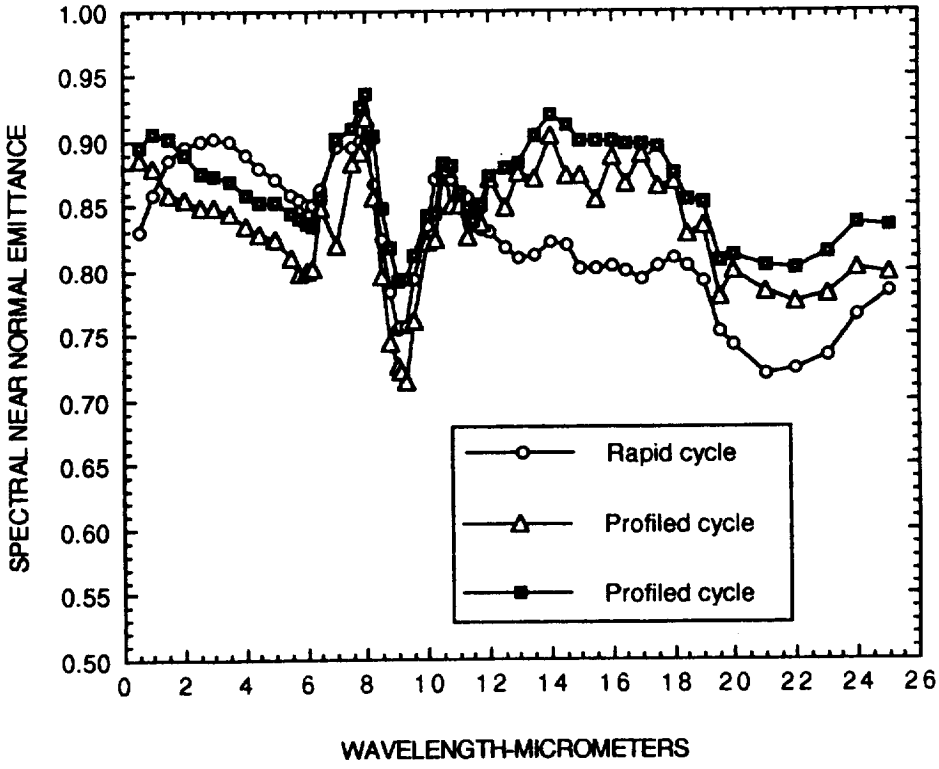

Figure B-38. Effect of heating and cooling rate of cyclic oxidation exposure on spectral near normal emittance of Type 1 coated Alpha2 substrate, maximum temperature of 1260 K, 100 cycles.

REPORT DOCUMENTATION PAGE

Form Approved
OMB No. 0704-0188

1. AGENCY USE ONLY *(Leave blank)*	2. REPORT DATE	3. REPORT TYPE AND DATES COVERED
	April 1993	Technical Memorandum

4. TITLE AND SUBTITLE

THERMAL COATINGS FOR TITANIUM-ALUMINUM ALLOYS

5. FUNDING NUMBERS

WU 506-73-43-01

6. AUTHOR(S)

George R. Cunnington, Ronald K. Clark, and John C. Robinson

7. PERFORMING ORGANIZATION NAME(S) AND ADDRESS(ES)

NASA Langley Research Center
Hampton, VA 23681-0001

8. PERFORMING ORGANIZATION REPORT NUMBER

9. SPONSORING/MONITORING AGENCY NAME(S) AND ADDRESS(ES)

National Aeronautics and Space Administration
Washington, DC 20546-0001

10. SPONSORING/MONITORING AGENCY REPORT NUMBER

NASA TM-107760

11. SUPPLEMENTARY NOTES

Cunnington and Robinson: Lockheed Missiles & Space Company, Inc., Palo Alto, CA; Clark: Langley Research Center, Hampton, VA.

12a. DISTRIBUTION/AVAILABILITY STATEMENT

Unclassified-Unlimited

Subject Category: 26

12b. DISTRIBUTION CODE

13. ABSTRACT *(Maximum 200 words)*

Titanium aluminides and titanium alloys are candidate materials for hot-structure and heat-shield components of hypersonic vehicles. In order to utilize their maximum temperature capability, they must be coated to resist oxidation and to have high emittance and a low value of recombination efficiency for dissociated boundary-layer species. Very thin chemical-vapor deposition (CVD) boron-silicon alloy coatings are promising for this application because of durability and low weight characteristics. Boron-silicon and aluminum-boron-silicon coatings were applied to alpha2, super-alpha2, and gamma titanium aluminides and the beta-21S titanium alloy. Coated specimens were exposed to a simulated hypersonic flight environment at temperatures to 1255 K to determine oxidation resistance, emittance, recombination efficiency, and thermal shock resistance. Results are presented for three types of coatings: (1) single-layer boron-silicon, (2) single-layer aluminum-boron-silicon and (3) multilayer of aluminum-boron-silicon with an outer layer of boron-silicon. The range of coating thicknesses was 2.4 to 19.6μm. Coating weights were 0.0056 to 0.0446 kg/m^2. Oxidation and thermal shock resistance were excellent and total emittance was 0.80 or greater in all cases. Recombination efficiency for 10 h of environmental exposure was 0.06 or less.

14. SUBJECT TERMS
Hypersonic vehicle thermal control coatings; Emittance; Oxidation resistance; Recombination efficiency; Simulated reentry exposure testing; Coating morphology and composition

15. NUMBER OF PAGES
131

16. PRICE CODE
A07

17. SECURITY CLASSIFICATION OF REPORT	18. SECURITY CLASSIFICATION OF THIS PAGE	19. SECURITY CLASSIFICATION OF ABSTRACT	20. LIMITATION OF ABSTRACT
UNCLASSIFIED	UNCLASSIFIED	UNCLASSIFIED	